100

NUCLEAR ENERGY

FOR ROCKET PROPULSION

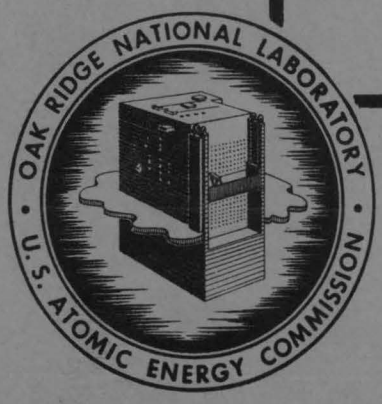

OAK RIDGE NATIONAL LABORATORY
OPERATED BY
CARBIDE AND CARBON CHEMICALS COMPANY
A DIVISION OF UNION CARBIDE AND CARBON CORPORATION
UCC
POST OFFICE BOX P
OAK RIDGE, TENNESSEE

ORNL
Central Files Number
53-6-6

This document consists of 94 pages.
Copy 11 of 29 copies. Series A.

Contract No. W-7405-eng-26

NUCLEAR ENERGY FOR ROCKET PROPULSION

R. W. Bussard

Date Issued

OAK RIDGE NATIONAL LABORATORY
Operated by
CARBIDE AND CARBON CHEMICALS COMPANY
A Division of Union Carbide and Carbon Corporation
Post Office Box P
Oak Ridge, Tennessee

DISTRIBUTION LIST

1. F. H. Abernathy
2. W. P. Berggren
3. R. C. Briant
4. E. S. Bettis
5. R. W. Bussard
6. C. E. Center
7. D. D. Cowen
8. L. B. Emlet (Y-12)
9. A. P. Fraas
10. W. B. Humes (K-25)
11. J. R. Johnson
12. C. E. Larson
13. F. Kertesz
14. W. D. Manly
15. C. B. Mills
16. A. J. Miller
17. H. F. Poppendiek
18. P. M. Reyling
19. A. M. Weinberg

20-23. ANP Library

24-25. Technical Information, Service, Oak Ridge

26-29. Frank Ward, AEC, Wash., D.C.

NUCLEAR ENERGY FOR ROCKET PROPULSION

INTRODUCTION

Since the advent of nuclear energy, there has been considerable discussion of the possibility of its application as a power source for the propulsion of high-velocity rocket vehicles. The use of nuclear energy for rocket propulsion appears attractive because the choice of propellant is not limited by considerations of combustion energy, therefore low molecular weight propellants such as pure hydrogen may be used. This is advantageous because the performance of any rocket vehicle is primarily a function of the exhaust velocity of its propellant gases, and, for a given peak gas temperature, the exhaust velocity is inversely proportional to the square root of the molecular weight of the exhaust gas. For example, for rocket motor operation at a chamber pressure of 300 psia, a peak gas temperature of 4500°F, and nozzle expansion to 15 psia, the liquid-oxygen–hydrazine propellant system produces an exhaust velocity of 8300 ft/sec, whereas pure hydrogen will attain an exhaust velocity of 22,700 ft/sec at the same conditions. This is an increase in exhaust velocity by a factor of 2.73. The required vehicle mass ratio for any desired burnout velocity is an exponential function of the exhaust velocity, thus the mass ratio of the hydrogen-propelled rocket will be equal to the mass ratio of the liquid-oxygen–hydrazine rocket raised to the 1/2.73 (= 0.367) power.

The logical method of determining the applicability of nuclear energy to rocket propulsion would seem to be through an investigation of the performance of feasible nuclear-powered rocket vehicles over a wide range of load carrying capacities and vehicle velocities (that is, over a wide range of vehicle sizes). A survey of the literature* reveals that no such general investigation has been made. The purpose of this report is to present the results of an investigation of this type in order to show the potential range of applicability of nuclear energy to rocket propulsion and to point out some of the major problems that would be involved in the actual construction of nuclear-powered rocket vehicles.

The basic difference between chemical- and nuclear-powered rocket vehicles is in the method of obtaining the energy required for vehicle propulsion. The chemical rocket obtains energy from the combustion or decomposition of the propellants, whereas the propellant of the nuclear rocket provides no intrinsic energy but is heated by a nuclear reactor.

The body of this report is divided into two major parts. The first part is an investigation of the potential performance of nuclear-powered rocket vehicles over a wide range of load carrying capacities and vehicle velocities, and nuclear rocket motor design conditions that might conceivably be achieved in a reasonable period of time are used. The second part covers an investigation of several nuclear reactor designs based on the conditions assumed in the first part of the report. Four reactor core designs were considered; each has a lower ratio of heat transfer surface area to heat transfer structure volume than its predecessor.

---

*E. P. Carter, *The Application of Nuclear Energy to Rocket Propulsion; a Literature Search*, Y-931 (Dec. 29, 1952).

SUMMARY

The results of the rocket vehicle study (Part I) indicate that nuclear-powered rocket vehicles will be lighter than comparable chemically powered vehicles for vehicle velocities greater than 15,000 ft/sec with payload weights of 1,000 to 10,000 lb, or for vehicle velocities greater than 7,000 ft/sec with payload weights greater than 10,000 pounds.

The reactor core design study (Part II) shows that high reactor core bulk power densities might be achieved without an undue gas pressure drop across the reactor or an excessive temperature drop from the fuel element to the gas. The best core design appears to be one that utilizes thin, parallel, solid graphite plates as the heat transfer elements.

Since the propellant gases are predominantly hydrogen, the use of graphite as the basic structural material will require the development of a hydrogen-resistant coating to be applied to the surfaces of the graphite heat transfer elements of the reactor core in order to inhibit chemical reactions between the gas and the graphite. The feasibility of the reactor core designs considered thus depends on the efficacy of the protective coatings proposed for the graphite heat transfer elements. Thus, the first step in a program of development of a nuclear rocket should be an experimental investigation of protective coatings for graphite for operation in hydrogen.

PART I
NOMENCLATURE

SYMBOL	MEANING	UNITS
a	Acceleration of rocket vehicle	ft/sec^2
a_b	Vehicle acceleration at end of rocket motor operation	ft/sec^2
a_0	Initial vehicle acceleration (at takeoff)	ft/sec^2
A_e	Exhaust nozzle exit area	ft^2
A_t	Exhaust nozzle throat area	ft^2
A_{st}	Propellant tank surface area	ft^2
c_{pg}	Mean specific heat of propellant gases	$Btu/lb \cdot {}^\circ F$
D	Propellant tank diameter	ft
D_r	Nuclear rocket motor outside diameter	in.
f_s	Design safety factor	
F_b	Rocket motor thrust at propellant burnout	lb
F_0	Initial thrust of nuclear rocket motor	lb
g_c	Acceleration of gravity at sea level	$32.2\ ft/sec^2$
J	Thermal-mechanical energy conversion factor	778 ft-lb/Btu
k	Propellant gas specific heat ratio	
k_i	Thermal conductivity of propellant tank insulation (see Fig. 2)	$Btu/hr \cdot ft \cdot {}^\circ F$
m	Weight of rocket vehicle	lb
m_b	Vehicle weight at end of rocket motor operation (at burnout)	lb
m_e	Weight of turbines, pumps, valves, propellant lines, and exhaust gas vane system	lb
m_f	Weight of fins	lb
m_L	Dead load weight	lb
m_0	Total loaded vehicle weight	lb
$m_{0(crit)}$	Total loaded weight of minimum size (4-in. dia) vehicle	lb
m_p	Total propellant weight	lb
m_r	Nuclear rocket motor weight	lb
m_s	Weight of propellant tank reinforcing structure	lb
m_t	Propellant tank skin weight	lb
mw	Molecular weight of propellant gases	lb/lb·mole
N	Number of equal increments of thrust, or number of equal-power rocket motors required to propel vehicle (stepped thrust system)	
p	Maximum absolute pressure within propellant tank	$lb/in.^2$
p_e	Propellant gas absolute pressure at nozzle exit	$lb/in.^2$
p_c	Absolute gas pressure within rocket motor prior to expansion through nozzle	$lb/in.^2$
$\overline{p}$	Rocket motor specific power	megawatt/lb

SYMBOL	MEANING	UNITS
P_d	Propellant pump discharge pressure	lb/in.^{2}
P_0	Maximum power required to propel vehicle	megawatt
P_r	Nuclear rocket motor power output	megawatt
R_u	Universal gas constant	$1544 \left(\frac{\text{lb}}{\text{ft}^2}\right) \left(\frac{\text{ft}^3}{\text{lb}\cdot\text{mole}}\right) \left(\frac{1}{^\circ\text{R}}\right)$
t_b	Nuclear rocket motor operating (burning) time	sec
t_t	Propellant tank wall thickness	ft
T_c	Gas temperature within rocket motor prior to expansion	$^\circ$R
T_e	Gas temperature at nozzle exit	$^\circ$R
T_0	Propellant temperature at reactor inlet	$^\circ$R
ΔT_t	Gas temperature drop through turbine	$^\circ$F (or $^\circ$R)
v	Vehicle velocity	ft/sec
v_b	Velocity of vehicle at end of rocket motor operation (at burnout)	ft/sec
v_e	Propellant gas exhaust velocity	ft/sec
v_L	Axial component of pump turbine gas exhaust velocity	ft/sec
v_m	Maximum theoretical propellant gas exhaust velocity	ft/sec
V_t	Propellant tank volume	ft^3
w_0	Initial (maximum) propellant weight flow rate	lb/sec
w_p	Propellant weight flow rate	lb/sec
w_t	Turbine gas weight flow rate	lb/sec
α	Fraction of total propellant not used as propulsive material	
α_e	Fraction of total propellant lost by evaporation in the propellant tanks	
β	Fraction of total propellant used as the vehicle propulsive jet	
γ_p	Liquid propellant density	lb/ft^3
γ'_p	Liquid propellant specific gravity	
γ_t	Propellant tank material density	lb/ft^3
γ'_t	Propellant tank material specific gravity	
λ_n	Over-all nozzle efficiency	
λ_p	Over-all efficiency of propellant pumps	
λ_t	Over-all efficiency of pump turbines	
η_c	Bulk power density within rocket motor reactor core	megawatts/ft^3
σ	Propellant tank material yield strength	lb/in.^{2}

PART I. VEHICLE PERFORMANCE

DISCUSSION

In an examination of the possible use of nuclear energy as the power source for rocket propulsion of vehicles, it is of little use to attempt to design nuclear-powered rocket motors to operate at high propellant specific impulse values without an investigation of the over-all performance characteristics of the vehicle in which the motor is to be used.

Nuclear reactors must be of a certain minimum size and weight in order to function at all, but once this size range has been reached, the power output is limited only by the capacity of the "non-nuclear" components of the system (that is, pumps, heat exchangers, etc.) and by the maximum temperature limitations imposed by available materials of construction.

The minimum reactor rocket motor diameter and weight will be of the order of 4 ft and 6,000 lb for a useful rocket reactor, therefore any rocket for which a nuclear reactor drive is proposed must start with a weight handicap of about 6,000 lb as compared to chemically powered rockets. Thus, in spite of the high performance offered by the possible use of low molecular weight propellants in nuclear reactor rocket motors, it will be necessary to go to rockets of over-all gross weights of the order of hundreds of thousands of pounds before the nuclear rocket can demonstrate a significant advantage over its chemically powered brothers*. Such large (by present standards) rockets are of interest only for tasks that require exceedingly long ranges or heavy payloads.

The present study is concerned with the investigation of the performance characteristics of single-stage nuclear rockets, over a wide range of vehicle burnout velocities and dead load capacities, using each of six different propellants. The optimum propellant to produce a given burnout velocity is that which yield a vehicle design with minimum total loaded weight (take-off weight) for the maximum dead load weight. The results are presented in the form of curves that give the ratio of loaded to dead load weight as a function of burnout velocity for the six propellants considered. For comparison, the performance of several chemically powered rockets is plotted on the same scales. These curves show that hydrogen is the best propellant for use in nuclear rocket vehicles despite its low liquid density and attendant tankage weight. Production and handling problems as well as propellant cost may indicate that ammonia, hydrazine, or an ammonia-hydrogen bipropellent system is more desirable than pure liquid hydrogen, depending upon the specific vehicle design and required performance.

Since, by present standards, the required vehicle size is quite large for the performance range in which nuclear rockets are most practical, it was considered reasonable to neglect the effects of atmospheric drag. Further, all calculations were based upon flight in a gravitational-field-free space. Chemical rocket performance was computed on the same basis.

GENERAL CONCEPT OF VEHICLE GEOMETRY AND OPERATION

The single-stage vehicle is shown schematically in Fig. 1.

The dead load carried by the vehicle is located in the rocket nose just forward of the propellant and propellant tanks. The propellant pumps, turbines, reactor, fins, and other major propulsion unit and control

*The validity of this conclusion was clearly shown by the results of a nuclear rocket study performed by Consolidated Vultee Aircraft Corp. (Convair Report FZA-9-504, Feb. 8, 1952) in which it was shown that nuclear powered rockets of V-2 size, payload, and general geometry, with arbitrary reactor weights as low as 4000 lb, will have about the same performance as the chemically powered V-2. This result is not surprising because the nuclear rocket cannot prove to be significantly better than a chemical rocket in a vehicle as small as the V-2 with payloads as small as those carried by the V-2.

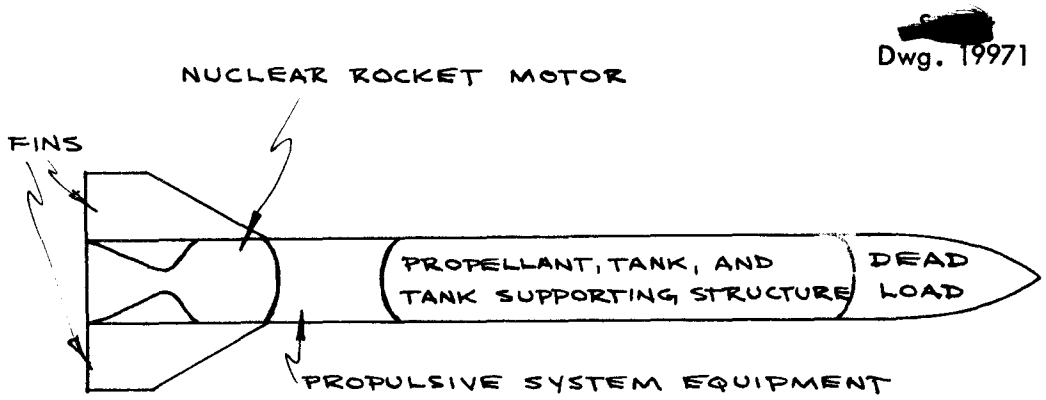

SINGLE STAGE VEHICLE

FIG. 1

mechanisms are all located aft of the main propellant and tank section. The propellant carried in the tank section is pumped to the reactor by means of centrifugal pumps driven by turbines that are powered by reactor bleed gas. The propellant is then vaporized and heated to the desired temperature within the reactor, is expelled through a converging-diverging exhaust nozzle, expands approximately adiabatically to supersonic velocity, and produces the thrust to drive the rocket. Fins may be carried by the vehicle during flight through the atmosphere in order to assure that the center of pressure will be aft of the center of gravity; however, movable gas-deflector vanes located in the propellant exhaust stream are provided for stability and control of the vehicle's flight during the take-off period and during the power-on portion of flight above the atmosphere. In certain cases it may be desirable to drop the fins after they are no longer useful as vehicle stabilizers; however, this weight saving was not considered in the calculations made for this report.

Brief consideration of the vehicle flight program is in order, as the required shield weights are influenced by the flight duration, vehicle acceleration, and reactor "burning" time. (See section on "Shielding Considerations.")

The flight program chosen as representative of the launching and "burning" portions of flight of the vehicle generally follows the familiar V-2 flight pattern. The vehicle initially stands in a vertical position on the ground, propellant is slowly bled through the reactor during reactor warmup, the propellant fill lines and other external control connections with the rocket are broken, the reactor is brought up to full power, the rocket rises vertically through the atmosphere with an initial acceleration of 3 to 5 times the normal gravitational acceleration, and the completion of burning occurs well above the effective atmosphere. Burning times considered are of the order of 200 to 500 sec for vehicles in the performance range most suitable to nuclear-energy rockets.

The vehicle performance for several different possible propellants was investigated over a wide range of dead load capacities. The performance is indicated by the take-off weight required to propel a given dead load to a given velocity. A high-performance vehicle is defined as one that has a low ratio of total loaded weight to dead load weight for a given dead load and burnout velocity.

In order to determine the total to dead load weight ratio as a function of vehicle burnout velocity and dead load capacity, it is necessary to

relate the familiar vehicle mass ratio equation to equations that describe the weight of the vehicle components.

The mass ratio equation is obtained as follows:

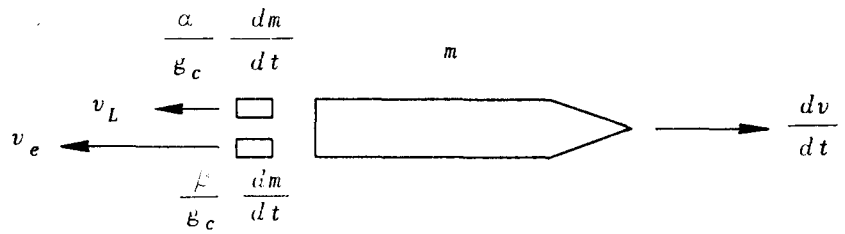

Assume a vehicle of instantaneous mass, m/g_c, that moves in a gravitational-field-free space and expels mass at a rate $(1/g_c)/(dm/dt)$ in a direction opposite to that of the vehicle motion. Further assume that a fraction α of the mass flow rate is being expelled with a velocity v_L, relative to the vehicle, and a fraction β with a velocity v_e. It will be shown later that α and β correspond, respectively, to the fraction of vehicle propellant mass lost by evaporation and other causes, and to the fraction of total propellant mass used as the vehicle propulsive jet. By conservation of momentum, we can write

$$(1)\quad m\,dv = -\beta v_e\,dm - \alpha v_L\,dm = -(\beta v_e + \alpha v_L)\,dm .$$

By integrating from initial vehicle velocity and mass, v_0 and m_0, to final velocity and mass, v_b and m_b, we have

$$\int_{m_0}^{m_b}\frac{dm}{m} = -\int_{v_0}^{v_b}\frac{dv}{(\beta v_e + \alpha v_L)}$$

$$(2)\qquad \ln\frac{m_b}{m_0} = -\frac{v_b - v_0}{\beta v_e + \alpha v_L}$$

or

$$\frac{m_0}{m_b} = e^{(v_b - v_0)/(\beta v_e + \alpha v_L)} .$$

The total mass expelled is obviously that of the propellant and is designated by m_p. Now, for a rocket initially at rest $v_0 = 0$, and since $m_0 - m_b = m_p$, Eq. 2 becomes

$$(3)\quad \frac{m_0}{m_p} = \frac{e^{v_b/(\alpha v_L + \beta v_e)}}{e^{v_b/(\alpha v_L + \beta v_e)} - 1} .$$

VEHICLE COMPONENT WEIGHT RELATIONS

For purposes of this study, the vehicle is divided into six basic component weights, which are the (1) dead load weight, m_L; (2) the propellant tank, m_t, and tank structural and reinforcement weight, m_s; (3) the fin weight, m_f; (4) the nuclear reactor rocket motor weight, m_r; (5) the propulsive system equipment weight, m_e; and the (6) propellant weight, m_p. The total loaded vehicle weight can thus be written as

$$(4)\quad m_0 = m_L + m_t + m_s + m_f + m_e + m_p + m_r .$$

Dead Load Weight, m_L. The dead load is defined as the sum of the weights of the useful payload carried, the shield required, the guidance equipment and instrumentation, and all the necessary supporting and enclosing structure.

Propellant Tank and Tank Structural Weight, $m_f + m_s$. The prime function of the propellant tank is to carry the propellant required to propel the vehicle to the desired burnout velocity. Thrust loads from the reactor motor are to be transmitted through the pressurized tank to the forward end of the vehicle, partly by the tank skin and partly by the tank reinforcing structure. The reinforcing structure would typically consist of stringers, stiffeners, and thrust columns, and its weight was taken as 15% of the weight of the tank.[1] A positive tank pressure should be maintained

to provide satisfactory pump inlet pressures and to ensure that the tank skin will always be under tensile loading so that buckling will be avoided.

Tank volume in excess of that necessary for the required amount of propellant must be provided for liquid expansion, gas space above the initial liquid surface, and propellant that is vaporized by heating of the tank walls resulting from aerodynamic skin friction.

For the purposes of this study, it was specified that the total initial propellant volume should be 97% of the total tank volume, thus 3% of the tank volume would be provided for liquid expansion and excess gas space. The ratio of cylindrical tank length to tank diameter was taken as 5:1, and 2:1 ellipsoidal tank end caps were specified.

At first glance, it seems desirable to consider the use of a double-walled tank construction (insulated or vacuum jacketed) for the extremely low boiling point propellants in order to prevent the loss of propellant by evaporation. However, it can be shown that in nearly all cases involving large vehicles, the increased tank weight required to maintain the specified mass ratio (and hence burnout velocity) with a double-walled construction will be greater than the propellant weight saved by the reduction of evaporation.[2,3] Thus, double-walled tank construction was deemed undesirable, and in the case of the low boiling point propellants, it was found possible to provide sufficient thermal insulation to reduce evaporation loss to an acceptable level without utilizing such construction.

Heat transfer from a heated metal surface to nondynamic liquid hydrogen and nitrogen has been investigated at the Los Alamos Scientific Laboratory.[4] By using values of heat transfer rates given in the Los Alamos report, it is possible to determine the fraction of propellant lost by evaporation during any arbitrary heating time for a given temperature difference between the tank wall and the propellant. These losses will be a function of the tank size since heat transfer area varies as the square of the tank dimensions while total propellant weight varies as the cube. The propellant is expelled as the rocket's reaction mass, therefore the available heat transfer surface of the tank constantly decreases with time, and the time-average heat transfer area is less than the total cylindrical surface area - the difference depends on the choice of burning time or vehicle acceleration. Based upon V-2 skin heating data, it is felt that a total heating time of 30 sec is a reasonable estimate for calculations based upon a maximum tank skin temperature of 250°F.[5]

For very long range vehicles operating at reasonable accelerations (that is, 3 g_c to 9 g_c), the minimum burning times will be of the order of 200 sec, therefore the time-average heat transfer area will be roughly 85% of the total tank cylindrical area. The results of calculations made by using heat transfer data from the Los Alamos report are presented in Fig. 2, which shows the fraction of propellant lost by evaporation as a function of tank size for four of the six propellants considered. The two propellants not shown are hydrazine and water, which were omitted because their boiling points are so much higher than those of liquid ammonia, methane, or hydrogen that the available temperature differences and hence heat transfer rates are insufficient to cause any significant evaporation in tanks of greater than 6 in. in diameter under the specified heat transfer conditions.

It can be seen in Fig. 2 that the propellant loss in negligible for all the propellants considered except for hydrogen and the hydrogen-ammonia system. The evaporative losses of these two propellants will be excessive if no insulation is provided for the tank wall; however, these losses can be drastically reduced by the use of a 0.010 in. thick insulation layer lining the tank inner wall. The

[redacted]

Dwg. 19972

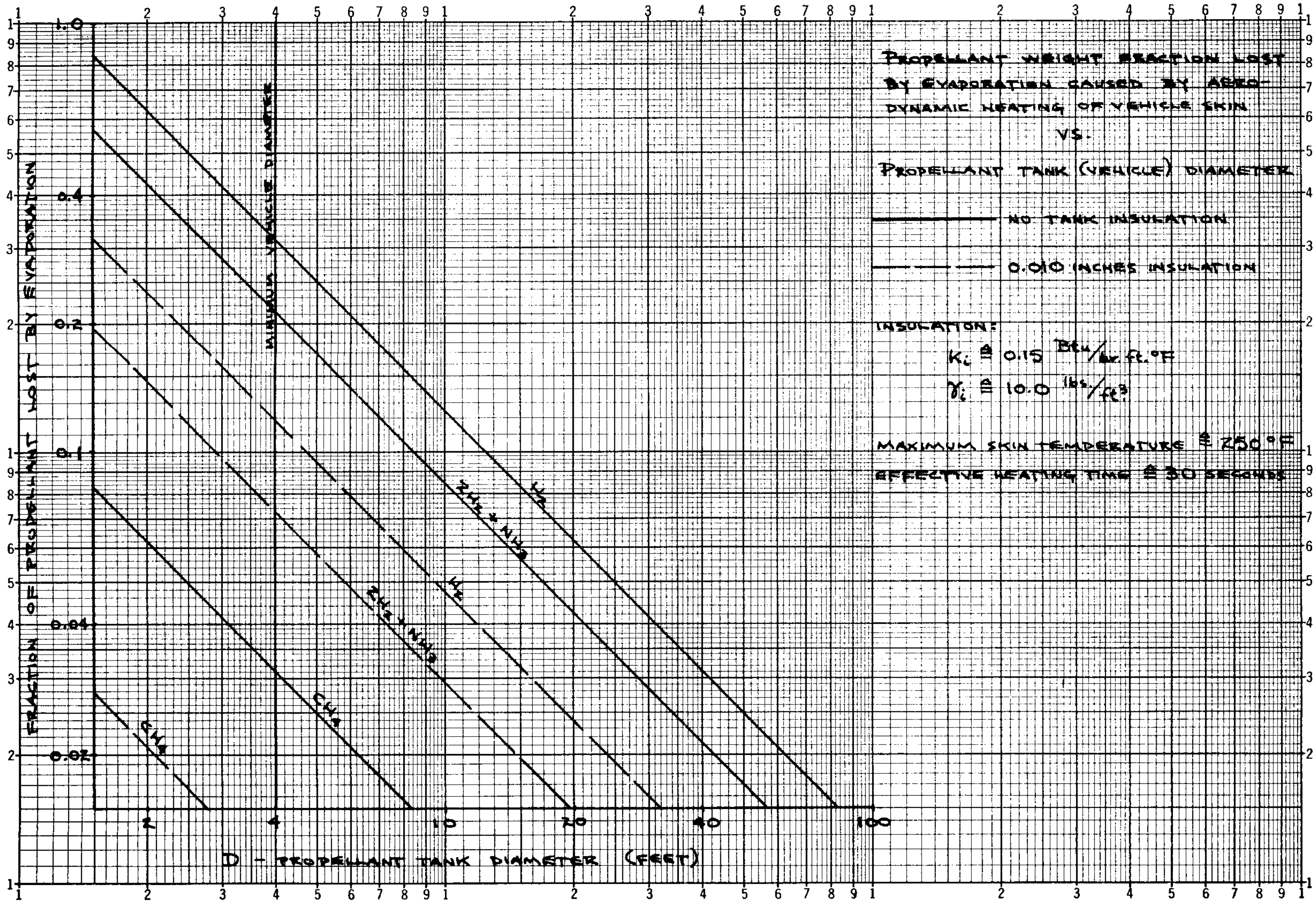

FIG. 2

insulation layer could be composed of ground cork or sawdust bonded to the tank skin by a pyroxylin plastic compound. The thermal conductivity of this material is estimated as less than 0.15 Btu/hr·ft·°F, and the bulk density as less than 10 lb/ft^3. Because of the thinness and low bulk density of the insulation layer as compared to the tank wall structure, the insulation weight will be small compared to the total tank weight and is therefore neglected in tank weight calculations.

The tank and structure weight can be related to the propellant weight by

$$m_s = 0.15\, m_t ,$$

as previously discussed. Thus,

$$(5) \qquad m_t + m_s = 1.15\, m_t .$$

Tank wall weight is given by

$$m_t = \gamma_t t_t A_{st}$$

where

$$A_{st} = 5\pi D^2 + \frac{\pi D^2}{2} + \frac{\pi\left(\frac{D}{4}\right)^2}{\frac{1}{2}} \ln \frac{1 + \frac{1}{2}}{1 - \frac{1}{2}}$$

for a tank with a cylindrical length to diameter ratio of 5, and 2:1 ellipsoidal end caps as specified.

Now,

$$t_t = \frac{pDf_s}{2\sigma} .$$

Thus,

$$(6) \qquad m_t = 2.819\, \pi\gamma_t \frac{pD^3 f_s}{\sigma} .$$

However, $m_p = 0.97\, \gamma_p V_t$ for the case of 3% tank volume initially unfilled to allow for liquid expansion and excess gas space. Here $V_t = (4/3)\, \pi D^3$ for the tank geometry previously specified.

Thus,

$$(7) \qquad m_p = 1.293\, \pi D^3 \gamma_p$$

or

$$m_p = 253.9\, \gamma_p' D^3 .$$

By combining Eqs. 6 and 7,

$$(8) \qquad m_t = 2.180\, \frac{\gamma_t}{\gamma_p} \frac{pf_s}{\sigma}\, m_p$$

which, when combined with Eq. 5, gives

$$(9) \qquad m_t + m_s = 2.506\, \frac{\gamma_t'}{\gamma_p'} \frac{pf_s}{\sigma}\, m_p .$$

It is obvious from Eq. 9 that a material with a high yield-strength to density ratio is desired in order to minimize tank weight. Further, the strength characteristics of the material must not be adversely affected by low temperatures, because two of the propellants considered boil at temperatures below -250°F. In addition, it is desired that a material with a reasonably low density be selected so that the tank walls will be thick enough to have some semblance of stiffness, and thus assure that local skin buckling will not occur under the anticipated conditions of loading. The best material is 75S, heat-treatable aluminum alloy, hardened to the T6 condition. The yield strength, ultimate strength, and modulus of elasticity of 75S-T6 all increase slightly (10 to 15%) with a change in temperature from 70 to -400°F, while the impact strength and per cent elongation to failure do not change significantly over this temperature range. The yield strength at 70°F for sheet and plate thicker than 0.040 in. and thinner than 2.0 in. is 67,000 psi,[6,7,8,9] and the specific gravity of the metal is 2.79. By using these values and by specifying that the safety factor be 2.0 and the tank pressure be equal to 35 psia, Eq. 9 can be reduced to obtain

$$(10) \qquad m_t + m_s = \frac{0.007305}{\gamma_p'}\, m_p .$$

Fin Weight, m_f. For weight study purposes, the fin weight can be taken as 1% of the total loaded weight of the vehicle. This figure, though somewhat arbitrary, was based upon considerations of the fin weight of existing chemically powered rocket vehicles. It is quite conceivable that fins would not be found useful for stabilization and control of large

nuclear-powered rockets if an exhaust-gas deflector system is used during the power-on portion of flight. The fin weight, as defined, is given by

$$m_f = 0.01\, m_0 \quad (11)$$

Rocket Motor Weight, m_r. The weight of the rocket motor is defined to include the reactor core structure, reflector, external pressure shell, and rocket exhaust nozzle. For high performance vehicles it is desirable to obtain rocket motors with high power-output to total-weight ratio (specific power) so that the motor weight will become a small fraction of the total loaded vehicle weight. The specific power of the rocket motor is not a constant for any given reactor core design, however, but varies with the size of the motor itself.

In order to determine the nuclear rocket motor weight as a function of the output power, it is necessary to determine the variation of rocket motor specific power and total weight with rocket motor outside diameter. When this relationship has been established, the total power output of any size and weight motor can be computed and an analytical expression relating weight and power output can determined.

The rocket motor specific power for the optimum reactor core design is shown in Part II (section on "Rocket Motor Structure") to be determined from

$$\frac{\eta_c}{\bar{p}} = \frac{52.23 + 5674\left(\frac{1}{D_r} - \frac{25.62}{D_r^2} + \frac{182.3}{D_r^3}\right)}{\left(1 - \frac{21.35}{D_r}\right)^3} + 136.8 \quad (12)$$

Total rocket motor weight (see Part II) is given by the sum of the motor component weights as

$$m_r = 0.0706\,(D_r^3 - 16.35\, D_r^2 + 220.9\, D_r - 1573) \quad (13)$$

where rocket motor outside diameter, D_r, is in inches.

Obviously, the total reactor power output is

$$P_r = m_r \bar{p} \quad (14)$$

For a fixed maximum bulk core power density η_c, the rocket motor power output and total weight for any given motor size can be determined from Eqs. 12, 13, and 14, thus the motor weight can be obtained as a function of the power output. From the results of the stacked-plate reactor core study in Part II, it seems possible that bulk core power densities of 300 megawatts/ft^3 might be attainable with refined, though sturdy, core heat transfer structures, with gas pressure drops within the reactor core of 200 to 300 psi and plate-to-gas mean temperature differences of 300 to 400°F. The results of calculations made by using η_c = 300 megawatts/ft^3 are shown in Fig. 3 and give total rocket motor weight as a function of power output. Figure 4 shows motor weight vs. outside diameter from Eq. 13. It was found possible to fit an equation of the form $m_r = AP_r + B$ to the curve in Fig. 3 with reasonable accuracy over the range of primary interest for the vehicle study. This equation and its deviation from the motor weight vs. power output relationship shown in Fig. 3 are given by:

$$m_r = 0.85\, P_r + 4570 \quad (15)$$

POWER OUTPUT RANGE	DEVIATION OF MOTOR WEIGHT
$2000 < P_r < 6 \times 10^6$ megawatts	Maximum ~20.6% Average ~11.7%

The minimum motor size marked in Figs. 3 and 4 is that of a 4-ft-dia

[redacted]
Dwg. 19973

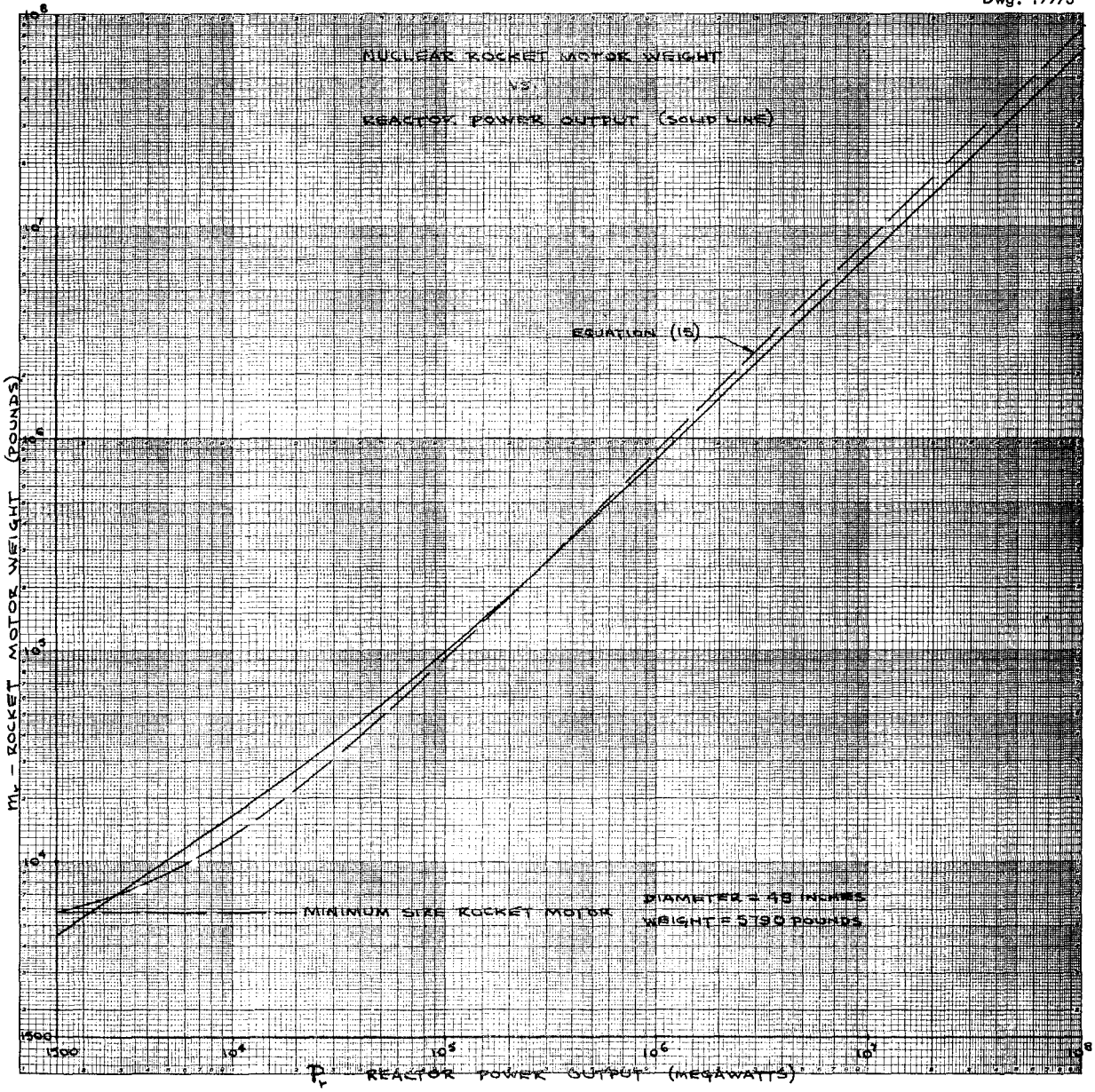

FIG. 3

[redacted] Dwg. 19974

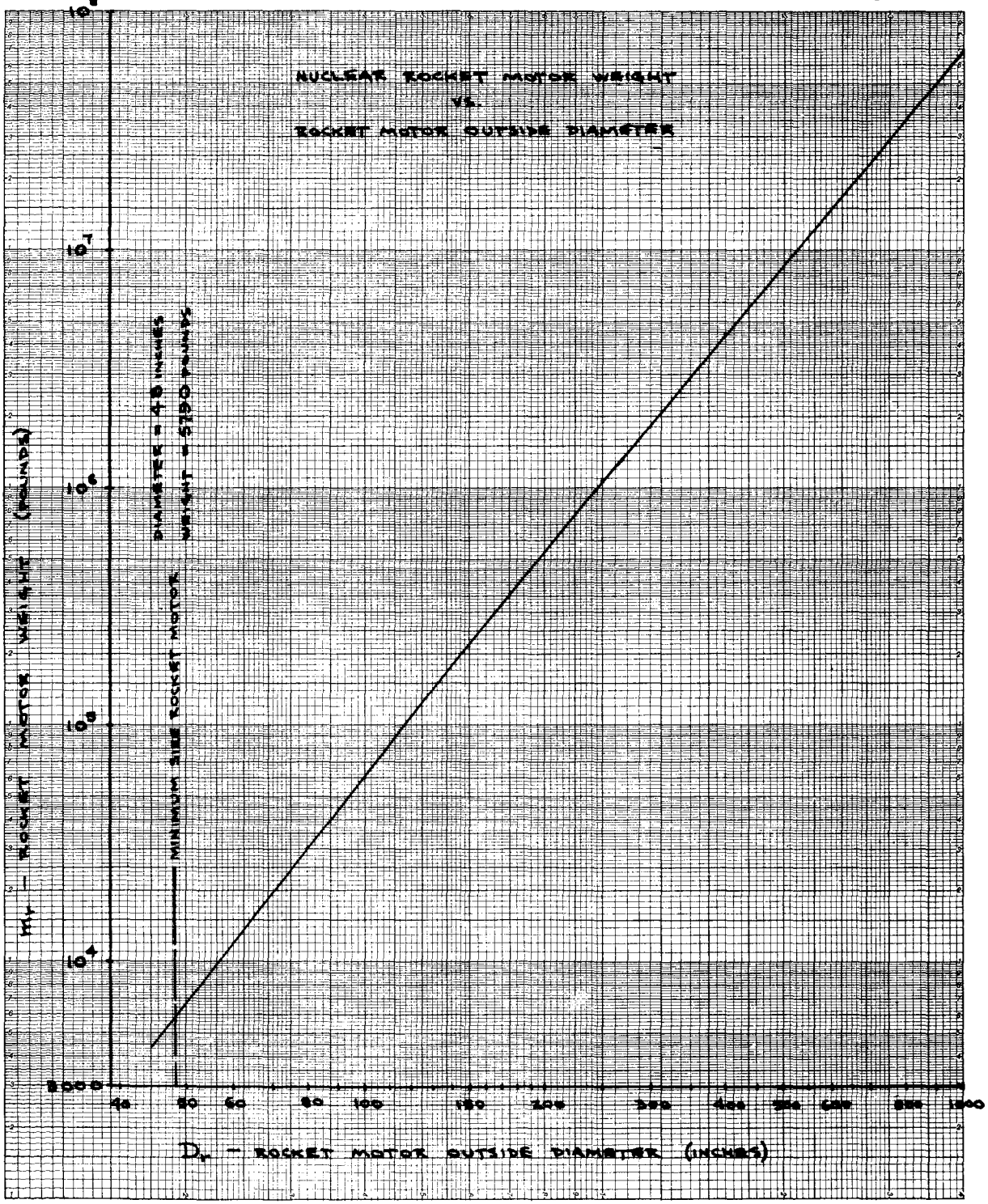

FIG. 4

motor. Because of limitations set by the maximum allowable uranium density within the core volume (see Part II), this diameter has been set as the minimum value for practical reactor construction.

The reactor power output must be equal to the total power required to vaporize and heat the propellant gases flowing through the reactor. This power output (in megawatts) is expressed by

$$(16) \qquad P_r = 0.678 \frac{w_p}{g_c} \left(\frac{v_m}{10^3}\right)^2 .$$

The required gas weight flow rate, w_p, is determined by the desired initial thrust; hence by the initial acceleration. For flight in a gravitational-field-free space, the flow rate and vehicle acceleration are related (by a simple force balance) by

$$(17) \qquad w_p = \frac{ma}{v_e} .$$

From Eq. 17 it can be seen that the maximum flow rate will always be required at takeoff, for any given vehicle acceleration, since the total vehicle mass decreases steadily with time. For constant-thrust rocket motors, this flow rate will remain constant throughout the motor operation time and is given by

$$(18) \qquad w_0 = \frac{m_0 a_0}{v_e}$$

The maximum required reactor power may then be found from Eqs. 16 and 18 to be

$$(19) \qquad P_r = 0.678 \frac{m_0 a_0}{g_c v_e} \left(\frac{v_m}{10^3}\right)^2 .$$

By combining Eqs. 15 and 19, the rocket motor weight may now be related to the total loaded vehicle weight as follows:

$$(20) \qquad m_r = 0.5763 \frac{m_0 a_0}{g_c v_e} \left(\frac{v_m}{10^3}\right)^2 + 4570 .$$

When it is assumed that the initial vehicle acceleration is 3 g_c, Eq. 20 becomes

$$(21) \qquad m_r = 1.729 \frac{\left(\frac{v_m}{10^3}\right)^2}{v_e} m_0 + 4570 .$$

Equation 21 can only be used for vehicles which require more power than that available from the minimum size reactor discussed previously (see also Part II). For all vehicles with lower power requirements, the reactor weight will necessarily remain constant at the minimum value of 5790 lb. In order to propel these vehicles, the reactor would be required to operate at bulk core power densities considerably lower than the assumed maximum of 300 megawatts/ft^3.

The total loaded vehicle weight corresponding to the minimum size rocket motor operating at maximum core power density can be determined from the known minimum rocket motor size, weight, and specific power (see Fig. 20, Part II), that is, the known maximum total power output, and from the relation between reactor power and total loaded vehicle weight as given by Eq. 19. The minimum motor values are:

Minimum motor weight, m_r = 5790 lb

Minimum motor diameter, D_r = 48 in.

Ratio of bulk core power density to motor specific power, given by Fig. 20, $\eta_c/\overline{p}$ = 820; for η_c = 300 megawatts/ft^3 (maximum), $\overline{p}$ = 0.366

Thus, maximum power output of minimum size motor, $m_r\overline{p}$ = 2120 megawatts.

From Eq. 19 and the information given above, the critical total loaded vehicle weight is found to be

$$(22) \qquad m_{0(crit)} = 1042 \frac{v_e}{\left(\frac{v_m}{10^3}\right)^2} .$$

Both v_e and v_m, the actual and theoretical maximum exhaust velocities, respectively, are functions of the

propellant gas properties, and are listed in Table 4. By using values from this table, $m_{0(crit)}$ was determined for each propellant considered. These calculated critical total loaded vehicle weights are listed in Table 1.

TABLE 1. CALCULATED CRITICAL TOTAL LOADED VEHICLE WEIGHTS

PROPELLANT	$m_{0(crit)}$ (lb)
Hydrogen	29,930
Methane	55,460
Ammonia	61,670
Hydrazine	68,990
Water	68,170
Hydrogen and ammonia	48,460

For all vehicles of total loaded weight less than $m_{0(crit)}$, the nuclear-reactor rocket motor weight is constant and fixed at

$$m_r = 5790 \tag{23}$$

and this weight was used in the solution of the performance equation. For all vehicles of m_0 greater than $m_{0(crit)}$, the motor weight as given by Eq. 21 was used in the performance equation.

Propulsive System Equipment Weight, m_e. The propulsive system equipment weight is defined to include the pumps, turbines, valves, piping, exhaust-gas deflector vanes, vane motors, support structure, and pump section structure of the vehicle. There will be little difference in these component weights as compared to a chemical system even though the pumps and other equipment are to be used on nuclear-powered rather than chemically powered vehicles. The major weight difference will be that entailed by the probable requirement that the pumps and some of the plumbing be jacketed with propellant as the coolant in order to remove the heat generated within the structure by neutron and gamma radiation from the reactor core. This radiation heating problem indicates that the pumps and turbines should be located several feet forward of the rocket motor and shielded from core radiation by at least 4 ft of liquid propellant (see Part II).

In general, the equipment weight will be a function of the propellant pump discharge pressure, P_d, the propellant volumetric flow rate, w_p/γ_p, and the pumping power requirements. The pumping power requirements are proportional to the product of the pump discharge pressure and the volumetric flow rate, therefore the equipment weight is actually a function of only these two variables. A study performed by Rand Corporation[10] shows that the weight of the pump turbines, piping, valves, and vane control system will vary approximately linearly with the pumping power requirements, while the pump weight will vary roughly as the product of the volumetric flow rate raised to a power slightly greater than 1.0 and the pump discharge pressure raised to a power on the order of 0.3. The equipment weight is herein assumed to vary as the product of the pump discharge pressure raised to the 1/3 power and the propellant volumetric flow rate – an approximation sufficiently good for the purposes of this study.

The volumetric flow rate is a maximum at take-off conditions for the vehicle flight pattern previously discussed, hence equipment weight is based upon the initial flow rate. Thus

$$m_e = c_1 \frac{w_0}{\gamma_p} (P_d)^{1/3} + c_2 \tag{24}$$

or, from Eq. 18,

$$m_e = c_1 \frac{a_0 m_0}{\gamma_p v_e} (P_d)^{1/3} + c_2$$

where c_1 and c_2 are constants to be determined. Weight data on chemically powered rockets of relatively advanced design give c_1 and approximate value of 10.5 and c_2 a value of 500. Again, specifying that $a_0 = 3\ g_c$, Eq. 24 becomes

$$m_e = 1014 \frac{m_0}{\gamma_p v_e} (P_d)^{1/3} + 500\ , \tag{25}$$

or

$$m_e = 16.22 \frac{m_0}{\gamma_p' v_e} (P_d)^{1/3} + 500 .$$

The pump discharge pressure must, of course, be equal to the desired gas pressure within the rocket motor prior to expansion plus the gas pressure drop through the nuclear reactor motor core plus the pressure drop in the supply plumbing. For a desired gas pressure of 1500 psi and a gas pressure drop of 200 psi (see Part II), it would seem conservative to specify a pump discharge pressure of 1900 psi; a plumbing pressure drop of 200 psi is thus allowed. For this specified discharge pressure, the equipment weight is related to the total vehicle weight by

$$m_e = 201 \frac{m_0}{\gamma_p' v_e} + 500 . \quad (26)$$

Figure 5 shows propulsive system equipment weight for several existing and proposed chemically powered rockets as a function of the volumetric flow rate times the pump discharge pressure to the 1/3 power. Pump plus turbine weight curve based on the results of a study performed by Rand Corporation[10] are also shown in Fig. 5 as a comparison with Eq. 24. It will be noted that the pump and turbine weight (hence the total equipment weight) based upon the Rand study increases more rapidly with

$$(w_0/\gamma_p)(P_d)^{1/3}$$

than does the equipment weight as given by Eq. 24. Even if this is the case, it should still be possible to attain equipment weight values as given by Eq. 24 at any value of

$$(w_0/\gamma_p)(P_d)^{1/3}$$

simply by using many small pumps and turbines in parallel.

Propellant Weight, m_p. As previously discussed, the propellant has been assumed to occupy 97% of the total tank volume when the tanks are fully loaded. Not all of this propellant can be used for vehicle propulsion, however, since some will be used for nozzle cooling, some for powering the pump turbines and auxiliary equipment, and some will be lost by evaporation within the propellant tank.

The minimum practical vehicle diameter is 4 ft (minimum rocket motor diameter), therefore it can be seen from Fig. 2 that propellant evaporation losses are negligible for all the propellants except hydrogen and the hydrogen-ammonia combination. The evaporative loss with these two propellant systems is a function of the tank diameter and hence of the propellant weight. In order to show this effect in the performance calculations over a large range of vehicle sizes, the evaporation loss was determined for each point that had been computed for the performance curves for the hydrogen and the hydrogen-ammonia propellants.

The most practical method of cooling the nozzle walls of the nuclear reactor rocket motors considered appears to be by the use of gas-transpiration cooling of a porous nozzle wall structure. Calculations based on the studies of Green and Duwez[11,12] indicate that the nozzle coolant weight flow rate can be as low as 2½% of the rocket motor propellant weight flow rate and still provide adequate cooling for a properly designed porous-wall nozzle.

The propellant pumping power requirements, in horsepower, are given by

$$HP_p = \frac{0.262\ w_p P_d}{\lambda_p \gamma_p} \quad (27)$$

where λ_p is the over-all pump efficiency, and other symbols are as defined previously.

The pump turbine power output, in horsepower, can be approximately expressed as

$$HP_t = 1.415\ c_{pg}\ \Delta T_t\ w_t \lambda_t \quad (28)$$

where ΔT_t is the gas temperature drop through the turbine, c_{pg} is the mean specific heat of the gas over the turbine operating temperature range, w_t is the gas weight flow rate, and

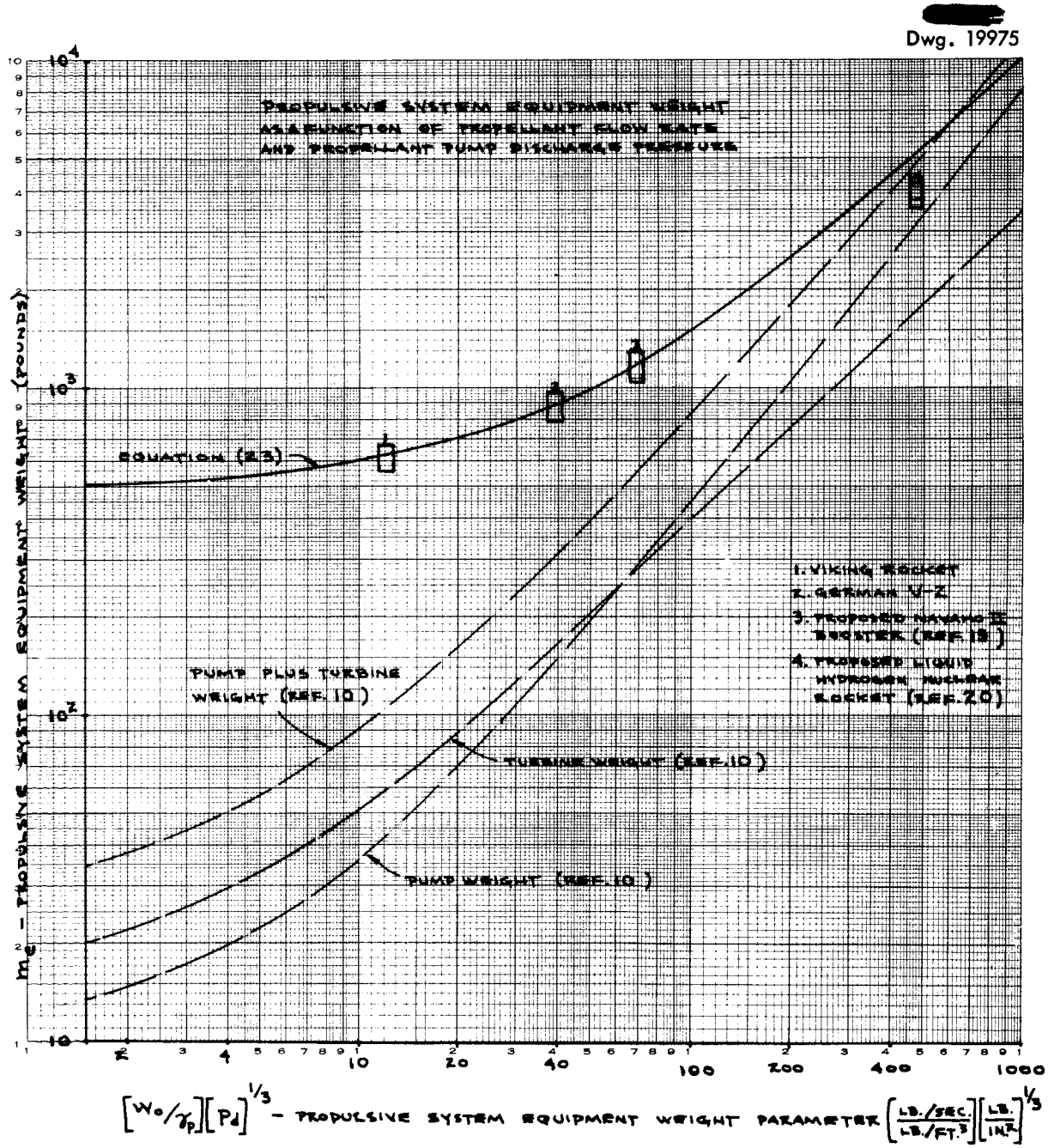
Dwg. 19975
PROPULSIVE SYSTEM EQUIPMENT WEIGHT AS A FUNCTION OF PROPELLANT FLOW RATE AND PROPELLANT PUMP DISCHARGE PRESSURE
EQUATION (E3)
PUMP PLUS TURBINE WEIGHT (REF. 10)
TURBINE WEIGHT (REF. 10)
PUMP WEIGHT (REF. 10)
1. VIKING ROCKET
2. GERMAN V-2
3. PROPOSED NAVAHO BOOSTER (REF. 18)
4. PROPOSED LIQUID HYDROGEN NUCLEAR ROCKET (REF. 20)
me - PROPULSIVE SYSTEM EQUIPMENT WEIGHT (POUNDS)
$[W_o/\gamma_p][P_d]^{1/3}$ - PROPULSIVE SYSTEM EQUIPMENT WEIGHT PARAMETER $\left[\frac{LB./SEC.}{LB./FT.^3}\right]\left[\frac{LB.}{IN.^2}\right]^{1/3}$

FIG. 5

λ_t is the over-all power conversion efficiency of the turbine.

By combining Eqs. 27 and 28, the ratio of the turbine gas weight flow rate to the propellant pump weight flow rate is determined to be

$$\frac{w_t}{w_p} = \frac{0.185}{\lambda_p \lambda_t} \frac{P_d}{\Delta T_t \, \gamma_p c_{pg}} . \tag{29}$$

By assuming the over-all turbine-pump efficiency, $\lambda_p \lambda_t$, to be 0.60, the pump discharge pressure to be 1900 psi (as previously), and the turbine gas temperature drop to be 1200°F, Eq. 29 is reduced to

$$\frac{w_t}{w_p} = \frac{0.462}{\gamma_p c_{pg}} . \tag{30}$$

This will be a maximum for hydrogen, which has the lowest value of $\gamma_p c_{pg}$ of any of the propellants considered. For hydrogen, γ_p = 4.4 lb/ft^3, and c_{pg} = 3.4 Btu/lb·°F for the temperature range 400 to 1600°F. Thus,

$$\left.\frac{w_t}{w_p}\right|_{H_2} = 0.0309 . \tag{31}$$

The average per cent propellant lost to pumping power requirements for all propellants considered will be taken as 2½% of the total propellant weight. The propellant required in the nuclear rocket motor as a fast neutron and gamma radiation shield (see Part II) has been neglected in the calculations, although it could be used to provide additional total impulse to the vehicle.

Thus, the effective propellant weight useful for vehicle propulsion is that contained initially in the tank volume (m_p) less that lost to nozzle cooling (0.025 m_p), pumping power (0.025 m_p), and evaporation loss ($\alpha_e m_p$). The parameters α and β in the vehicle mass ratio equation (Eq. 2) are determined from the figures given above as α = 0.05 + α_e (fraction lost), and β = 1 − α = 0.95 − α_e (useful propellants). Assuming the axial exhaust velocity v_L of the noneffective gases to be zero, the mass ratio equation becomes

$$\frac{m_0}{m_b} = e^{v_b/(0.95-\alpha_e)v_e} \tag{32}$$

or

$$\frac{m_0}{m_p} = \frac{e^{v_b/(0.95-\alpha_e)v_e}}{e^{v_b/(0.95-\alpha_e)v_e} - 1} = \Phi(v_b) .$$

The propellants considered herein are listed in Table 2 together with some of their physical properties. All the propellants were chosen primarily because of their high hydrogen content, which yields a low molecular weight

TABLE 2. PHYSICAL PROPERTIES OF LIQUID PROPELLANTS

PROPELLANT	CHEMICAL FORMULA	FREEZING POINT AT 1 ATM PRESSURE (°F)	BOILING POINT AT 1 ATM PRESSURE (°F)	LIQUID SPECIFIC GRAVITY AT GIVEN TEMPERATURE
Hydrogen	H_2	-434.5	-423	0.071 at -425°F
Methane	CH_4	-300	-259	0.42 at -265°F
Ammonia	NH_3	-108	-28	0.70 at -60°F
Hydrazine	N_2H_4	34.5	236	1.04 at 40°F
Water	H_2O	32	212	1.00 at 40°F
Hydrogen and ammonia	$2H_2 + NH_3$	see hydrogen and ammonia		0.25 for H_2 at -425°F, NH_3 at -60°F

product when the material is in the decomposed gaseous form. The bipropellant system of hydrogen and ammonia is carried throughout this report to serve as an indication of the possibilities of obtaining higher performance at lower cost than is possible with any one of the five basic propellants.

Liquid helium is worth mention as a possible nuclear rocket propellant only because of its chemical inertness which would eliminate the possibility of chemical reaction with the graphite reactor structure at 4500°F. However, the boiling point of helium is -452°F, hence it is difficult and costly to liquefy. The heat of vaporization of liquid helium at 1 atm pressure is only 10.8 Btu/lb, therefore it would be of little value as a coolant. The specific gravity of the liquid at the boiling point is only 0.122. This, coupled with the low boiling point, makes the storage problem quite severe, and heavy insulated double-walled propellant tanks would be absolutely necessary. Liquid helium was given no further consideration in the study covered by this report.

PROPELLANT PERFORMANCE

As can be seen from Eq. 32, the over-all vehicle performance is primarily a function of the exhaust velocities attainable with the propellants considered. The propellant is to be vaporized within the reactor, heated to the desired temperature, and expanded adiabatically, through a converging-diverging nozzle, to exhaust with velocity v_e. The exhaust velocity is a function of the nozzle geometry and the thermodynamic properties of the propellant gases at the chamber and nozzle exit conditions.

High exhaust velocities are obtained by high pressure-expansion ratios, but the maximum pressure ratio is limited by the allowable maximum ratio of nozzle exit area to nozzle throat area. The nozzle exit area is limited for aerodynamic reasons by the vehicle diameter, while the nozzle throat area is primarily a function of the desired thrust of the rocket motor. Calculations indicate that a maximum feasible nozzle area ratio is of the order of 35:1 under these restrictions, and this value has been used for calculations of propellant performance.

The specified area ratio determines the maximum attainable pressure ratio for each propellant gas, and thus determines the ratio of actual exhaust velocity to maximum theoretical exhaust velocity for adiabatic expansion to zero pressure. The pressure ratio is related to the area ratio by

$$\frac{A_t}{A_e} = \left(\frac{k+1}{2}\right)^{1/(k-1)} \left(\frac{p_e}{p_c}\right)^{1/k} \sqrt{\frac{k+1}{k-1}\left[1 - \left(\frac{p_e}{p_c}\right)^{(k-1)/k}\right]} \tag{33}$$

while the velocity ratio is related to the pressure ratio by

$$\frac{v_e}{v_m} = \lambda_n \sqrt{1 - \left(\frac{p_e}{p_c}\right)^{(k-1)/k}} \tag{34}$$

where

$$v_m = \sqrt{\frac{2\, g_c k}{k-1} \frac{R_u}{mw} T_c} \tag{35}$$

and λ_n is the nozzle efficiency.

The ratio of propellant gas exit temperature to chamber temperature is given by

$$\frac{T_e}{T_c} = \left(\frac{p_e}{p_c}\right)^{(k-1)/k} . \tag{36}$$

The value of k to be used in the above equations is the mean of the ratios of specific heats at the chamber temperature and at the gas exit temperature, hence this relation is required in order to determine the exhaust gas temperature.

By combining Eqs. 33 and 34, the following relation between nozzle area

ratio and exhaust velocity ratio is obtained:

$$(37) \qquad \frac{A_t}{A_e} = \left(\frac{k+1}{2}\right)^{1/(k-1)} \left[1 - \left(\frac{v_e}{\lambda_n v_m}\right)^2\right]^{1/(k-1)} \left(\frac{v_e}{\lambda_n v_m}\right) \sqrt{\frac{k+1}{k-1}} .$$

By combining Eqs. 33 and 36,

$$(38) \qquad \frac{A_t}{A_e} = \left[\left(\frac{k+1}{2}\right)\left(\frac{T_e}{T_c}\right)\right]^{1/(k-1)} \sqrt{\frac{k+1}{k-1}\left(1 - \frac{T_e}{T_c}\right)} .$$

Before the velocity ratios can be determined for each propellant, it is necessary to determine the propellant gas compositions at the chamber conditions, and to evaluate the thermodynamic properties of the gas mixtures at the specified chamber temperature and at exit temperatures determined from Eq. 38 by use of assumed values of the specific heat ratio.

Throughout the expansion process, the gas composition is considered as being "frozen" at the equilibrium composition existing in the rocket motor at maximum gas temperature, thus the molecular weight of the propellant gas will be that of the equilibrium mixture in the chamber. The maximum propellant gas temperature was chosen as 4500°F on the basis of the strength characteristics of graphite, the desired reactor structural material. The chamber pressure was specified to be 1500 psi primarily for reasons of fluid flow and heat transfer within the reactor.

The equilibrium gas compositions at chamber conditions, the pertinent thermodynamic properties of the gases at chamber and exit conditions, and average values of these properties between chamber and exit conditions are given in Table 3 for each propellant. The calculations necessary for the determination of this information were based upon equilibrium constants and gas property data obtained from refs. 13, 14, 15, 16, 17, and 18.

The theoretical maximum exhaust velocities and the ratio of actual to theoretical exhaust velocities were calculated from Eqs. 35 and 37; the average values of molecular weight and specific heat ratio given in Table 3 were used. Table 4 lists the maximum theoretical exhaust velocities, the ratio of actual to theoretical exhaust velocities, and the actual obtainable exhaust velocity, which is determined by use of Eqs. 35 and 37 and an arbitrarily defined nozzle efficiency, λ_n, of 0.985.

The decomposition of methane at high temperatures may result in the precipitation of solid carbon on the heat transfer surfaces of the reactor at the temperature and pressure conditions assumed for the rocket motor chamber. The precipitation of carbon would probably preclude the use of methane as a rocket propellant; however, calculations for methane are included because it is felt that the possible decomposition should be verified by experiment before this promising propellant is discarded.

DETERMINATION OF VEHICLE PERFORMANCE

The equations relating component weights to propellant weight or total loaded vehicle weight may now be combined with the vehicle mass ratio equation to obtain an expression relating the vehicle burnout velocity to the component weights.

TABLE 3. THERMODYNAMIC PROPERTIES AND COMPOSITION OF PROPELLANT GASES

PROPELLANT	GAS IN CHAMBER AND NOZZLE EXIT		SPECIFIC HEAT RATIO AT CHAMBER CONDITIONS, k_c	GAS EXIT TEMPERATURE, T_e (°F)	SPECIFIC HEAT RATIO AT EXIT CONDITIONS, k_e	AVERAGE SPECIFIC HEAT RATIO BETWEEN CHAMBER AND EXIT, k_a
	Composition (mole fraction)	Average Molecular Weight				
Hydrogen	0.9963 H_2 0.0073 H	1.993	1.298	450	1.400	1.349
Methane	0.449 C_2H_2 0.030 CH_4 1.485 H_2 0.011 H 0.073 C	7.813	1.267	620	1.354	1.311
Ammonia	0.5 N_2 0.011 H 1.494 H_2	8.48	1.297	450	1.398	1.348
Hydrazine	1.00 N_2 1.993 H_2 0.014 H	10.64	1.296	450	1.397	1.347
Water	0.9907 H_2O 0.0070 H_2 0.0047 OH 0.0023 O_2	17.92	1.187	1180	1.258	1.223
Hydrogen and ammonia	0.026 H 3.487 H_2 0.5 N_2	5.23	1.298	450	1.399	1.349

From Eqs. 10, 11, 21 or 23, and 26 combined with Eq. 4, the total loaded vehicle weight is:

(39) for $m_0 > m_{0(crit)}$,

$$m_0 = (m_L + 5070) + m_p\left(1 + \frac{0.007305}{\gamma_p'}\right) + m_0\left[0.01 + \frac{201}{\gamma_p' v_e} + 1.729\,\frac{\left(\frac{v_m}{10^3}\right)^2}{v_e}\right] ;$$

and for $m_0 < m_{0(crit)}$,

$$m_0 = (m_L + 6290) + m_p\left(1 + \frac{0.007305}{\gamma_p'}\right) + m_0\left(0.01 + \frac{201}{\gamma_p' v_e}\right) .$$

By combining Eqs. 39 with Eq. 32:

(40) for $m_0 > m_{0(crit)}$,

$$\frac{m_0}{m_p} = \Phi(v_b) = \frac{\left(1 + \frac{0.007305}{\gamma_p'}\right) + \left(\frac{m_L + 5070}{m_p}\right)}{\left[0.990 - \frac{201}{\gamma_p' v_e} - 1.729\,\frac{\left(\frac{v_m}{10^3}\right)^2}{v_e}\right]} ;$$

and for $m_0 < m_{0(crit)}$,

$$\frac{m_0}{m_p} = \Phi(v_b) = \frac{\left(1 + \frac{0.007305}{\gamma_p'}\right) + \left(\frac{m_L + 6290}{m_p}\right)}{\left(0.990 - \frac{201}{\gamma_p' v_e}\right)} .$$

These can be represented by:

(41) for $m_0 > m_{0(crit)}$,

$$\frac{m_0}{m_p} = \Phi(v_b) = \frac{A_p + \left(\frac{m_L + 5070}{m_p}\right)}{B_p - C_p} ;$$

and for $m_0 < m_{0(crit)}$,

$$\frac{m_0}{m_p} = \Phi(v_b) = \frac{A_p + \left(\frac{m_L + 6290}{m_p}\right)}{B_p}$$

where the terms A_p, B_p, and C_p are functions of the propellant properties alone, for given system operating conditions, and are listed in Table 5.

Since the performance parameter of interest is the ratio of total loaded weight to dead load capacity, m_0/m_L, Eqs. 41 were solved for m_0/m_L as:

(42) for $m_0 > m_{0(crit)}$,

$$\frac{m_0}{m_L} = \left[\frac{\Phi}{(B_p - C_p)\,\Phi - A_p}\right]\left[\frac{m_L + 5070}{m_L}\right] ;$$

and for $m_0 < m_{0(crit)}$,

$$\frac{m_0}{m_L} = \left[\frac{\Phi}{B_p\Phi - A_p}\right]\left[\frac{m_L + 6290}{m_L}\right] .$$

The results of computations made by using Eqs. 42 to determine vehicle performance are shown graphically in Figs. 6*a* through 6*f* which portray m_0/m_L vs. v_b for each of the six propellants and for several different values of dead load weight. Values of v_b were determined from postulated values of Φ used in the solution of Eqs. 42.

It will be noted from the figures that m_0/m_L approaches infinity at a certain limiting vehicle burnout velocity for each propellant. It is evident from Eqs. 41 that the maximum

TABLE 4. PROPELLANT GAS EXHAUST VELOCITIES

PROPELLANT	MAXIMUM THEORETICAL EXHAUST VELOCITY, v_m (ft/sec)	RATIO OF ACTUAL TO THEORETICAL EXHAUST VELOCITY, v_e/v_m	ACTUAL ATTAINABLE EXHAUST VELOCITY AT 98.5% NOZZLE EFFICIENCY, v_e (ft/sec)
Hydrogen	31,010	0.892	27,650
Methane	16,360	0.872	14,260
Ammonia	15,050	0.892	13,420
Hydrazine	13,450	0.892	11,990
Water	12,320	0.807	9,940
Hydrogen and ammonia	19,150	0.892	17,070

TABLE 5. PROPELLANT CONSTANTS

PROPELLANT	A_p	B_p	C_p	$B_p - C_p$
Hydrogen	1.10289	0.88762	0.06013	0.82749
Methane	1.01739	0.95644	0.03245	0.92399
Ammonia	1.01044	0.96860	0.02919	0.93941
Hydrazine	1.00702	0.97388	0.02609	0.94779
Water	1.00731	0.96978	0.02640	0.94338
Hydrogen and ammonia	1.02922	0.94290	0.03714	0.90576

limiting vehicle velocity is obtained for an infinite propellant weight if the dead load weight is finite. Obviously, for an infinite propellant weight the total loaded vehicle weight will be greater than the critical weight, thus the limiting velocity is determined by the first of Eqs. 41 as

$$\Phi(v_{b(max)}) = \frac{A_p}{B_p - C_p} . \tag{43}$$

Furthermore, it will be noted that the m_0/m_L vs. v_b curves are asymptotic to the curve labeled $m_L = \infty$ in Figs. 6*a* through 6*f*. This limiting performance curve occurs as the dead load weight becomes infinite, and is obtained from the first of Eqs. 42 as

$$\frac{m_0}{m_L} = \frac{\Phi}{(B_p - C_p)\,\Phi - A_p} . \tag{44}$$

COMPARATIVE CHEMICAL ROCKET PERFORMANCE

Calculations were made for an optimum performance, liquid-hydrogen - liquid-oxygen, single-stage, chemical rocket vehicle to provide a comparison with the nuclear vehicle performance curves. The equations used for the weight of propulsive system equipment, fins, propellant, dead load, and propellant tank and tank structure were the same as those used for the nuclear vehicle. The equation for the weight of the chemical rocket motor was based roughly on the results of a rocket vehicle component weight study performed by the Rand Corporation [10] and is

$$m_r = 0.03\, m_0 \tag{45}$$

for an initial vehicle acceleration of 3 g_c, as for the nuclear vehicle. The chosen operating conditions of the hydrogen-oxygen rocket motor were

$$4H_2 + O_2 \longrightarrow 2H_2O + 2H_2$$

Oxidizer-to-fuel weight ratio = 4.0

p_c = 1500 psi

T_c = 5430°R

A_e/A_t = 35

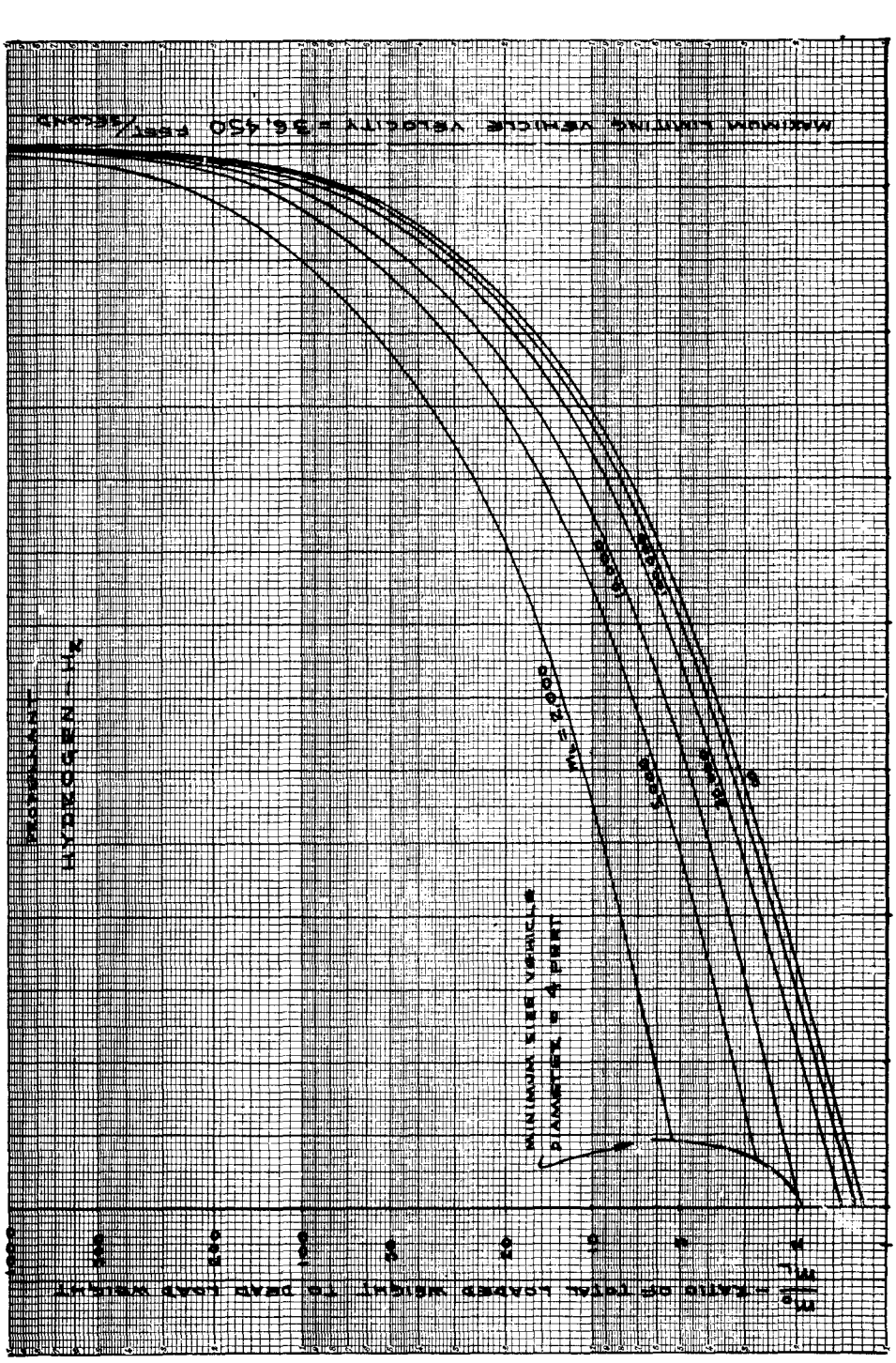
NUCLEAR ROCKET PERFORMANCE
Dwg. 19976
PROPELLANT
HYDROGEN - H2
MAXIMUM LIMITING VEHICLE VELOCITY = 36,450 FEET/SECOND
MINIMUM SIZE VEHICLE
DIAMETER = 4 FEET
Isp = 2000
2500
3000
3500
4000
4500
5000
$\frac{m_0}{m_L}$ = RATIO OF TOTAL LOADED WEIGHT TO DEAD LOAD WEIGHT
V_b - VEHICLE BURNOUT VELOCITY (FEET/SECOND)
0
5,000
10,000
15,000
20,000
25,000
30,000
35,000
40,000

FIG. 6a

[redacted] Dwg. 19977

NUCLEAR ROCKET PERFORMANCE

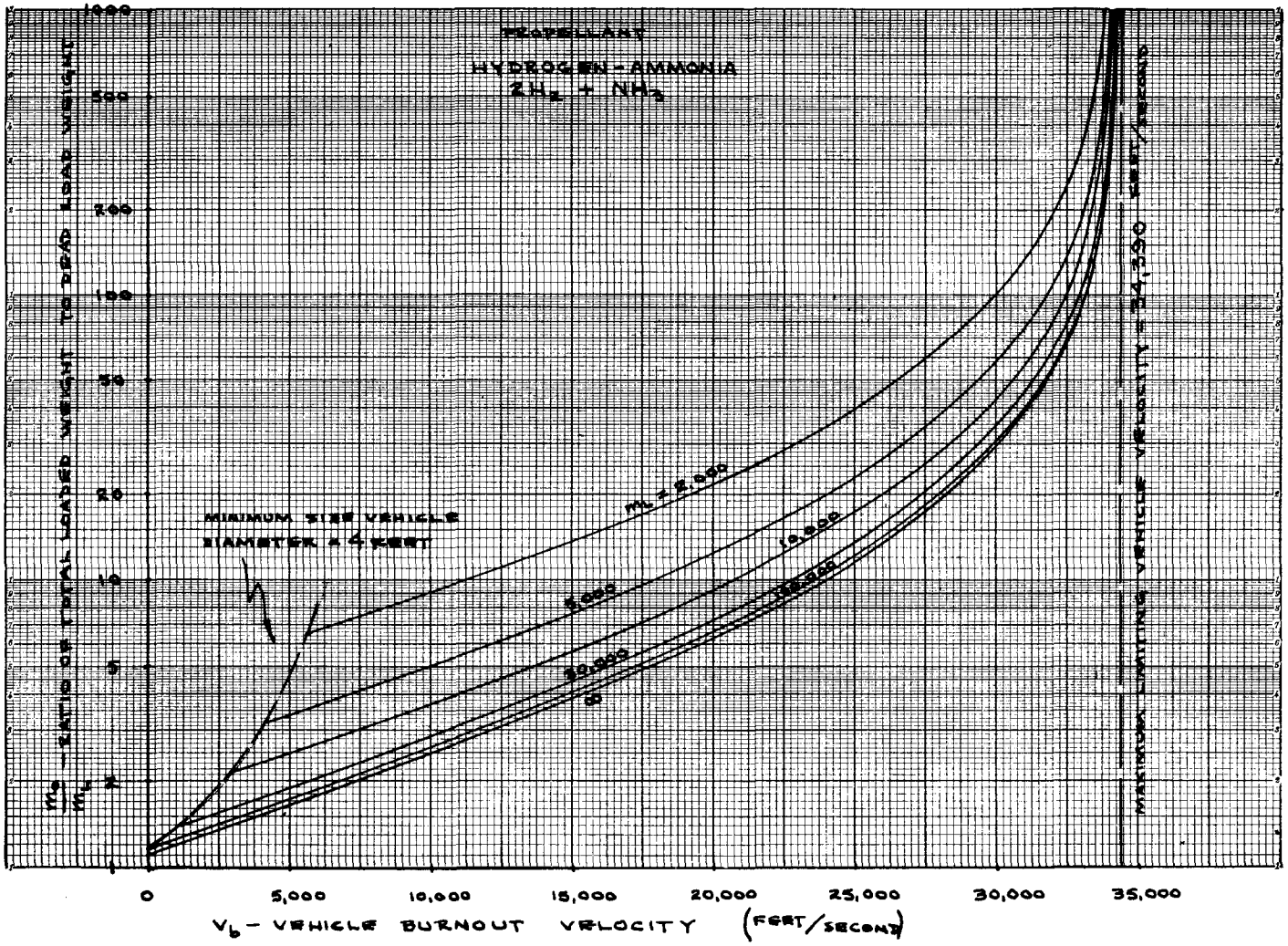

FIG. 6b

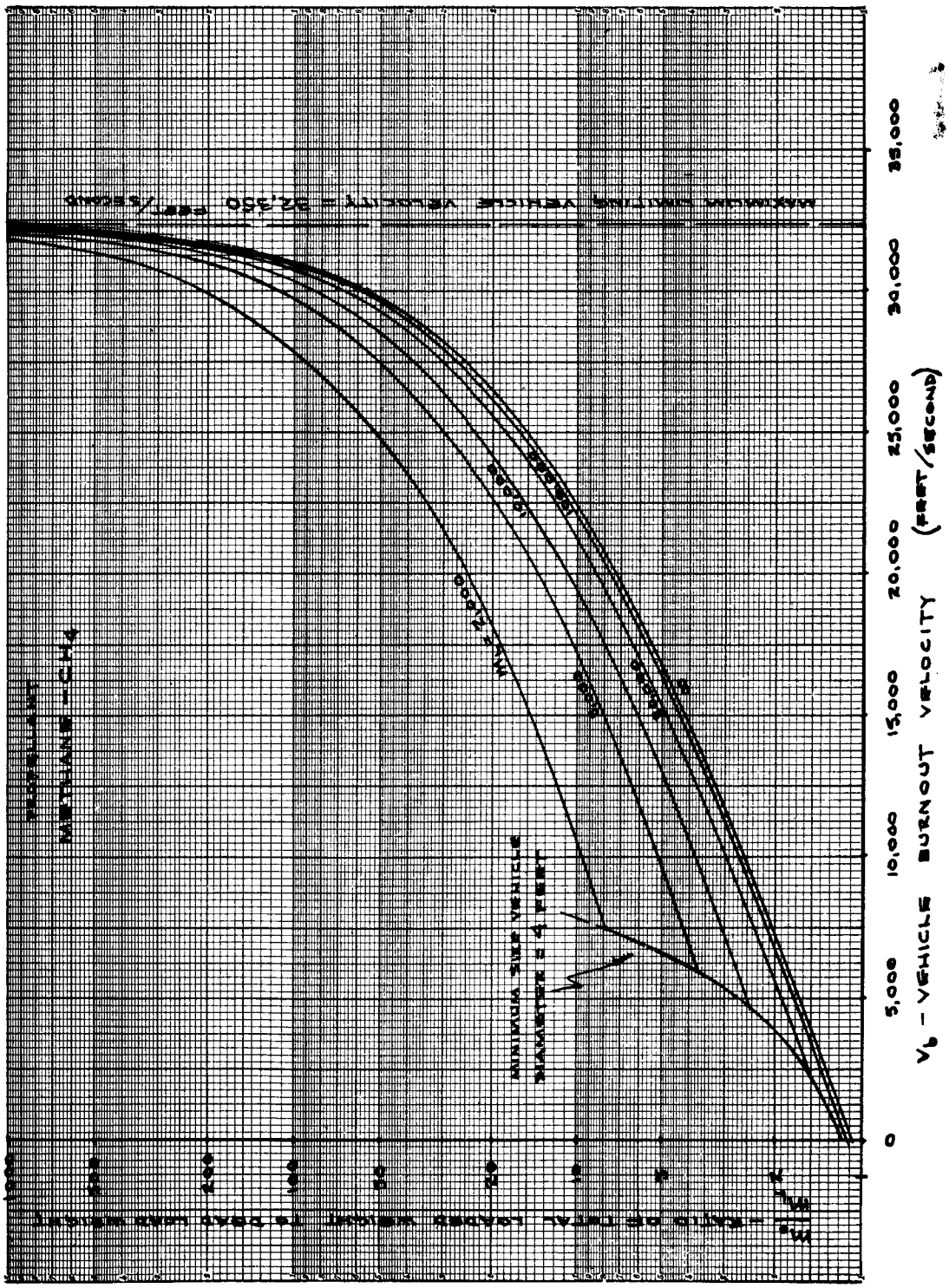
Dwg. 19978
NUCLEAR ROCKET PERFORMANCE
PROPELLANT
METHANE - CH4
MAXIMUM ALLOWABLE VEHICLE VELOCITY = 32,350 FEET/SECOND
MINIMUM SIZE VEHICLE
DIAMETER = 4 FEET
0
5,000
10,000
15,000
20,000
25,000
30,000
35,000
V_b - VEHICLE BURNOUT VELOCITY (FEET/SECOND)

FIG. 6c

[redacted] Dwg. 19979

NUCLEAR ROCKET PERFORMANCE

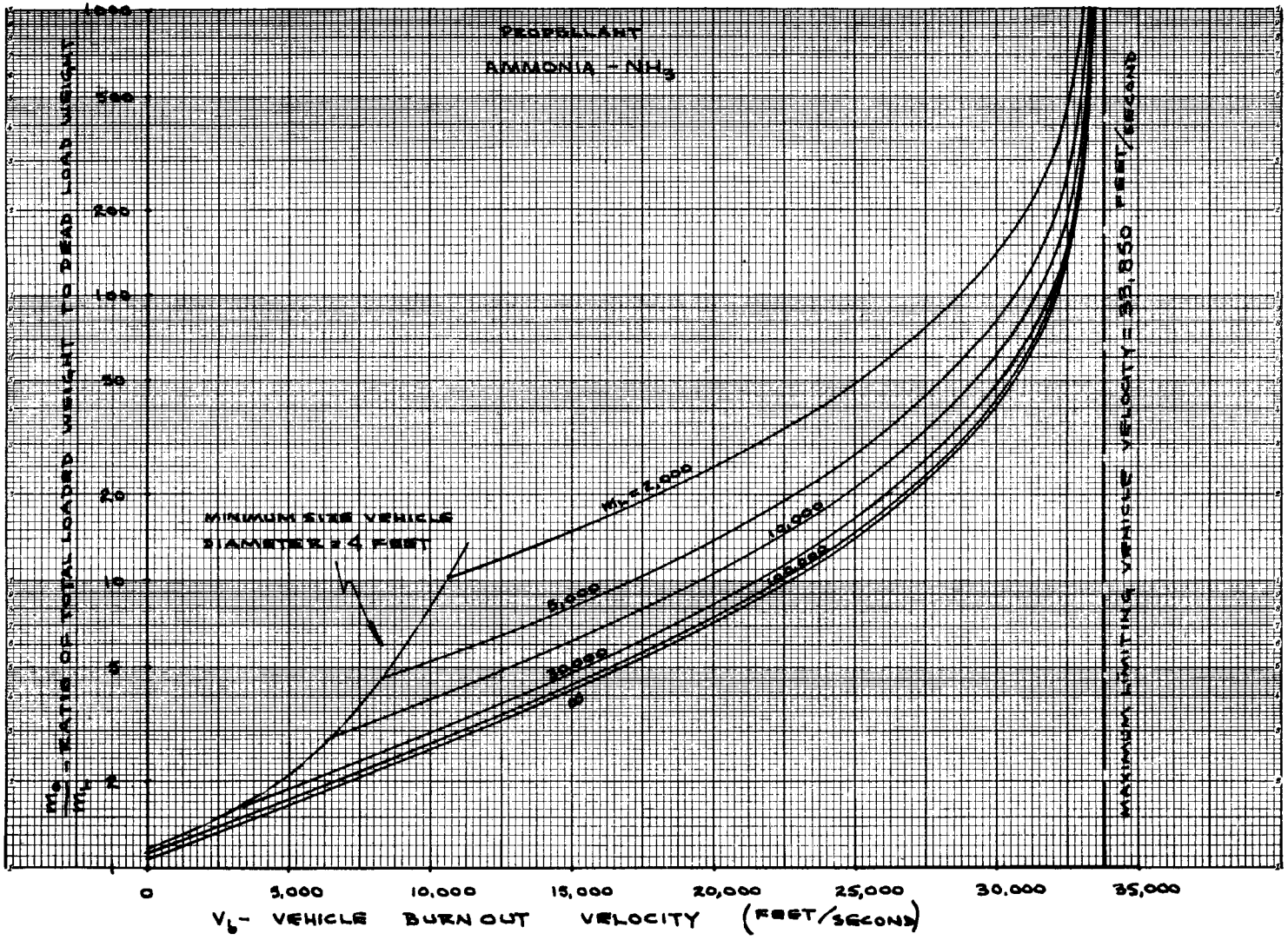

FIG. 6d

[redacted]

Dwg. 19980

NUCLEAR ROCKET PERFORMANCE

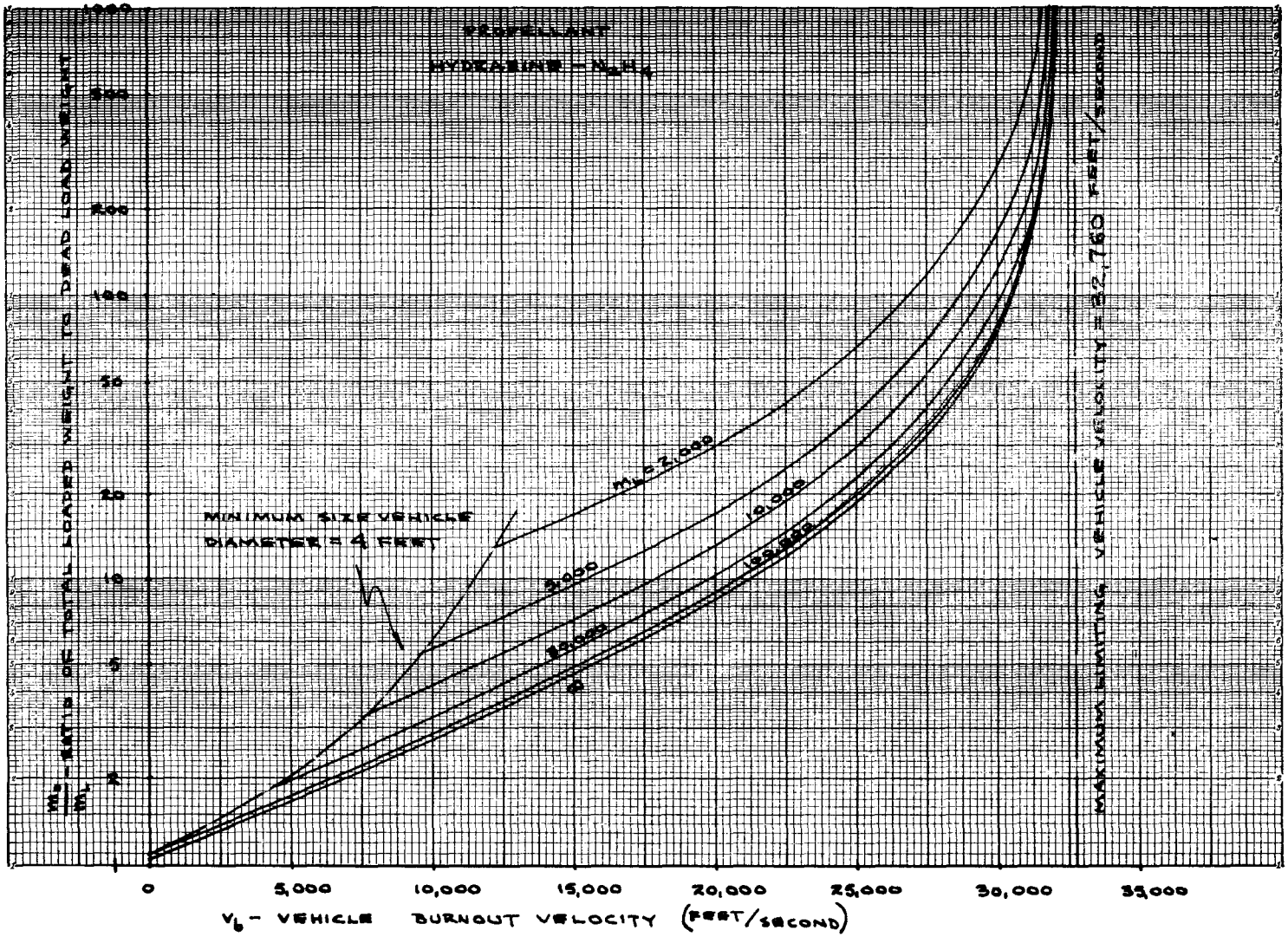

FIG. 6e

[redacted]

NUCLEAR ROCKET PERFORMANCE

[redacted] Dwg. 19981

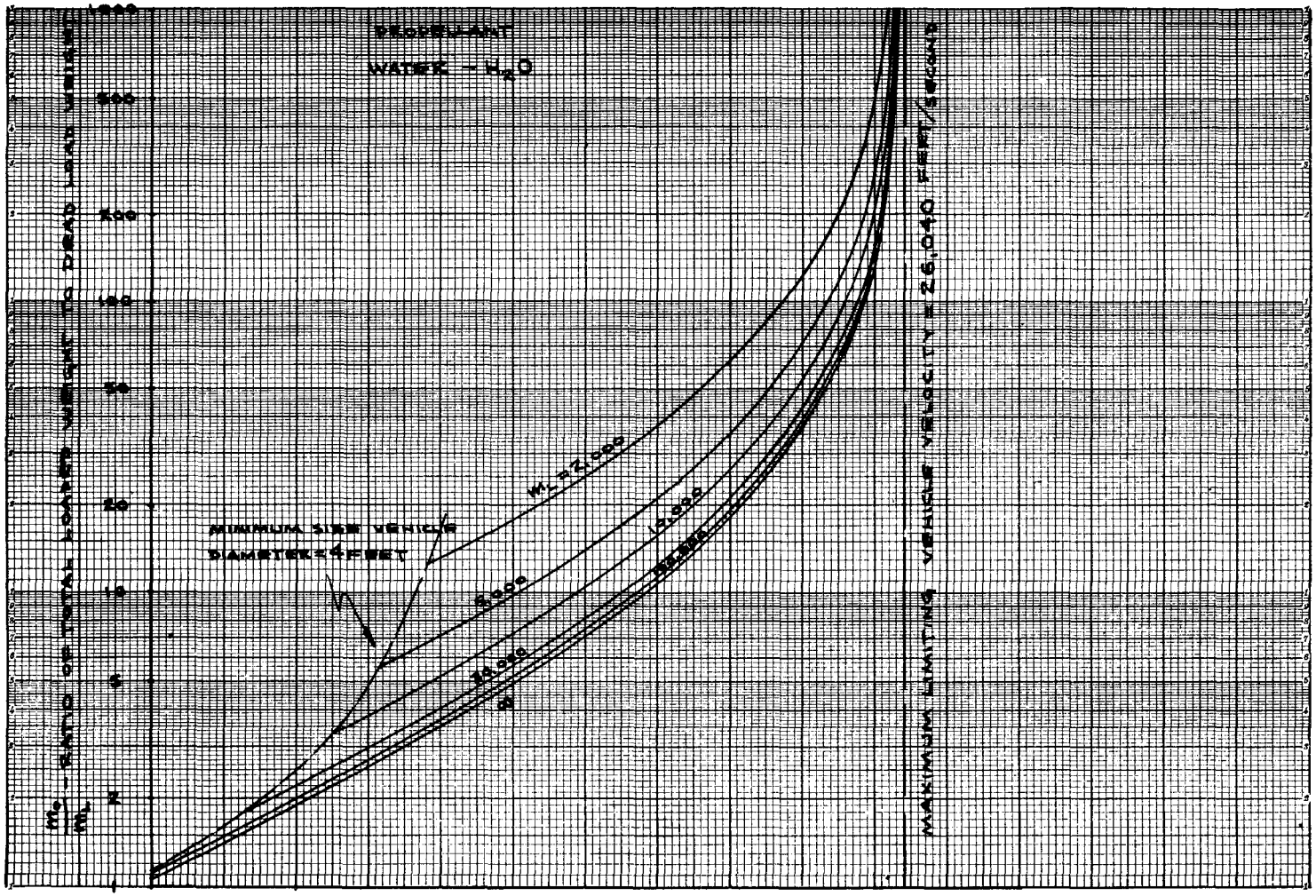

FIG. 6f

For these conditions, the average specific heat ratio of the propellant gases, between the chamber and exit, was found to be 1.267, and the average molecular weight was taken as 10.0. The propellant exhaust velocity was then determined to be 13,390 ft/sec.

The type of analysis indicated in Eqs. 39 through 44 was performed with the result that the chemical rocket performance equation is

$$(46) \qquad \frac{m_0}{m_L} = \left(\frac{\Phi}{B_p\Phi - A_p}\right)\left(\frac{m_L + 500}{m_L}\right)$$

and the limiting performance curve, for m_L approaching infinity, is obviously given by

$$(47) \qquad \frac{m_0}{m_L} = \frac{\Phi}{B_p\Phi - A_p} .$$

The maximum limiting velocity was found from

$$(48) \qquad \Phi(v_{b(max)}) = \frac{A_p}{B_p} .$$

For the hydrogen-oxygen vehicle, the terms A_p and B_p are

$$A_p = 1 + \frac{0.007305}{\gamma'_p} = 1.02566$$

and

$$B_p = 0.960 - \frac{201}{\gamma'_p v_e} = 0.90727 .$$

The results of calculations made by using Eqs. 46, 47, and 48, are shown in Fig. 7, which shows m_0/m_L vs. v_b for several values of dead load weight. Figure 7 also shows performance curves, for two ranges of dead load weight, for several existing and proposed chemical rocket vehicles. It will be noted that the hydrogen-oxygen rocket discussed above is far superior in performance to any rocket vehicle yet built. In fact, it may be considered as an upper limit on single-stage chemical rocket performance, barring the use of such esoteric fuels and oxidizers as liquid monatomic hydrogen and liquid ozone.

A comparison of the liquid hydrogen nuclear-powered vehicle performance curves with those for the hydrogen-oxygen chemical rocket shows that the nuclear vehicle is superior for burnout velocities higher than 26,000 ft/sec for all dead load capacities. A closer comparison shows that the dividing line between superior chemical or nuclear rocket performance is a function of the vehicle dead load capacity and that the points of intersection of the curves of equal dead load in the two figures define the vehicle burnout velocities at which the nuclear and chemical rocket performances are equal for the given dead load. It is thus possible to obtain a curve showing the regions of superior performance of each type of vehicle as a function of dead load capacity and vehicle burnout velocity. Figure 8 shows such a curve for a comparison of the liquid-hydrogen nuclear-powered vehicle with the hydrogen-oxygen chemical rocket. It is at once obvious that the nuclear rocket is superior to the chemical rocket for operation with high dead loads or for the attainment of high burnout velocities.

REACTOR POWER REQUIREMENTS

Before the problems of the reactor design are considered, it is desirable to know the power required to accelerate a rocket to any desired burnout velocity, with a given dead load weight and propellant.

The total energy required to produce a given exhaust velocity with a given amount of propellant is

$$E = Jm_p c_{pg} (T_c - T_0) \text{ ft-lb} .$$

This can also be expressed by

$$E = \frac{m_p v_m^2}{2 g_c} \text{ ft-lb} .$$

The rate of energy production, or the power, will be dependent on the burning time chosen for the vehicle. The burning time, in turn, is dependent on the allowable vehicle accelerations, and hence on the ratio of propellant weight to total loaded vehicle weight,

CHEMICAL ROCKET PERFORMANCE

[redacted] Dwg. 19982

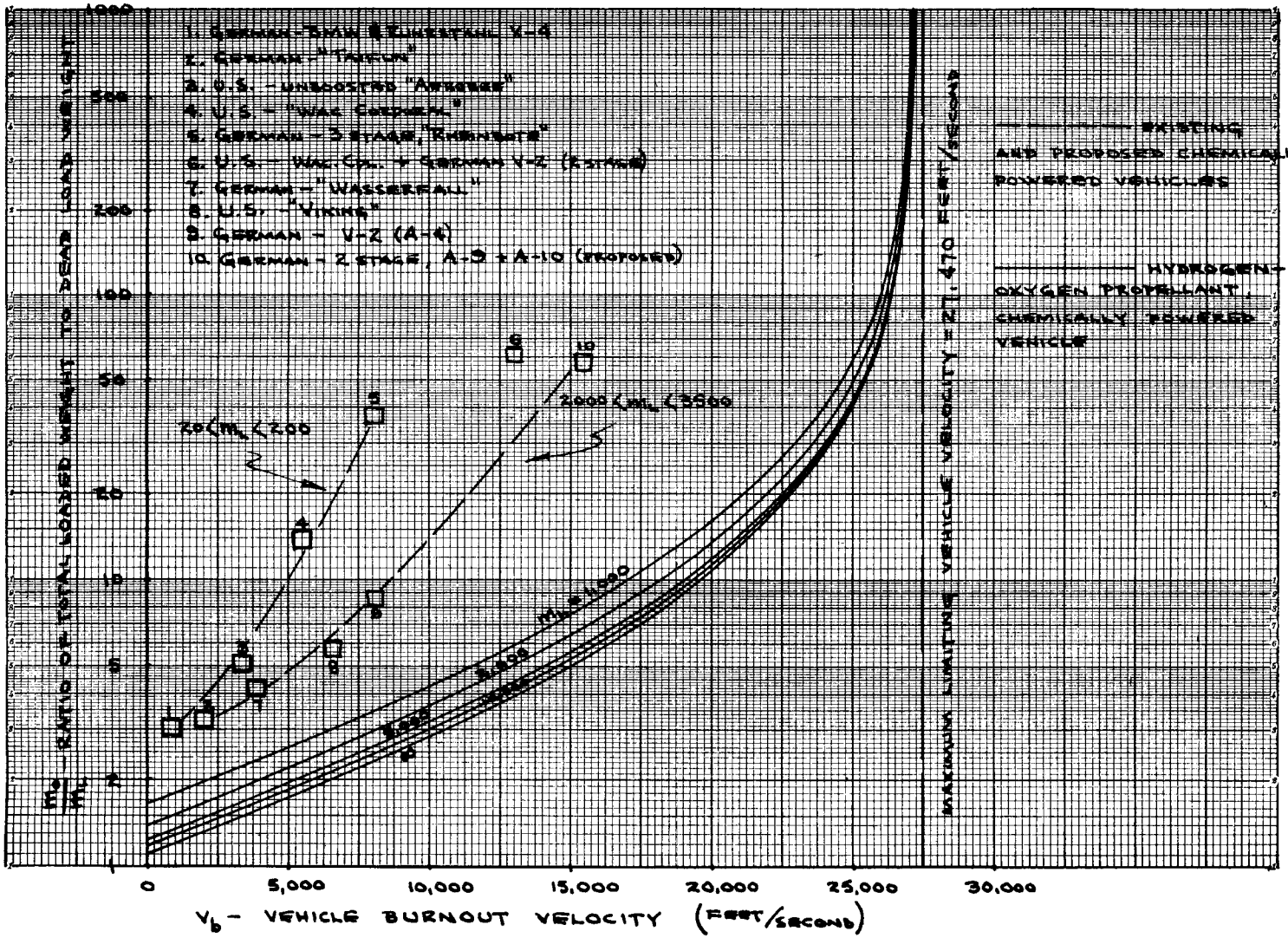

FIG. 7

Dwg. 19983

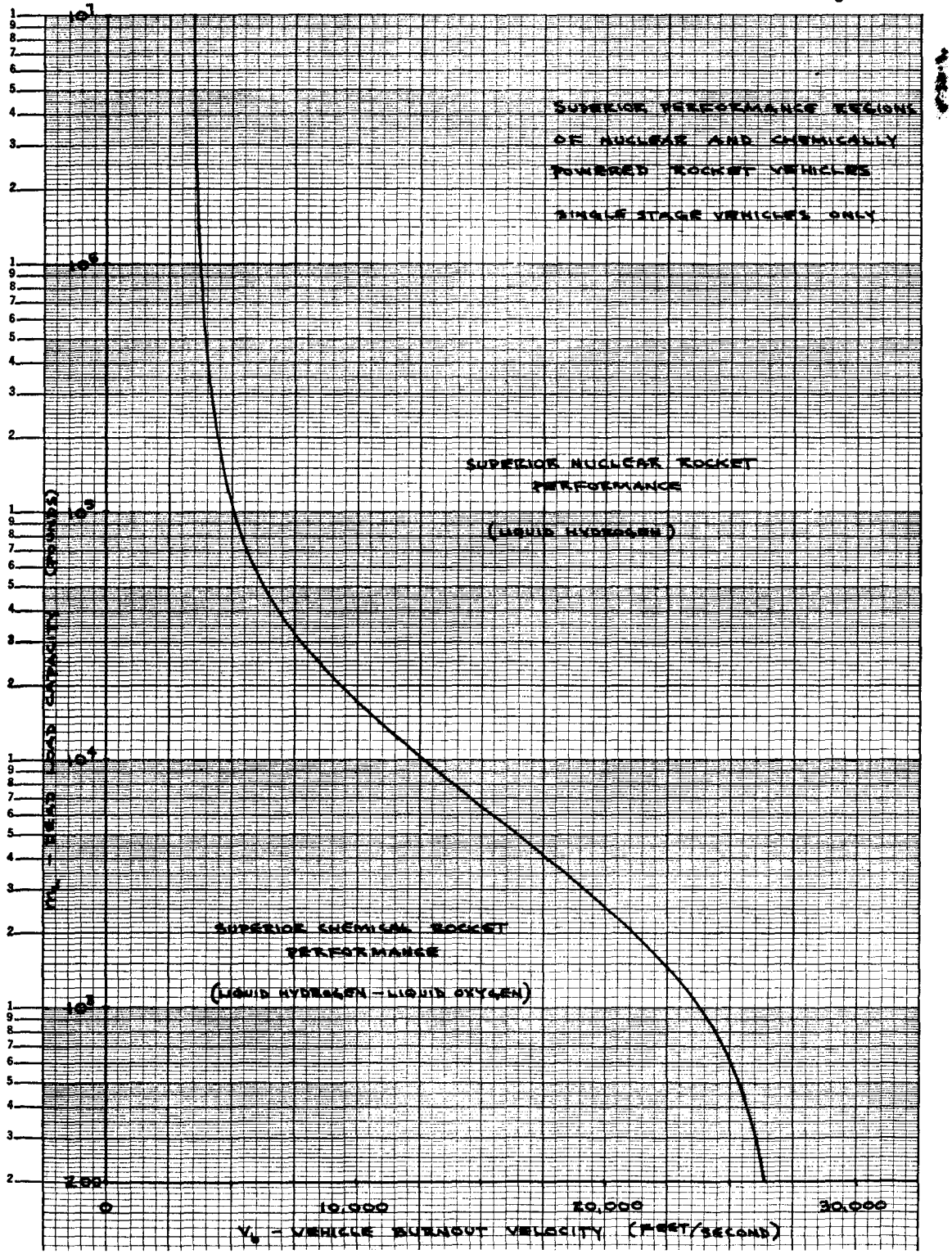

FIG. 8

m_p/m_0. In order to determine reactor power requirements, it is thus necessary to examine the relations between thrust, vehicle acceleration, and rocket burning time. For a rocket moving in a gravitational-field-free, airless space, the initial acceleration is given by

$$a_0 = \frac{F_0 g_c}{m_0} ,$$

where

$$F_0 = \frac{w_0 v_e}{g_c} ;$$

hence

$$a_0 = \frac{w_0 v_e}{m_0} . \tag{49}$$

However, for constant propellant flow rate (and constant thrust)

$$w_p = \frac{m_p}{t_b} .$$

Thus, the initial acceleration becomes

$$a_0 = \frac{v_e}{t_b}\left(\frac{1}{\frac{m_0}{m_p}}\right) . \tag{50}$$

Similarly, the final acceleration, just as the propellant is consumed, is

$$a_b = \frac{v_e}{t_b}\left(\frac{1}{\frac{m_0}{m_p} - 1}\right) . \tag{51}$$

Considerations of human capabilities and of acceleration loading of the vehicle structures indicate that the maximum allowable acceleration of the vehicle (at burnout) should be no greater than $9 g_c$. Also, in order to obtain reasonable performance, it seems desirable that the initial acceleration be no less than $3 g_c$. Thus the ratio a_b/a_0 must be equal to or less than 3 for all vehicles considered.

By combining Eqs. 50 and 51, the ratio a_b/a_0 becomes

$$\frac{a_b}{a_0} = \left(\frac{\frac{m_0}{m_p}}{\frac{m_0}{m_p} - 1}\right) , \tag{52}$$

and since $a_b/a_0 \leq 3$, then $m_0/m_p \geq 1.50$ or $m_p/m_0 \leq 2/3$. Therefore, for all vehicles of $m_0/m_p < 1.50$ (that is, propellant weight greater than 2/3 of total loaded weight), it is necessary to utilize a variable thrust system in order to keep the vehicle accelerations below the arbitrarily set limit of $3 a_0$.

Variable thrust may be accomplished by (1) changing propellants in flight, thus changing exhaust velocities, but keeping constant pump and reactor flow rates; (2) changing pump flow rates (speed control or throttle valving) and hence reactor operating pressure, thus altering the discharge rate of the propellant; (3) utilizing a variable nozzle throat diameter to control reactor chamber pressure, thus change exhaust velocity; and (4) utilizing several individually operated reactor motors, which may be "fired" in unison or in any desired combination so as to obtain a stepwise variation in thrust. Of these four schemes, (4) appears to be most attractive. The plan to change propellants in flight would incur many difficulties in the propulsion system design problem, because the reactor and pumps would then have to operate satisfactorily with two fluids of generally different viscosities, conductivities, heat capacities, liquid and gas densities, boiling points, etc. It is perhaps needless to point out that it is difficult enough to design a reactor to work satisfactorily with one fluid.

Thrust control by means of changes in pump flow rates would cause problems similar to those that would result from a change in propellants. The reactor would be required to operate properly at different system pressures.

In reactors of the type considered, it is quite difficult to change the flow rate and still operate the reactor at high power-to-weight ratios because the material stresses and heat transfer conditions are sensitive functions of pressure and flow rate.

The use of a variable nozzle throat area would be hampered by the same problems as the use of variable flow rates because the reactor system pressure would vary with changes in the nozzle throat area. Aside from this consideration, it is not at all certain that such a nozzle could be built and operated satisfactorily under the pressure, temperature, and flow conditions required for the desired vehicle performance.

The use of groups of separately controllable motors as a means of stepwise thrust control is quite satisfactory. All motors could operate at the proper reactor design point and the thrust could be varied by firing different numbers of motors at any one time. Certainly, if it is possible to build one successfully operating nuclear reactor rocket motor, a second could be built and coupled to the first to form a two-step controllable thrust unit. Although this method of thrust variation is not aesthetically attractive, it is the most straightforward and was adopted for the purposes of this study.

For N equal increments of thrust (or N equal thrust motors), the ratio of final to initial acceleration is related to the ratio of total loaded weight to propellant weight as follows:

$$F_0 = \frac{w_0 v_e}{g_c} \tag{53}$$

and

$$a_0 = \frac{F_0 g_c}{m_0} = v_e \frac{w_0}{m_0} \quad ;$$

$$F_b = \frac{F_0}{N} = \frac{w_0 v_e}{N g_c} \tag{54}$$

and

$$a_b = \frac{F_b g_c}{m_b} = v_e \frac{w_0}{N(m_0 - m_p)} \quad .$$

A combination of Eqs. 53 and 54 yields

$$\frac{a_b}{a_0} = \frac{m_0}{N(m_0 - m_p)} \tag{55}$$

or

$$\frac{a_b}{a_0} = \frac{\frac{m_0}{m_p}}{N\left(\frac{m_0}{m_p} - 1\right)} \quad ,$$

and since $a_b/a_0 \leq 3$ by definition, then, from Eq. 55 is obtained

$$\frac{m_0}{m_p} \geq \frac{3N}{3N - 1} \quad . \tag{56}$$

The allowable minimum values of m_0/m_p correspond to maximum values of v_b/v_e as shown by Eq. 32. Table 6 lists the permissible values of m_0/m_p and per cent propellant weight, $100(m_p/m_0)$, together with the maximum allowable values of v_b/v_e, for several values of N.

The maximum reactor power required is simply the maximum rate of energy expenditure; a rate which occurs at the time of takeoff for all rockets regardless of the number of incremental thrust units employed to reduce final accelerations.

The total maximum power is given by

$$P_{max} = P_0 = \frac{w_0}{2 g_c} v_m^2 \quad \text{ft-lb/sec} \quad . \tag{57}$$

However, from Eq. 49,

$$w_0 = \frac{a_0 m_0}{v_e} \quad ;$$

thus

$$P_0 = \frac{a_0 m_0}{2 g_c} \frac{v_m^2}{v_e} = \frac{a_0}{2 g_c} \frac{m_L \left(\frac{m_0}{m_L}\right) v_m^2}{v_e} \quad . \tag{58}$$

Since P_0 is the maximum power required by the vehicle, the power required of

TABLE 6. ALLOWABLE VEHICLE WEIGHT AND VELOCITY RATIOS FOR STEPWISE THRUST VARIATION

NUMBER OF EQUAL INCREMENTS OF THRUST,* N	MINIMUM ALLOWABLE RATIO OF m_0/m_p	PROPELLANT WEIGHT (%) $m_p/m_0 \times 100$	MAXIMUM ALLOWABLE RATIO OF v_b/v_e
1	1.5	66.7	1.0437
2	1.20	83.3	1.7022
3	1.125	88.9	2.0873
4	1.091	91.7	2.3607
5	1.071	93.4	2.5727
6	1.059	94.4	2.7459

*Number of equal thrust motors.

the individual reactors will be given by $P_r = P_0/N$ where N is the number of equal thrust motors, or equal power reactors, and is determined from Eq. 56 or Table 6.

The maximum required power, in megawatts, is given by Eq. 59 for $a_0 = 3g_c$.

$$(59) \quad P_0 = 2.034 \frac{m_L \left(\frac{m_0}{m_L}\right)}{v_e} \left(\frac{v_m}{10^3}\right)^2 .$$

The results of calculations that cover the vehicle performance range previously considered are shown in Figs. 9*a* through 9*f*, in which total rocket motor power, $P_0 = P_r N$, is plotted against vehicle burnout velocity, v_b, for several arbitrary dead load weights.

Although the total power requirements shown in Figs. 9*a* through 9*f* are extremely high, for the optimum operating range of nuclear powered vehicles, it should be pointed out that the total energy outputs required appear quite reasonable when compared with existing and proposed chemically powered, high-velocity vehicles. The operating time of the nuclear rocket motors required for propulsion of high-dead-load, high-velocity vehicles is of the order of 200 to 500 sec, thus the total energy outputs required will be approximately 500 to 5000 megawatt-hours. As a comparison, the total energy output of the B-52 aircraft for a 10-hr flight is approximately 600 megawatt-hours, while the energy output of proposed nuclear powered aircraft is of the order of 2500 megawatt-hours for a 10-hr flight.

SHIELDING CONSIDERATIONS

If it is desired to carry a crew in a nuclear-powered rocket vehicle, or if radiation-sensitive electronic equipment is required for flight guidance, some sort of radiation shielding will be necessary. The exact size, weight, and shape of such a shield will depend almost entirely on the desired use of the vehicle, therefore no attempt is made in this report to present a generalized shield design study. The total radiation flux incident on the crew compartment and electronic equipment in the vehicle nose during reactor operation is the sum of two components: (1) direct radiation, along the vehicle axis, from the reactor, and (2) radiation scattered from the atmosphere external to the vehicle. The relative importance of these two components will vary with time and position of the vehicle along its vertical flight path. Initially, at take-off, the propellant tanks would be full and would provide complete shadow shielding for the direct radiation from the reactor, but radiation resulting from air scattering would be at a maximum. At burnout the

[redacted] Dwg. 19984

NUCLEAR ROCKET – MAXIMUM POWER REQUIREMENTS

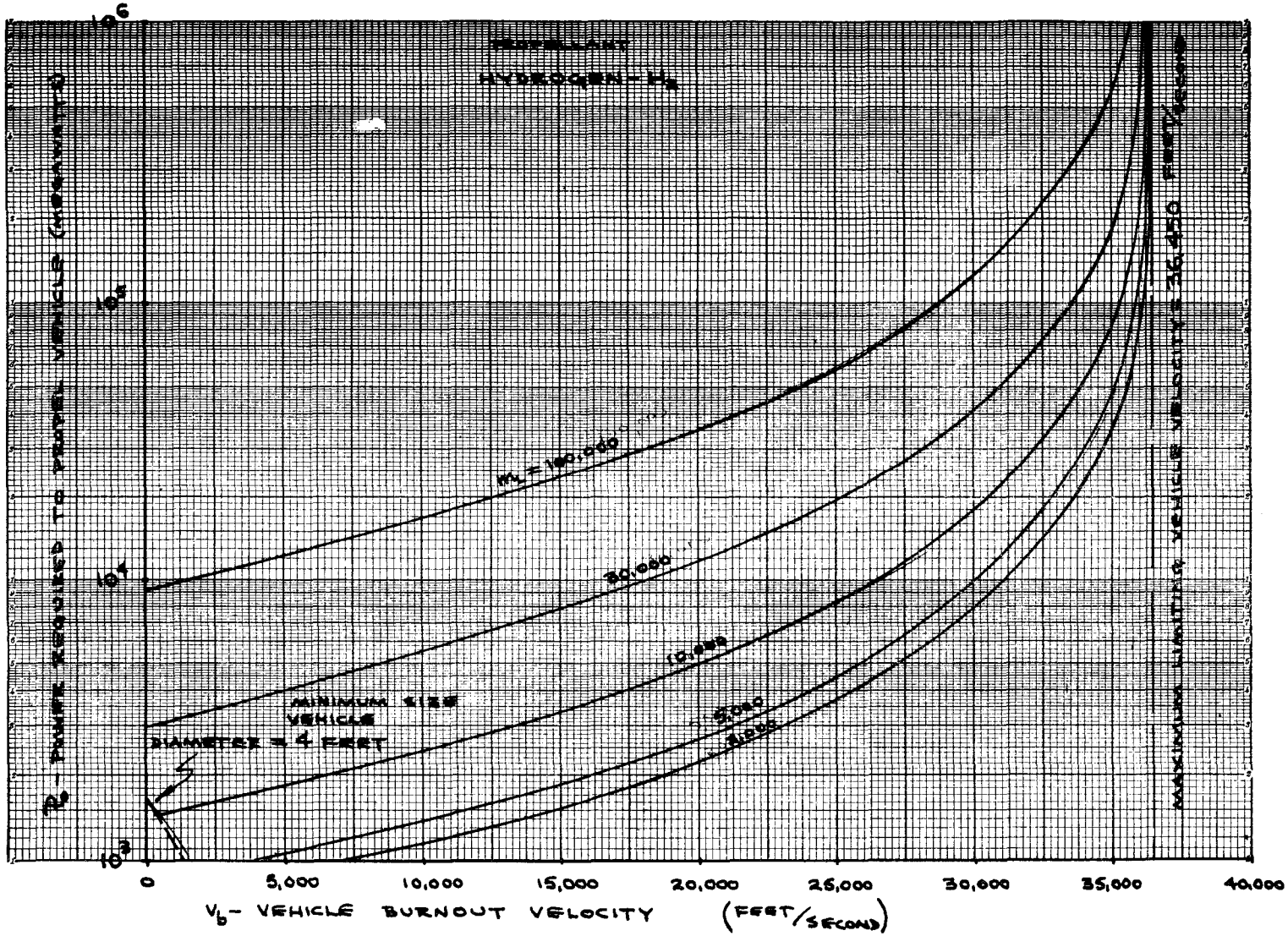

FIG. 9a

[redacted] Dwg. 19985

NUCLEAR ROCKET – MAXIMUM POWER REQUIREMENTS

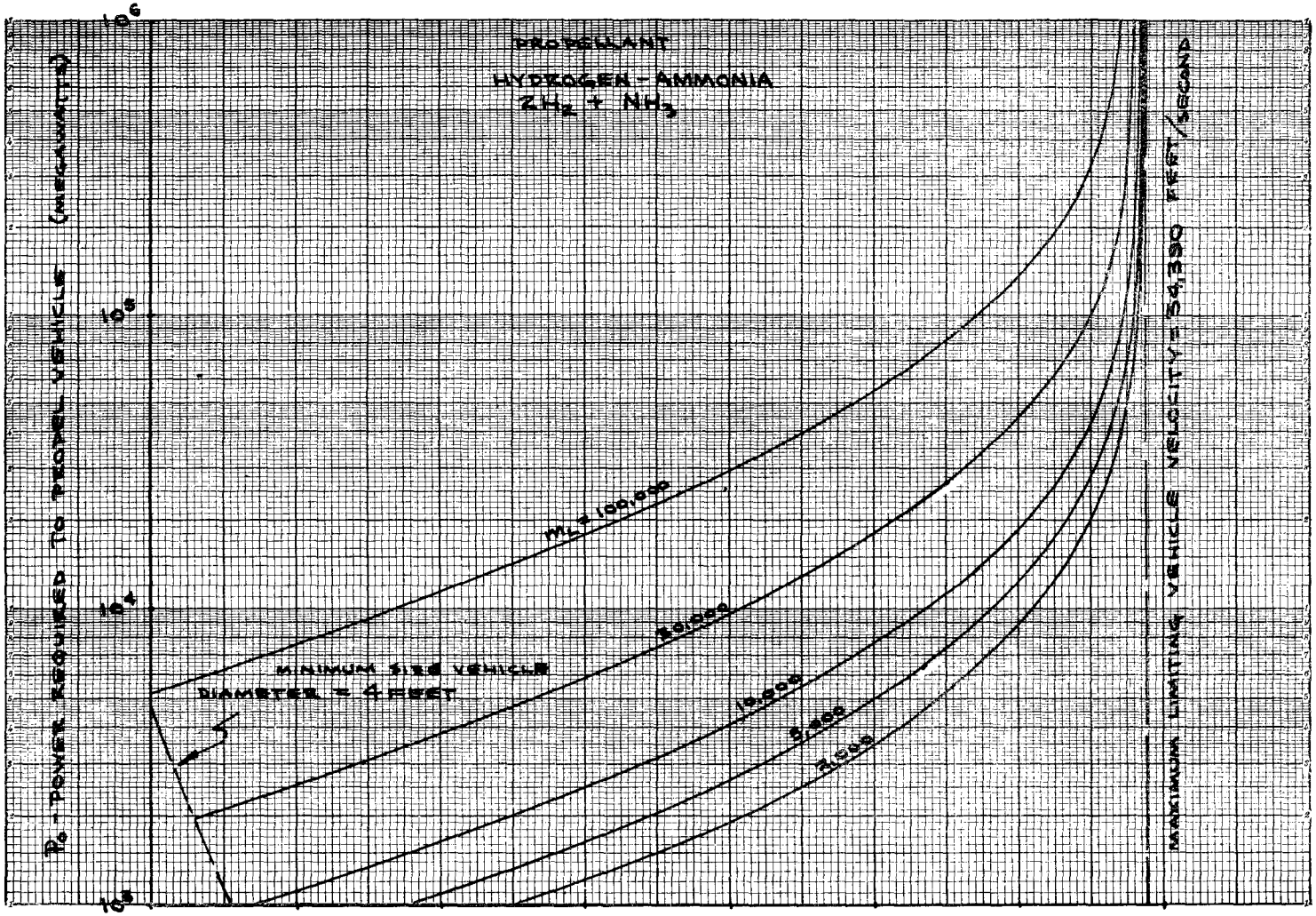

FIG. 9b

[redacted] Dwg. 19986

NUCLEAR ROCKET – MAXIMUM POWER REQUIREMENTS

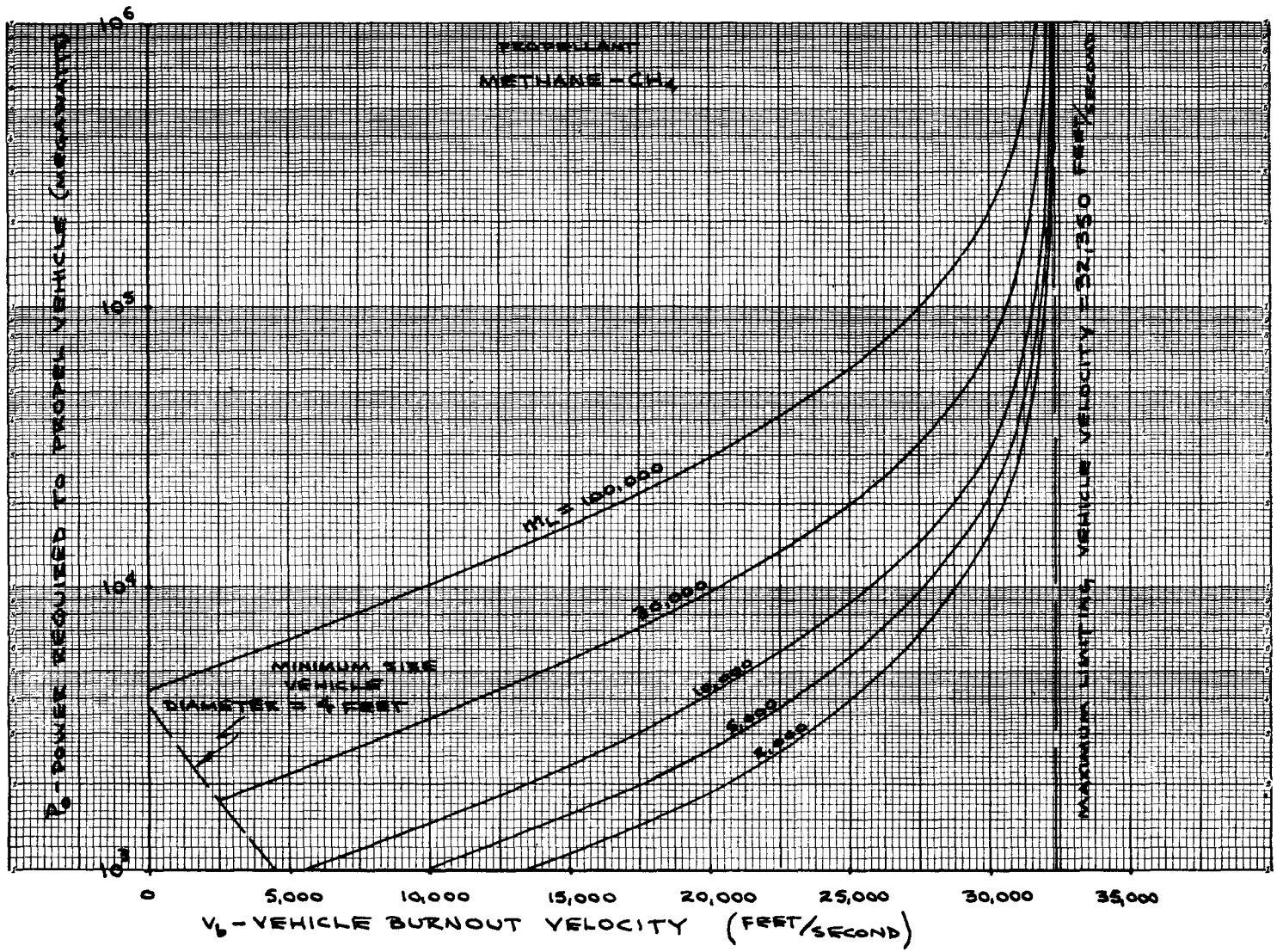

FIG. 9c

[redacted]

[redacted] Dwg. 19987

NUCLEAR ROCKET – MAXIMUM POWER REQUIREMENTS

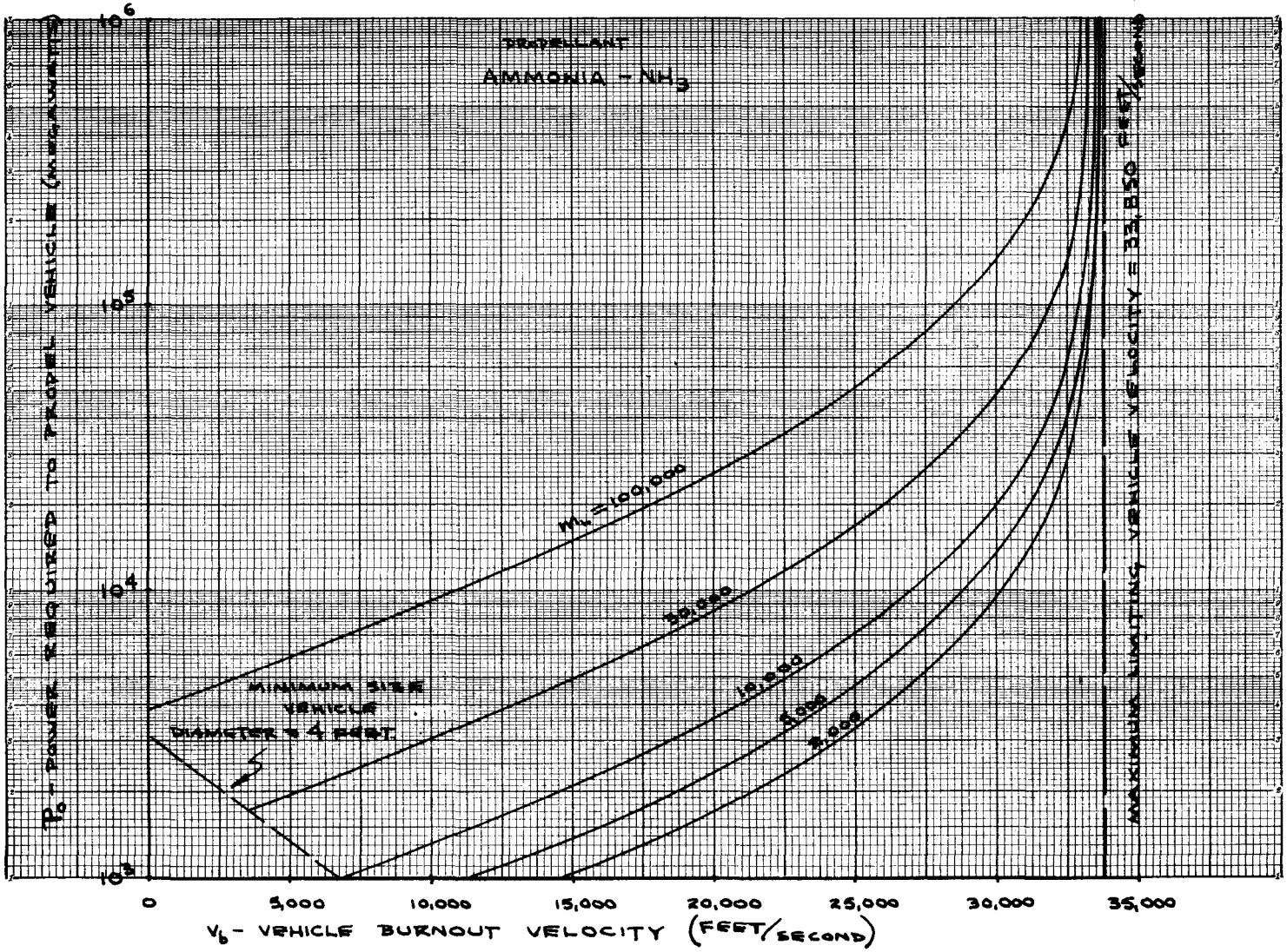

FIG. 9d

[redacted] Dwg. 19988

NUCLEAR ROCKET – MAXIMUM POWER REQUIREMENTS

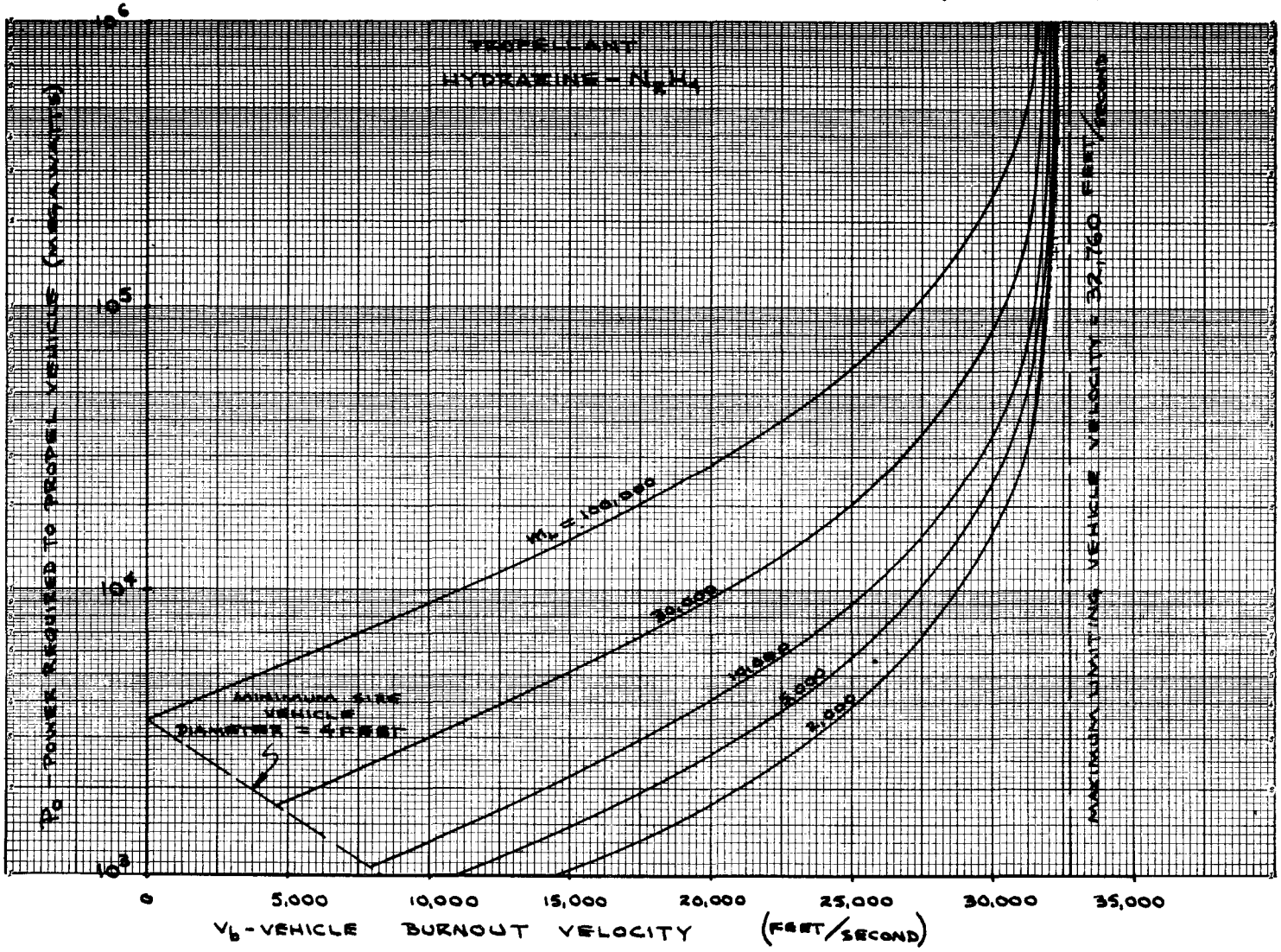

FIG. 9e

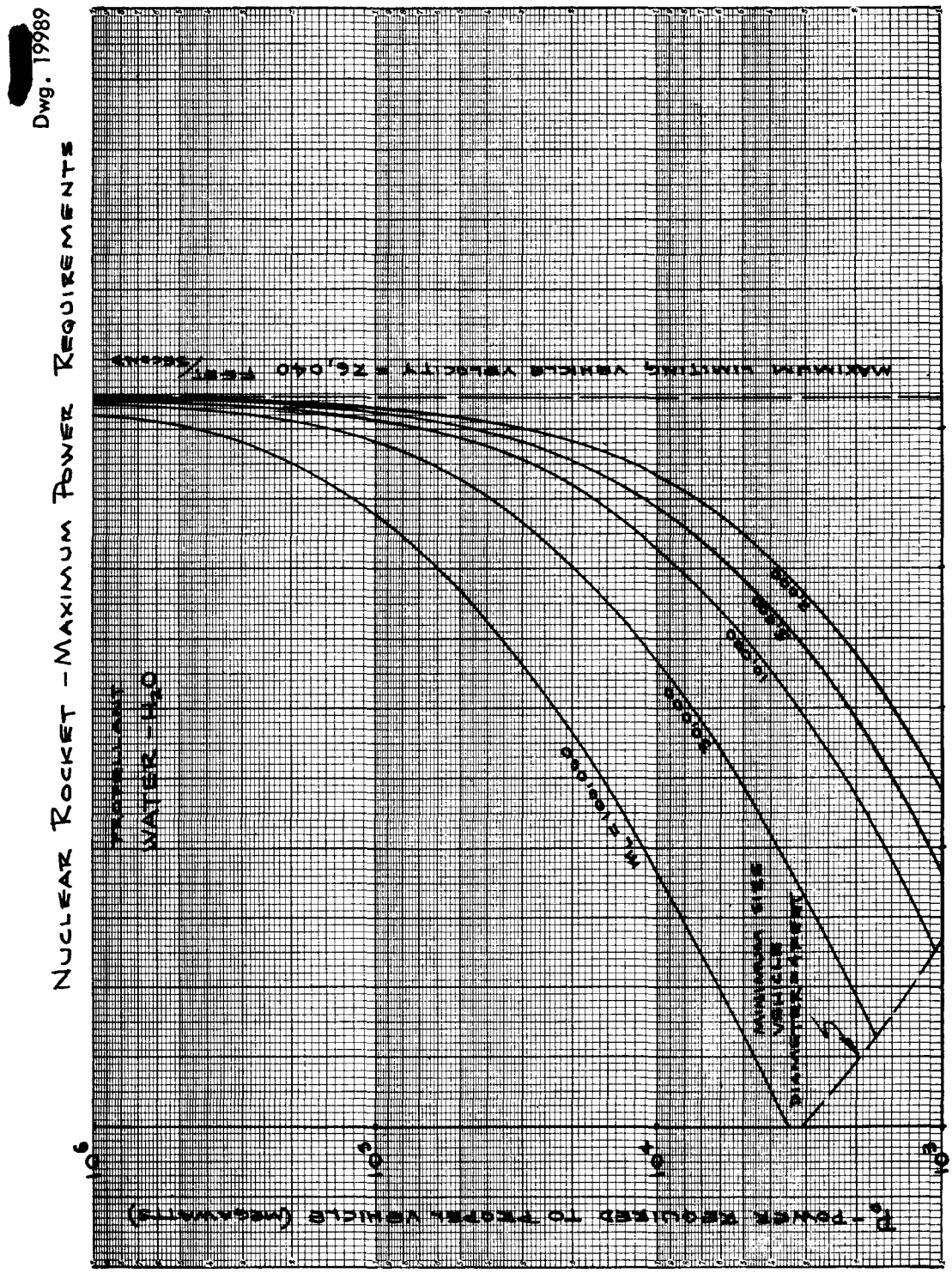
NUCLEAR ROCKET - MAXIMUM POWER REQUIREMENTS
Dwg. 19989
PROPELLANT
WATER - H_2O
MAXIMUM LIMITING VEHICLE VELOCITY = 26,040 FEET/SECOND
P_e - POWER REQUIRED TO PROPEL VEHICLE (megawatts)
V_b - VEHICLE BURNOUT VELOCITY (FEET/SECOND)
10^6
10^5
10^4
10^3
0
5,000
10,000
15,000
20,000
25,000
30,000
MINIMUM SIZE VEHICLE
DIMENSIONLESS

FIG. 9f

propellant tanks would be empty, hence no protection from direct radiation would exist, but the vehicle would be above the atmosphere and air scattered radiation would be reduced to zero. This inversion of conditions would take place within the brief, 200- to 500-sec, operating life of the rocket motor.

The variation of flux intensity incident on a unit volume within the vehicle nose as a function of time would be roughly as shown below.

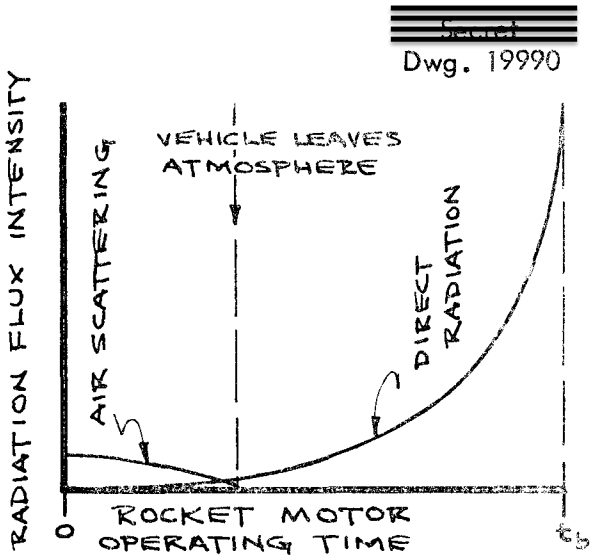

FLUX VARIATION AT VEHICLE NOSE AS A FUNCTION OF MOTOR OPERATING TIME

Very rough calculations indicate that crew shield weights of the order of tens of thousands of pounds would be required for a liquid-hydrogen orbital satellite vehicle with dead load capacities of hundreds of thousands of pounds. It should be pointed out that required shielding need not be useless dead weight, since it may be possible to utilize the useful payload as shield material by proper arrangement with respect to the spaces to be shielded.

REFERENCES

1. A. N. McDonald, *Determination of Propellant Tank Weights and Optimum Pump Inlet Pressure for Orbiting Rocket,* NEPA-457-EAM-C7, p. 6 (March 10, 1948).
2. *J. Brit. Interplanet. Soc.* **10,** No. 6, 288 (1951).
3. *Feasibility of Nuclear Powered Rockets and Ramjets,* NA-47-15, p. 40 (Feb. 11, 1947).
4. R. N. Mulford and J. P. Nigon, *Heat Exchange Between a Copper Surface and Liquid Hydrogen and Nitrogen,* IA-1416 (May 21, 1952).
5. *Op. cit.,* NA-47-15, pp. 155-157.
6. P. L. Teed, *The Properties of Metallic Materials at Low Temperatures,* chap. 3, John Wiley and Sons, New York, 1950.
7. *Mechanical Properties of Metals at Low Temperatures,* NBS-520, chap. 5 (May 1952).
8. G. F. Titterton, *Aircraft Materials and Processes,* chap. 11, Pitman Publishing Co., New York, 1947.
9. *Strength of Metal Aircraft Elements,* ANC-5a, chap. 3 (May 1949).
10. S. L. Gendler, R. M. Salter, H. A. Koch, and L. P. Holliday, *Long Range Surface-to-Surface Rocket and Ramjet Missiles - Propulsion and Fuels,* R-180 (May 1, 1950).
11. L. Green, Jr. and P. Duwez, "Fluid Flow Through Porous Metals," *J. Appl. Mechanics* **18,** 39 (1951).
12. L. Green, Jr., "Gas Cooling of a Porous Heat Source," *J. Appl. Mechanics* **19,** 173 (1952).
13. G. P. Sutton, *Rocket Propulsion Elements,* chap. 4, John Wiley and Sons, New York, 1949.
14. V. N. Huff, S. Gordon, and V. E. Morrell, *General Method and Thermodynamic Tables for Computation of Equilibrium Composition and Temperature of Chemical Reactions,* NACA-1037 (1951).

15. B. Lewis and G. von Elbe, *Combustion, Flames, and Explosions of Gases,* app. A, Academic Press, New York, 1951.

16. *Handbook of Chemistry and Physics,* 30th ed., Chemical Rubber Publishing Co., Cleveland, 1947.

17. J. O. Hirschfelder, F. T. McClure, and C. F. Curtiss, *Thermochemistry and the Equation of State of the Propellant Gases,* OSRD-547 A-48 (May 1942).

18. E. W. Geyer and E. A. Bruges, *Tables of Properties of Gases,* p. 19 ff., Longmans, Green and Co., London, 1948.

19. *Aerodynamic Summary, Navaho II Missile and Booster,* NA-AL-1372, p. 16 - III (Dec. 15, 1951).

20. *Op. cit.* NA-47-15, pp. 360-361.

PART II
NOMENCLATURE

SYMBOL	MEANING	UNITS
a_m	Maximum acceleration of rocket vehicle	ft/sec^2
A_H	Mean total cylindrical area of porous graphite tubes	$in.^2$
A_{plate}	Total surface area of graphite plates	$in.^2$
A_{rods}	Total surface area of graphite rods	$in.^2$
A_{sph}	Total surface area of graphite spheres	$in.^2$
$\overline{A}$	Ratio of area radiating to liquid propellant to total radiating area of nuclear rocket motor	
b	Gas constant ($= 12\ R_u/mw$)	$in./^\circ R$
B	Coefficient of thermal expansion of graphite heat transfer structure	$in./in.\cdot^\circ F$
c	Width of flat graphite plates	in.
c_{pg}	Mean specific heat of propellant gases	$Btu/lb\cdot^\circ F$
$\overline{c}_p$	Mean molar specific heat of propellant gases	$Btu/mole\cdot^\circ F$
C	Total width of all graphite plates ($= Nc$)	in.
d_h	Gas flow passage "hydraulic" diameter	in.
D_c	Unit reactor core diameter	in.
D_H	Mean diameter of porous graphite tubes	in.
D_r	Rocket motor outside diameter	in.
D_s	Diameter of graphite rods or spheres	in.
E	Modulus of elasticity of graphite heat transfer structure	$lb/in.^2$
$f,\ f',\ f''$	Gas flow friction factors	
f_c	Reactor core graphite volume fraction	
f_e	Fraction of fission energy escaping the reactor core in photon and fast neutron radiation	
f_{Mo}	Reactor core molybdenum volume fraction	
f_v	Reactor core void volume fraction	
f_{Zr}	Reactor core zirconium volume fraction	
f_s	Design safety factor	
F_T	Total normal load at any one contact point between any two spheres	lb
g_c	Acceleration of gravity at sea level	$32.2\ ft/sec^2$
G	Propellant gas weight flow rate per unit area	$lb/sec\cdot in.^2$
h_c	Heat transfer structure surface heat transfer coefficient	$Btu/sec\cdot in.^2\cdot^\circ F$
H_v	Heat of vaporization of liquid propellant	Btu/lb
J	Thermal-mechanical energy conversion factor	778 ft-lb/Btu
k_g	Thermal conductivity of propellant gas	$Btu/sec\cdot in.\cdot^\circ F$
k_s	Thermal conductivity of graphite heat transfer structure	$Btu/sec\cdot in.\cdot^\circ F$
L	Unit reactor core length, or length of porous tubes or solid graphite plates	in.

SYMBOL	MEANING	UNITS
L_c	Unit reactor core length	in.
m	Required number of porous tubes in porous tube reactor core	
m_r	Nuclear rocket motor weight	lb
m_u	Uranium weight required for reactor criticality (assumed homogeneous distribution)	lb
mw	Molecular weight of propellant gases	lb/lb·mole
N	Number of flat graphite plates in stacked plate reactor core	
N_{Re}	Reynolds number of propellant gas flow through reactor core (dimensionless)	
N_{Re_f}	Flow Reynolds number — Packed sphere reactor core only	
N_{Re_H}	Heat transfer Reynolds number — Packed sphere reactor core only	
N_{Pr}	Prandtl's number for propellant gases (dimensionless)	
p	Absolute pressure of propellant gases within reactor core	lb/in.^{2}
Δp	Gas pressure drop across reactor core	lb/in.^{2}
p_{avg}	Average absolute pressure of propellant gases within reactor core	lb/in.^{2}
p_i	Absolute pressure of propellant gases inside the porous tubes of the porous tube reactor core	lb/in.^{2}
p_0	Absolute pressure of propellant at reactor inlet	lb/in.^{2}
$\overline{p}$	Rocket motor specific power	megawatts/lb
P_r	Reactor power output	megawatts
q	Heat generation in the vehicle propellant due to neutron and gamma ray heating	Btu/sec
R_{rm}	Maximum radial thermal compressive stress in graphite spheres	lb/in.^{2}
R_u	Universal gas constant	$1544\left(\frac{\text{lb}}{\text{ft}^2}\right)\left(\frac{\text{ft}^3}{\text{lb·mole}}\right)\left(\frac{1}{^\circ\text{R}}\right)$
R'_u	Universal gas constant	$10.73\left(\frac{\text{lb}}{\text{in.}^2}\right)\left(\frac{\text{ft}^3}{\text{lb·mole}}\right)\left(\frac{1}{^\circ\text{R}}\right)$
s	Maximum compressive strength of graphite	lb/in.^{2}
s_L	Heat transfer structure stress due to pressure loading	lb/in.^{2}
s_s	Yield strength of rocket motor pressure shell material	lb/in.^{2}
s_{th}	Heat transfer structure thermal stress due to internal heat generation	lb/in.^{2}
s_{tot}	Total combined heat transfer structure stresses	lb/in.^{2}
t	Thickness of porous tube wall or solid graphite plate	in.
t_s	Thickness of rocket motor pressure shell	in.
T	Temperature	$^\circ$R

SYMBOL	MEANING	UNITS
T_{avg}	Average gas temperature within reactor core (defined in text)	$^{\circ}R$
T_c	Maximum propellant gas temperature within rocket motor prior to expansion	$^{\circ}R$
T_{gx}	Propellant gas temperature at any point within reactor core	$^{\circ}R$
T_0	Propellant temperature at reactor inlet	$^{\circ}R$
ΔT_H	Temperature drop across porous graphite tube wall	$^{\circ}F$ (or $^{\circ}R$)
ΔT_m	Mean temperature difference between graphite heat transfer structure surface and propellant gas	$^{\circ}F$ (or $^{\circ}R$)
ΔT_s	Temperature drop from center of graphite heat transfer structure to surface	$^{\circ}F$ (or $^{\circ}R$)
u	Separation distance between adjacent parallel graphite plates	in.
v_m	Maximum theoretical propellant gas exhaust velocity	ft/sec
V_c	Volume of reactor core	$in.^3$
V_H	Porous tube wall bulk volume	ft^3
V_n	Volume of material in porous nozzle	$in.^3$
V_0	Propellant gas velocity through core, based on the empty core cross section and the weight flow rate w	ft/sec
V_{refl}	Volume of 10-in. thick carbon reactor core reflector	$in.^3$
V_s	Volume of rocket motor pressure shell	$in.^3$
w, w_p	Propellant gas weight flow rate	lb/sec
w_{vap}	Rate of vaporization of propellant by internal power generation due to neutron and gamma ray heating	lb/sec
x	Length dimension	in.
α	Viscous flow resistance coefficient of porous material	$1/in.^2$
β	Inertial flow resistance coefficient of porous material	1/in.
γ_c	Density of graphite	lb/ft^3
γ_u	Uranium bulk density within reactor core	lb/ft^3
γ'_c	Density of carbon or graphite	$lb/in.^3$
γ'_{Mo}	Density of molybdenum	$lb/in.^3$
γ'_n	Density of nozzle material	$lb/in.^3$
γ'_{refl}	Density of reflector material	$lb/in.^3$
γ'_s	Density of pressure shell material	$lb/in.^3$
γ'_{Zr}	Density of zirconium	$lb/in.^3$
δ	Graphite heat transfer structure dimensional parameter (defined in text)	
ϵ_A	Ratio of maximum sphere cross sectional area to core cross sectional area	
ϵ_f	Ratio of void volume to core volume in packed rod reactor core	
ϵ_p	Fraction of total reactor power generated within graphite core heat transfer structure by neutron and gamma ray heating	

SYMBOL	MEANING	UNITS
ϵ_T	Ratio of total porous tube volume to reactor core volume	
ϵ_V	Ratio of total sphere volume to reactor core volume	
η_c	Reactor core bulk power density	megawatt/ft^3
η_H	Bulk power density within porous tube wall volume	megawatt/ft^3
θ	Reactor core power parameter (defined in text)	
λ	Reactor core dimensional parameter (defined in text)	
μ	Propellant gas viscosity	lb/sec·in.
μ'	Propellant gas viscosity	lb·sec/$in.^2$
ρ_x	Propellant gas density at any point within reactor core	lb/ft^3
σ	Poisson's ratio for graphite	
Φ_{ϕ_m}	Maximum tangential thermal tensile stress in graphite spheres	$lb/in.^2$

PART II. NUCLEAR REACTOR ROCKET MOTOR

DISCUSSION

The feasibility of nuclear-powered rocket vehicles is largely a function of the attainable specific power of the nuclear-reactor rocket motor. From the equations determining vehicle performance (see Part I), it can be shown that the specific power of the nuclear rocket motor must be greater than approximately 0.5 megawatt/lb of total rocket motor weight for a nuclear rocket vehicle to demonstrate any significant performance advantage over conventional chemically powered rocket vehicles for any reasonable range of vehicle burnout velocities and dead load capacities.

The results of analytical studies of four possible reactor core designs indicate that specific powers as high as 4 megawatts/lb are possible with delicate structural and heat transfer components in the core, and that specific powers of 1.0 megawatt/lb are attainable with relatively sturdy components in at least two of the four designs considered.

The type of reactor proposed for a rocket vehicle power plant is, in principle, simple in operation. The liquid propellant would be fed into the reactor core at a high pressure, vaporized and heated to 4500°F (2500°C) by heat transfer from the hot surfaces which comprise the main core structure, and exhausted through a nozzle cooled by gas transpiration and with an exit to throat area ratio of 35:1. The reactor power would be generated primarily in thin layers of uranium carbide sandwiched between hydrogen resistant metallic carbide coatings and the primary graphite core structure. A secondary source of power would be from neutron and gamma heating of the core structure, reflector, and propellant shield.

All reactors considered in this report utilize carbon and graphite as the reflector, moderator, and heat transfer structure materials. In order to keep the power density variation of the reactor core at a minimum during reactor operation, the maximum burnup should be held to 1%, or less, of the uranium mass. Since a typical required total energy output of a rocket vehicle reactor is of the order of 2×10^6 kw-hr (see Part I), the total uranium burnup would be roughly 1/2 lb of U^{235}. Thus the minimum allowable critical mass will be of the order of 50 to 100 pounds.

For homogeneous, carbon-reflected reactors containing various volume fractions of graphite, molybdenum (core support structure), and zirconium, columbium, or tantalum (protective coating material), multigroup analyses and calculations based upon the work of Mills[1] indicate that the minimum required critical mass for operation of physically feasible reactors is of the order of 50 to 150 pounds. Since useful nuclear rocket reactors will necessarily be relatively large, the uranium density will always be low. Thus, despite the required high critical mass, the majority of the fissions will result from thermal rather than fast neutrons. The basic types of nuclear rocket motor designs have been discussed elsewhere.[2,3] The type of motor considered here was chosen because it appears to offer considerably more promise from the practical standpoint than any other. In order to obtain a high power to total-weight ratio in the reactor, it is obviously necessary to operate the reactor at a high heat-transfer-rate to core-volume ratio. This in turn, requires a high surface-area to core-structure-volume ratio and a high gas mass velocity, if it is desired to operate the core structure at temperatures approaching the gas outlet temperature. Other requirements are that the gas pressure drop through the core be limited to a maximum value of the order of 30 to 40% of the propellant gas pressure at the core outlet (higher allowable pressure drops necessitate excessive pump weights), that the core structure must

be able to withstand the thermal and pressure loads imposed by the heat transfer and gas flow conditions, and the core material must not react chemically with the propellant gases (predominately hydrogen, for all useful propellants) at 4500°F.

Fluid flow and heat transfer conditions are optimized when the power density is constant across the reactor core in any plane normal to the fluid flow. Furthermore, the variation, with temperature, of gas properties such as viscosity and thermal conductivity is quite marked in the case of hydrogen; therefore variations in power density from point to point within the core would have a pronounced effect on the reactor rocket motor performance.[4]

Variation of power density in a direction parallel to the flow through the core is permissible, provided that the plane of maximum power density occurs at the propellant inlet end of the core and the minimum power density region occurs at the hot gas outlet. This maximum *axial* variation in power density should not exceed 25 to 30%.

A neutron reflector is necessitated by the requirement of constant power density across the core. With such a reflector it will still be necessary to vary the uranium concentration across the core in order to hold the radial variation in power density within 5 to 10%. The radial power density in any given plane normal to the gas flow should also remain constant within 5 to 10% throughout the time of reactor operation.

From the structural standpoint, carbon or graphite are the only known moderating materials with appreciable strength at temperatures above 4000°F.[5] Graphite was chosen as the material for the core structure primarily because of its high thermal conductivity as compared with carbon. Carbon was chosen as the reflector material because of its very low cost as compared to other reflector materials and because of its low thermal conductivity; it must also serve as a thermal insulator for the reactor pressure shell. Because of their high strength-to-density ratios and low absorption cross sections for thermal neutrons, aluminum or magnesium alloys are suitable for the reactor rocket motor pressure shell and external support structure. Proper cooling is, of course, essential to the use of these materials. The internal support structure in the core, which would be exposed to the propellant gas at 4500°F, could be made from tantalum, columbium, molybdenum, or zirconium. Molybdenum would be preferred because it is more readily available and less expensive than tantalum, zirconium, or columbium, and has more favorable thermal neutron absorption cross section than tantalum. The problem of protecting the hot core elements from chemical reaction with the predominantly hydrogen propellant gas is by no means solved; however, there are indications that satisfactory protective coatings can be made. Tests performed by North American Aviation with tantalum carbide coatings on graphite in flowing hydrogen at 3000°C showed that tantalum carbide will give excellent protection to graphite and does not react with hot hydrogen atmospheres. Comparison tests made on uncoated graphite samples showed serious erosion of the graphite during tests of 5 to 15 min duration.[6] Unfortunately, tantalum has a high macroscopic thermal neutron absorption cross section and is thus not well suited for reactor operation. Columbium, molybdenum, and zirconium, are chemically similar to tantalum, have much lower neutron absorption cross sections, and form carbides with sufficiently high melting points to make their use in the rocket reactor possible.

No experimental work has been done on the efficacy of protective coatings of the carbides of zirconium, columbium, or molybdenum in dynamic hydrogen atmospheres under the temperature and pressure conditions envisioned for a nuclear rocket motor. Until information from tests of this type is available, no such nuclear rocket motors can be considered as feasible. It should be

borne in mind that the required operational life of the protective coatings and, in fact, the nuclear rocket reactors will be of the order of 30 min or less for most practical rocket vehicles. Possible methods of coating graphite with the metal carbides are (1) the deposition upon the graphite of a metallic halide layer of the desired metal from a vapor phase, followed by heating to decompose the halide compounds and by continued heating to form the metallic carbides by reaction with the graphite surface; (2) surface coating of the graphite by impregnation of the surface with metallic compounds in an organic solution, followed by heating to vaporize the solvent, decompose the metallic compounds, and form the desired metallic carbides; and (3) in the case of zirconium, by dipping the graphite member to be coated directly into a bath of molten zirconium or zirconium-aluminum alloy, which would initiate the exothermic $Zr + C \rightarrow ZrC$ reaction.

For the purposes of this study, it was assumed that a metallic carbide protective coating could be found that would provide satisfactory protection for the graphite structure of the reactor core at 4500°F in flowing hydrogen and would not have an excessive neutron absorption cross section.

The core elements must also contain the nuclear fuel. It is contemplated that the fuel would be in the form of a layer of uranium carbide between the graphite body of the structural element and the external metallic carbide protective coating. Possible methods of applying the UC_2 coating to the graphite are similar in principle to those outlined for the metallic carbide coatings.

Four possible reactor designs appeared to give a sufficiently high heat transfer rate per pound of total reactor weight to make investigation worthwhile. The four designs are (1) the porous tube reactor; (2) the packed sphere reactor; (3) the packed rod reactor; and (4) the stacked plate reactor. All four configurations are similar in principle in that there exists a high ratio of heat transfer surface area to heat transfer structure volume; however, each configuration is geometrically "coarser" than the previous one (as listed above). Thus there is a continuous spectrum of required pressure drops and temperature differences when the four designs are viewed in sequence.

In Part I, it was noted that vehicle performance (as defined by the ratio of full weight to dead load weight of the vehicle) is an exponential function of the propellant exhaust velocity. For fixed nozzle geometry, the propellant exhaust velocity is approximately proportional to the square root of the absolute temperature of the propellant gas prior to expansion. The vehicle performance, therefore, falls off sharply as the maximum gas temperature is decreased. The maximum gas temperature in any reactor of the sort proposed for nuclear-rocket vehicles is limited by the maximum allowable operating temperature of the heat transfer structure and by the structure-to-gas temperature drop necessary to attain the required heat transfer rate. From data presented in Fig. 10, it would seem unreasonable to predicate reactor designs for a graphite structure operating at temperatures higher than 5000°F. Thus, if the desired maximum gas temperature is taken as 4500°F (as in this study), the absolute maximum allowable structure-to-gas temperature drop will be 500°F at the gas outlet end of the reactor.

The results of the design and performance studies of the packed sphere, packed rod, and stacked plate reactor cores are presented in the form of plots of the significant and characteristic dimensional parameters of each system as a function of the bulk power density within the core. The region of turbulent flow (that is, Reynolds number > 2100) is the only one of interest in the three designs because, although the calculated theoretical performance in the laminar region is more desirable than that in the turbulent flow region in

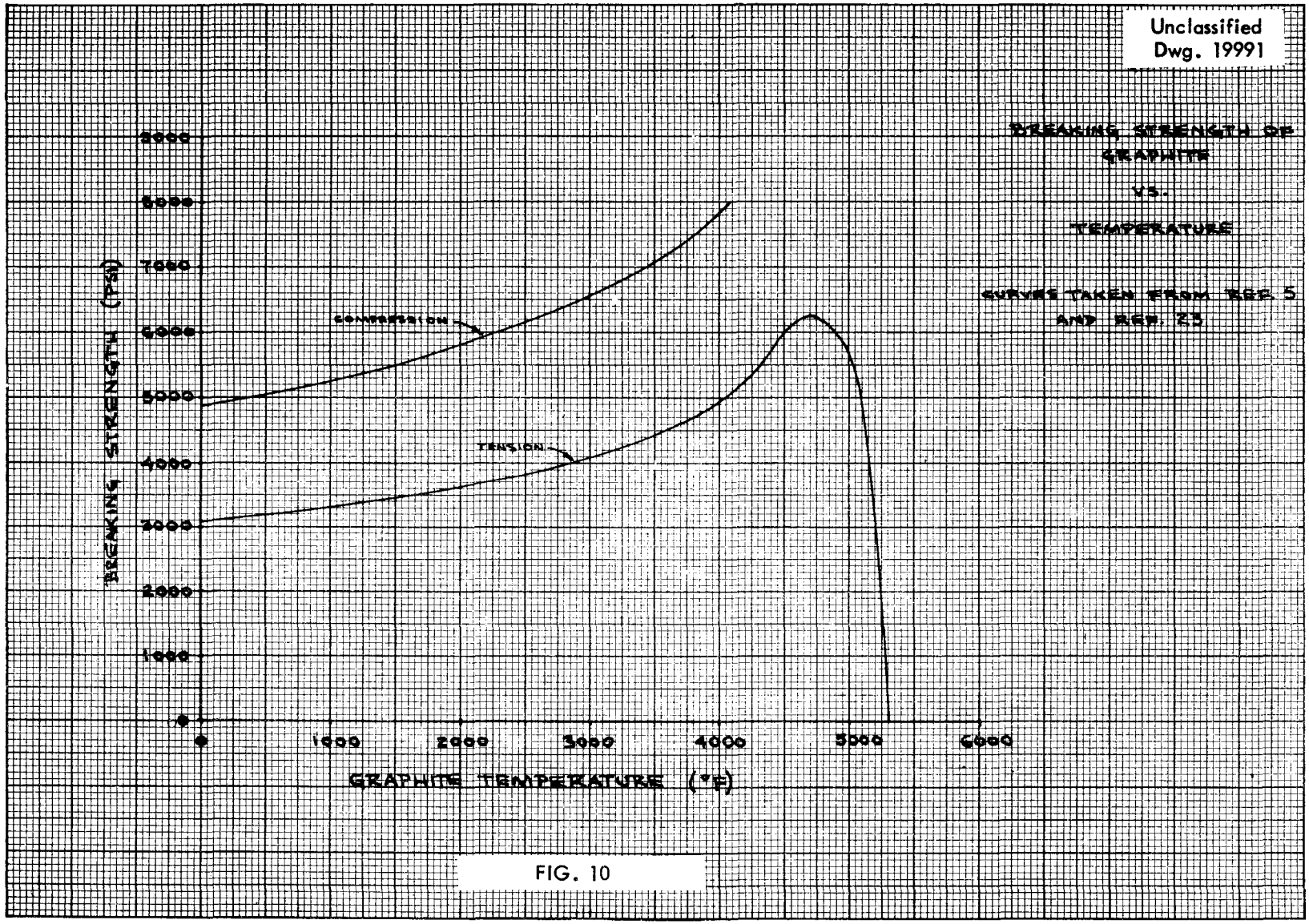
Unclassified
Dwg. 19991
BREAKING STRENGTH OF GRAPHITE
VS.
TEMPERATURE
CURVES TAKEN FROM REF. 5 AND REF. 25
COMPRESSION
TENSION
BREAKING STRENGTH (PSI)
8000
7000
6000
5000
4000
3000
2000
1000
0
1000
2000
3000
4000
5000
6000
GRAPHITE TEMPERATURE (°F)

FIG. 10

some cases, the structural requirements (that is, the very small size required of the core heat transfer elements) are so stringent as to make physical construction of the laminar region designs appear virtually impossible. The results of the porous tube reactor design and performance study are shown graphically in terms of the critical tube dimensions vs. a simple function of the reactor core bulk power density. Flow through and heat transfer within porous media cannot be handled conveniently by the conventional correlations of Nusselt, Prandtl, and Reynolds numbers and there are no clear-cut laminar and turbulent flow regimes. Thus, the equations relating temperature and pressure drops to heat transfer and fluid flow appear in somewhat different forms than those encountered in the packed sphere, packed rod, and stacked plate studies.

Figure 11 shows a schematic outline of the type of nuclear-powered rocket motor discussed.

REACTOR CORE DESIGN SUMMARY

Porous Tube Reactor. The possible use of porous graphite as a reactor core structure heat transfer medium for nuclear rockets is not new;[3] however, its potentiality had never been fully investigated by the use of recently available analytical tools to describe the flow and heat transfer conditions in porous heat sources.[7,8]

The porous tube reactor envisioned would have a basic heat transfer matrix consisting of a number of thin-walled porous graphite tubes, all parallel and spaced at equal intervals in an equilateral triangular array across the reactor core. The propellant would be pumped through the reflector as a coolant and then into the spaces external to the tubes. It would flow radially through the tube walls, being vaporized and heated in the process, and would finally flow axially down the length of the tubes to the converging-diverging exhaust nozzle. The axial porous graphite tubes could be supported at the gas exit end by a graphite plate. This plate would be designed to withstand the load imposed by the pressure drop across the tube walls and the acceleration forces on the core structure mass imposed by the contemplated vehicle accelerations. The surfaces of the pore passages through the porous graphite tubes would be coated with uranium carbide and a protective metallic carbide, possibly by a vapor-deposition process, and the power generation would be primarily on the pore surfaces of the tube that are exposed to the propellant gas. Reactor control might be accomplished by the use of one or more movable boron

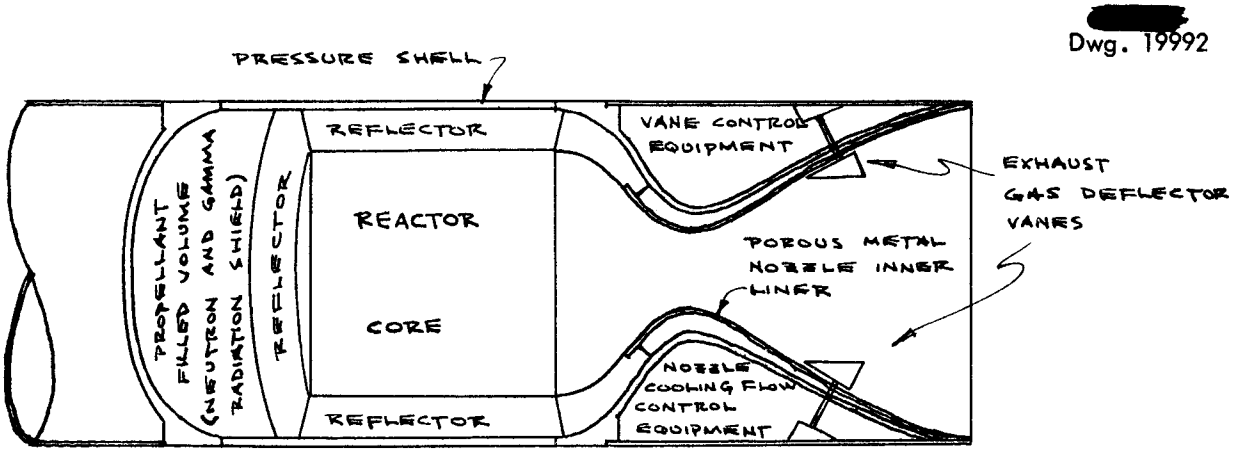

NUCLEAR POWERED ROCKET MOTOR

FIG. 11

carbide control rods extending into the reactor core, parallel to the porous tubes (that is, axially through the reactor), where they could be cooled by liquid propellant flowing around the rods in the rod hole jackets.

The optimum shape of the porous tubes to be used in the reactor is, of course, not cylindrical. For the case of straight cylindrical tubes, the gas pressure drop along the tube caused by the increasing dynamic head will cause a large variation in the pressure differential across the tube wall because the pressure on the external (gas supply) side of the tubes would be approximately constant. Because of this, the maximum pressure drop across the wall would be at the gas exit end of the tubes. For the same thermal and pressure stress conditions, the higher pressure drop across the wall would necessitate thicker tube walls at the gas exit end of the tubes than at the top of the tubes. A thicker wall, however, will cause a decrease in the gas through-flow. For the case of conical tubes, the internal gas pressure remains constant down the tube length; thus the gas pressure drop across the tube wall will remain constant. However, the tube diameter increases from the top of the tube to the gas exit end; hence the cone wall thickness must also increase to counteract increased pressure loads, and the wall through-flow will again be affected.

For purposes of this study, it was assumed that straight cylindrical porous graphite tubes of constant wall thickness would be used, and that the gas pressure drop across the tube wall would be constant throughout the tube length.

The basic result of this study is given by an equation relating porous tube diameter and tube wall thickness to the reactor core bulk power density. For a design safety factor of 1.0 this equation was found to be

$$\frac{\eta_c}{\epsilon_T} = \frac{10.45\ D_H}{t[D_H + t]^2} ,$$

where ϵ_T is the ratio of total porous tube volume to the reactor core volume. This equation is shown graphically in Fig. 12*a*. Figure 12*b* shows the effect of design safety factor on the bulk core power density for any given porous tube dimensions.

From Figs. 12*a* and 12*b*, it can be seen that reactors of bulk core power density greater than 100 megawatts/ft^3 can be achieved only by the use of small diameter and very thin-walled porous graphite tubes operating at low safety factors. The mechanical difficulties of fabricating the tubes and applying uranium carbide and protective metallic carbide coatings to the pore and tube surfaces would be very great compared to the problems associated with the construction of a solid graphite, surface coated type of core structure. It may be concluded that the porous graphite tube core structure is not the optimum method of rocket reactor construction, when compared with the packed rod or stacked plate core structure systems.

Packed Sphere Reactor. As an extension of the porous type of construction, the next possible reactor design to be considered was that in which the core structure consists of a "bed" of solid graphite spheres packed in a tetrahedral geometry. In this design, the propellant gas flow is assumed to pass axially through the reactor core, to absorb heat energy from the sphere surfaces, and to emerge at the core bottom at 4500°F prior to entering the converging-diverging exhaust nozzle. Each graphite sphere would be coated with a thin layer of uranium carbide covered by a thin, hydrogen-resistant coating of metallic carbide. The packed sphere core could be supported by a graphite plate designed to withstand the pressure and acceleration loads imposed by the flow system and vehicle performance. The pressure loads, of course, appear primarily as point contact loads between adjacent spheres and produce high local stresses. Reactor control might be accomplished by the use of boron carbide control rods, as mentioned

[redacted] Dwg. 19993

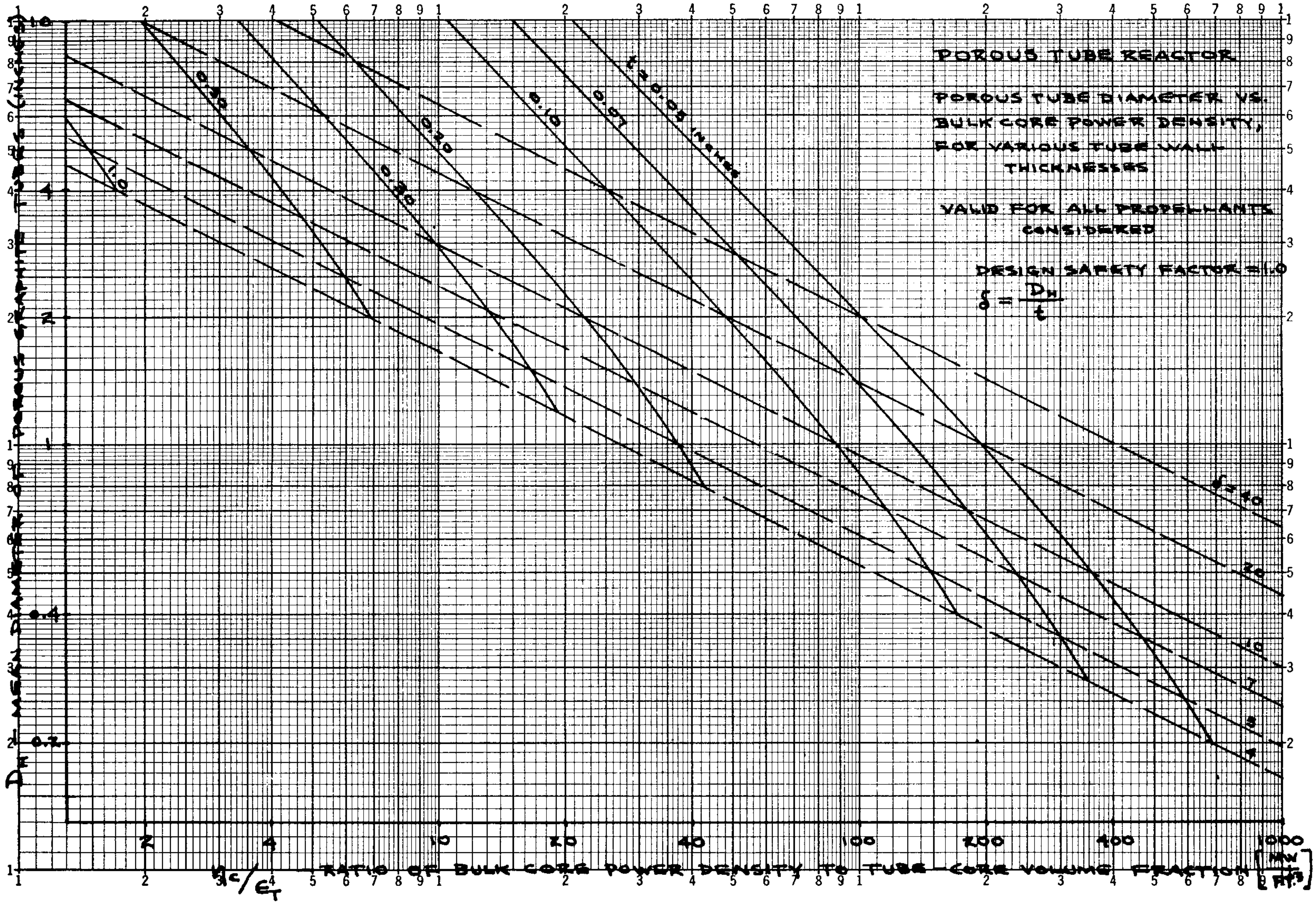

FIG. 12a

[redacted]

Dwg. 19994

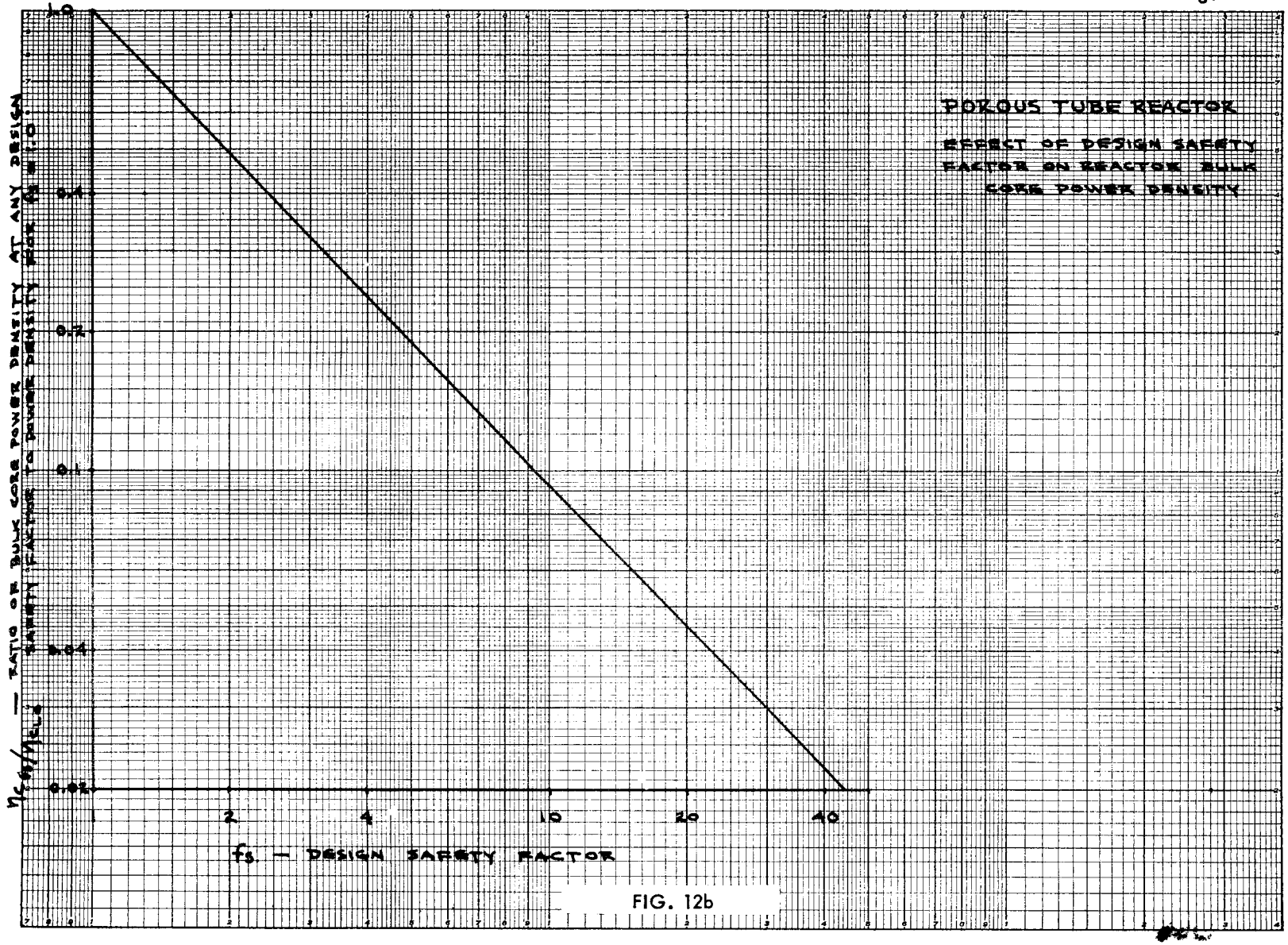

FIG. 12b

in the section on the porous tube reactor.

The most interesting result from the packed sphere reactor study is the relation between the bulk core power density, the gas pressure drop across the core, the mean temperature drop between the graphite spheres and the gas, and the graphite sphere diameter. This relation was found to be

$$D_s = \frac{1.305 \left(\frac{\Delta p}{200}\right)^{0.323} \left(\frac{\Delta T_m}{360}\right)^{0.446}}{(\eta_c)^{0.823} \left(\frac{mw}{\bar{c}_p^2}\right)^{0.323}}$$

and is shown graphically in Fig. 13, for $\Delta p = 200$ lb/in^2 and $\Delta T_m = 360°$F, for all the propellant gases considered. Values of Reynolds number are given at several points along the curve. For turbulent gas flow, the Reynolds number must be greater than 2100, and it can be seen from Fig. 13 that the maximum possible bulk core power density is thus 100 megawatts/ft^3 with a sphere diameter of 0.090 inch.

The difficulties that would be encountered in the fabrication and satisfactory coating of millions of small spheres for any reactor of sufficient power output to propel a rocket vehicle, while probably less than those inherent in the construction of the porous tube reactor system, would certainly be great enough to create serious doubt as to the wisdom, if not feasibility, of construction of the packed sphere type reactor. It thus seems reasonable to conclude that the packed sphere reactor does not appear to be the optimum type for rocket vehicle propulsion.

Packed Rod Reactor. In an effort to reduce the number of individual pieces that would be required for reactor core construction from that of the numerous spheres necessary in the previously discussed system, a reactor core consisting of axially packed rods was considered. This system appeared to offer advantages from the standpoint of more rugged construction and greater ease of manufacture and assembly than either of the two reactor types discussed thus far, and seemed to be no worse than either in respect to required wall-to-gas temperature drops and gas flow pressure drops.

The reactor core of this type would consist of numerous cylindrical solid graphite rods packed together in an equilateral triangular array with their axes parallel to the axis of the reactor core and the rocket vehicle. These rods might be coated with uranium carbide and a protective metallic carbide coating, and could be supported by either a graphite plate or a propellant cooled, molybdenum or columbium metallic structure, or by a combination of both. The propellant gas flow would, as in the previous types, pass axially through the core, and the propellant would be vaporized and heated to 4500°F during passage through the interstices between the packed rods. The hot propellant gas would leave the bottom of the reactor core and pass through the exhaust nozzle; thus furnishing thrust to propel the vehicle. Reactor control by propellant-cooled boron carbide rods inserted in the core seems feasible.

The relation between the bulk core power density, the gas pressure drop across the core, the mean temperature difference between the graphite rods and the gas, and the rod diameter was found to be

$$D_s = \frac{2.717 \left(\frac{\Delta p}{200}\right)^{0.328} \left(\frac{\Delta T_m}{360}\right)^{1.154}}{(\eta_c)^{0.828} \left(\frac{mw}{\bar{c}_p^2}\right)^{0.328}}.$$

This equation is shown graphically in Fig. 14, for $\Delta p = 200$ lb/in^2 and $\Delta T_m = 360°$F, for all the propellant gases considered. Values of Reynolds number are given at several points along the curve.

From Fig. 14, it would appear that packed rod reactors could be constructed to operate at core power

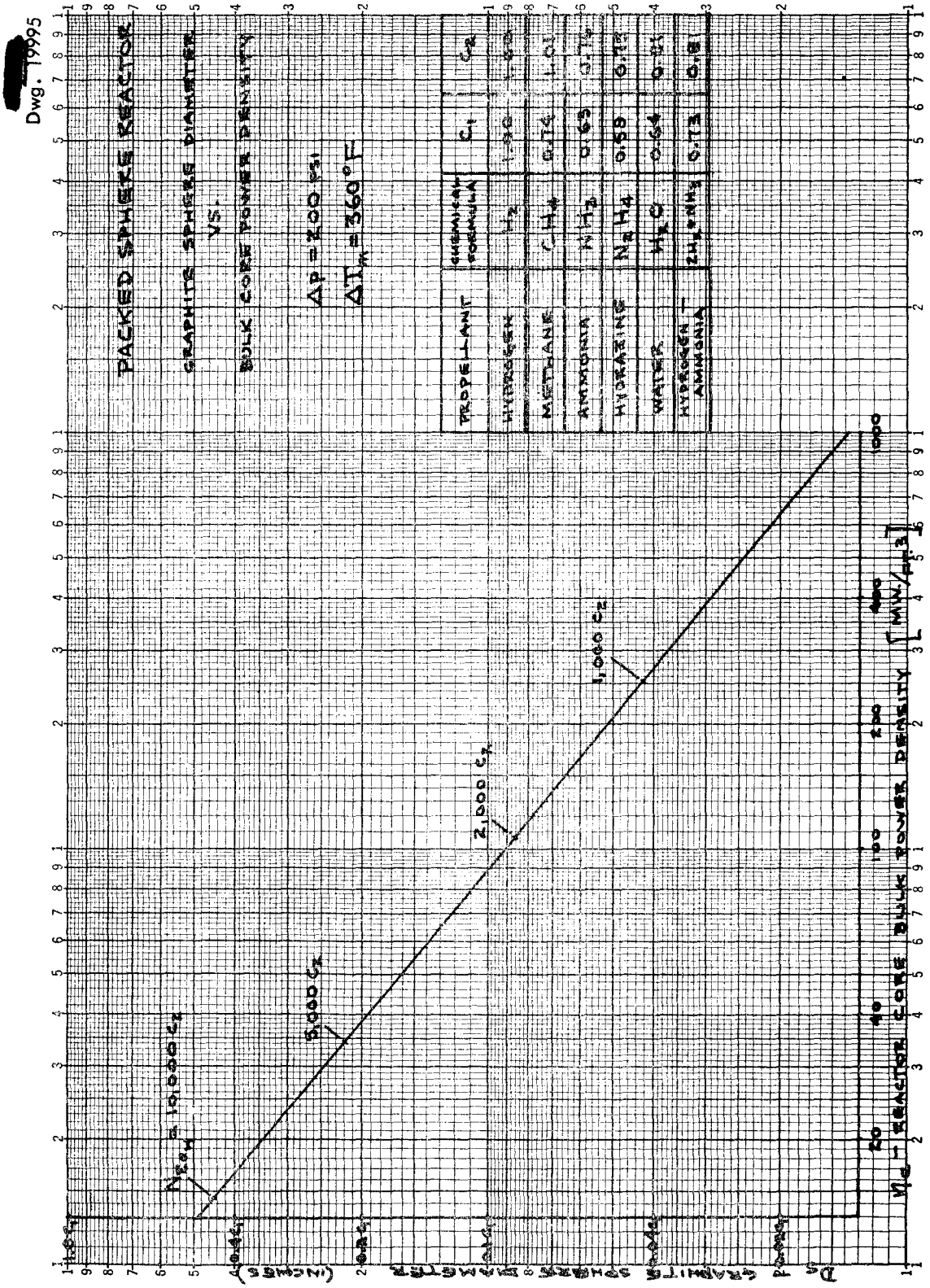
Dwg. 19995
PACKED SPHERE REACTOR
GRAPHITE SPHERE DIAMETER
VS.
BULK CORE POWER DENSITY
ΔP = 200 psi
ΔT_R = 360°F
PROPELLANT
CHEMICAL FORMULA
C1
C2
HYDROGEN
H2
1.30
1.92
METHANE
CH4
0.74
1.01
AMMONIA
NH3
0.63
0.79
HYDRAZINE
N2H4
0.58
0.78
WATER
H2O
0.64
0.82
HYDROGEN - AMMONIA
2H2+NH3
0.73
0.91
N_Re,H = 10,000 C2
2,000 C2
1,000 C2
GRAPHITE SPHERE DIAMETER, D_p (INCHES)
Mid - REACTOR CORE BULK POWER DENSITY [MW/ft3]
20
40
100
200
400
1000

FIG. 13

[redacted] Dwg. 19996

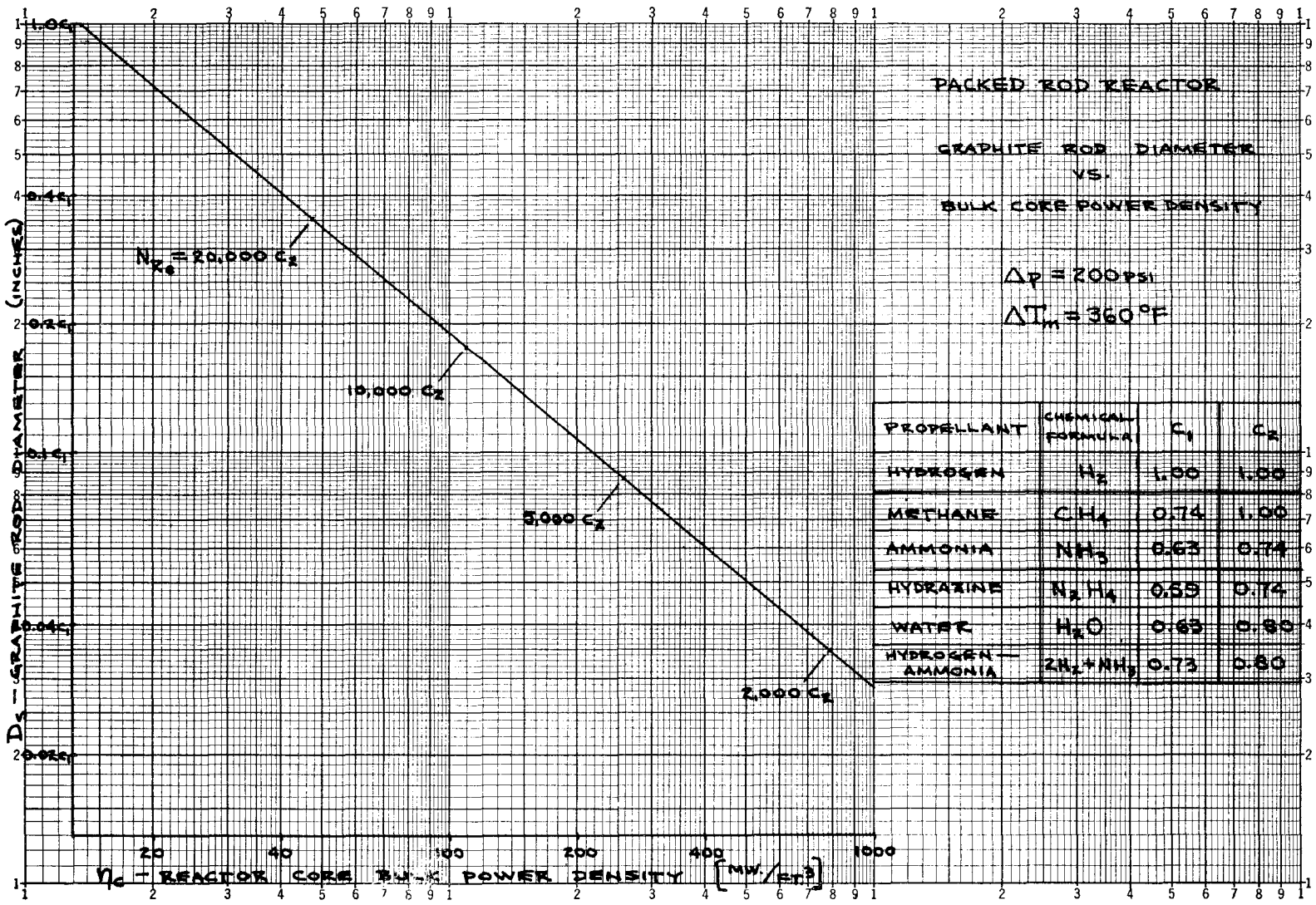

PROPELLANT	CHEMICAL FORMULA	C_1	C_2
HYDROGEN	H_2	1.00	1.00
METHANE	CH_4	0.74	1.00
AMMONIA	NH_3	0.63	0.74
HYDRAZINE	N_2H_4	0.55	0.74
WATER	H_2O	0.63	0.80
HYDROGEN — AMMONIA	$2H_2+NH_3$	0.73	0.80

FIG. 14

densities as high as 250 megawatts/ft^3 with rods of 0.090-in. in diameter and with the gas flow at a Reynolds number of 5000. This core power density is high enough to provide specific power above the minimum limit for useful nuclear rocket motors, and the rod diameter, though small, is sufficient to give some assurance of constructional feasibility. It would seem reasonable to conclude that the packed rod reactor core would be capable of use as a rocket vehicle power source. The construction of such a packed rod reactor, while much less difficult than the packed sphere or porous tube systems, would be a monumental task. The chief constructional difficulties would be the manufacture of the many small-diameter and satisfactorily coated rods and the fabrication and assembly of the internal rod support structure of the core. The most obvious means of supporting the rods is on metallic gridwork or on perforated plates; however, both methods suffer from the problems of local stress concentration at the support points and of serious gas flow restriction at the gas passage outlets if the rods and support structure holes fail to line up properly. It would probably be necessary to utilize a support plate that accurately located each rod in relation to the gas outlet passages, and although this might be accomplished by electroplating processes, among other methods, it would still prove to be a difficult and expensive task. It is believed that the stacked plate reactor system offers sufficient constructional advantages to offset its slightly smaller component dimensions at comparable power density levels.

Stacked Plate Reactor. A stacked plate reactor core structure consisting of thin parallel plates of graphite spaced at equal intervals was next considered with the aim of decreasing or eliminating the constructional difficulties that are inherent in each of the three reactor types considered previously. It seems self evident that the manufacture of a number of flat plates of given surface area and thickness will be simpler and cheaper than the manufacture of a number of rods of diameter comparable to the plate thickness and with the same total surface area. The difficulties and expense of the uranium carbide and hydrogen-resistant metallic carbide coating application would also be less for the flat plate system than for the packed rod, packed sphere, or porous tube reactor systems.

The flat plates could be supported within the core by a propellant-cooled molybdenum or columbium metallic structure and/or by graphite support plates. The use of a propellant-cooled, boron carbide, control rod inserted in the core seems feasible.

The most interesting result of the stacked plate reactor study is the relation between the bulk core power density, the gas pressure drop, the plate-to-gas temperature difference, the gas flow Reynolds number, and the plate thickness. This relation was found to be

$$t = \frac{1.130\left(\frac{\Delta p}{200}\right)^{1/2}\left(\frac{\Delta T_m}{360}\right)^{3/2}}{\eta_c\,(N_{Re})^{0.21}\,(k_g)^{0.21}\left(\frac{mw}{\bar{c}_p^2}\right)^{1/2}} - \frac{1.009\left(\frac{mw}{\bar{c}_p^2}\right)^{1/2}(k_g)^{1.01}\,(N_{Re})^{1.01}}{\left(\frac{\Delta p}{200}\right)^{1/2}\left(\frac{\Delta T_m}{360}\right)^{1/2}}$$

and is shown in Fig. 15, for $\Delta p = 200$ lb/in.^{2} and $\Delta T_m = 360°$F, for several values of Reynolds number for all the propellants considered.

For core gas flow in the turbulent regime, Fig. 15 indicates that bulk

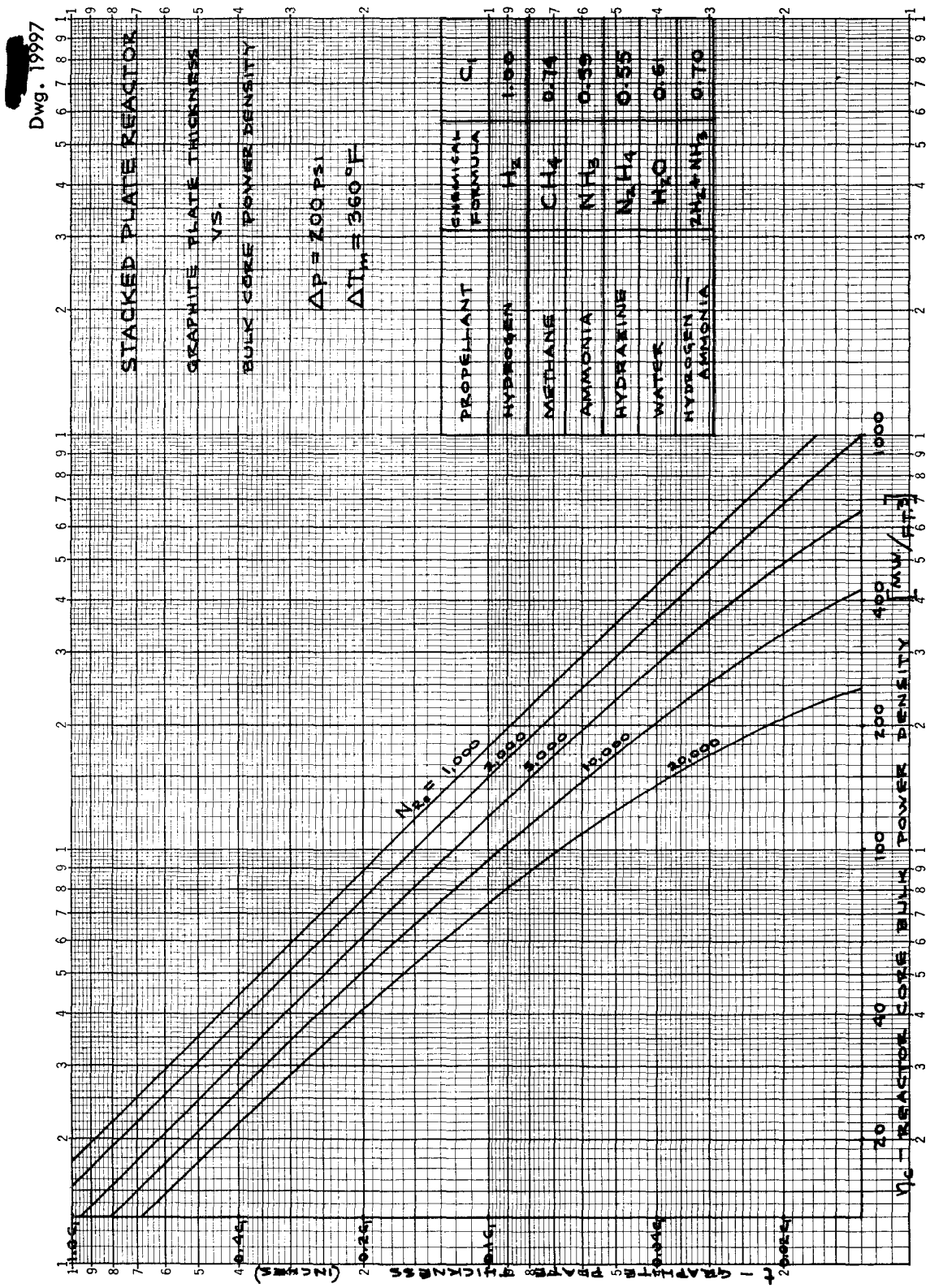
Dwg. 19997
STACKED PLATE REACTOR
GRAPHITE PLATE THICKNESS
VS.
BULK CORE POWER DENSITY
ΔP = 200 PSI
ΔTw = 360°F
PROPELLANT
HYDROGEN
METHANE
AMMONIA
HYDRAZINE
WATER
HYDROGEN — AMMONIA
CHEMICAL FORMULA
H2
CH4
NH3
N2H4
H2O
2H2+NH3
Cf
1.00
0.74
0.59
0.55
0.61
0.70
Nu = 1,000
2,000
5,000
10,000
20,000
ηc — REACTOR CORE BULK POWER DENSITY [MW/FT3]
20
40
100
200
400
1000

FIG. 15

core power densities of the order of 150 megawatts/ft^3 could be obtained with graphite plate thicknesses of 0.090 inch. This thickness is satisfactory from the fabrication standpoint and would provide sturdy core structural elements which could be manufactured relatively inexpensively, even on an experimental basis. In order to attain power densities of the order of 500 megawatts/ft^3, it would be necessary to consider plate thicknesses of 0.035 in., which would seem to be about the limit of constructional feasibility. Higher power densities may, of course, be obtained by operation at higher allowable gas pressure drops or plate-to-gas temperature drops.

Compared to the other systems, the stacked plate reactor core appears advantageous because of the larger component sizes (exclusive of thickness), hence fewer required pieces, simplicity of fabrication and assembly, and relative cheapness of construction. The support of the structural pieces of the core - porous tubes, rods, spheres, or plates - is obviously simpler for the stacked plate system than for any other. The reactor core could consist of a number of hexagonal "boxes" stacked together in a cylindrical pattern, each box could be made from molybdenum and would contain a specified number of graphite plates supported by molybdenum channels at the top and bottom of the plate sections. This arrangement would be much less complex than the support structure which would be required for the packed rod core, for example, where it might be necessary to use individual support pads at each rod end so that the gas flow would not be excessively restricted.

Because of the acceptably high power densities theoretically attainable from the stacked plate reactor core, and the reasonable simplicity of the core structural and heat transfer elements, it would appear that the stacked plate type of core structure offers the most promise for useful nuclear-powered rocket motors.

REACTOR NUCLEAR REQUIREMENTS

Approximate critical mass calculations based on the work of Mills[1] were made for a homogeneous carbon reflected reactor over a range of core graphite volume fractions. A constant zirconium (assumed coating material) volume fraction of 0.05 and a constant molybdenum (assumed structural material) volume fraction of 0.10 were used. The reflector thickness was taken as 10 in., and a typical core length and diameter of 90 in. was chosen.

Multigroup analyses of equivalent reflected reactor configurations were examined to supplement and to check the approximate solutions for several specific values of graphite core volume fraction. The results of these calculations are shown in Fig. 16. Further criticality calculations were made, over a range of molybdenum volume fractions, for a fixed graphite volume fraction of 0.50 and zirconium volume fraction of 0.05. The results are shown in Fig. 17. From Figs. 16 and 17, it may be concluded that excessive critical masses will be required for carbon volume fractions less than 0.35, and for molybdenum volume fractions greater than approximately 0.15.

To show the effect of reactor size on critical mass, approximate criticality calculations were made over a range of core diameters for a fixed graphite volume fraction of 0.50 and fixed zirconium and molybdenum volume fractions of 0.05 and 0.10, respectively. Multigroup calculations were performed to obtain the desired data for reactor cores smaller than 60 in. in diameter. The results of these calculations are shown in Fig. 18.

From Fig. 18, the uranium bulk density within the reactor core was determined as a function of the core diameter. The variation of uranium density with core diameter is shown in Fig. 19.

It can be seen from Fig. 19 that the uranium density within the core rises quite rapidly as the core diameter

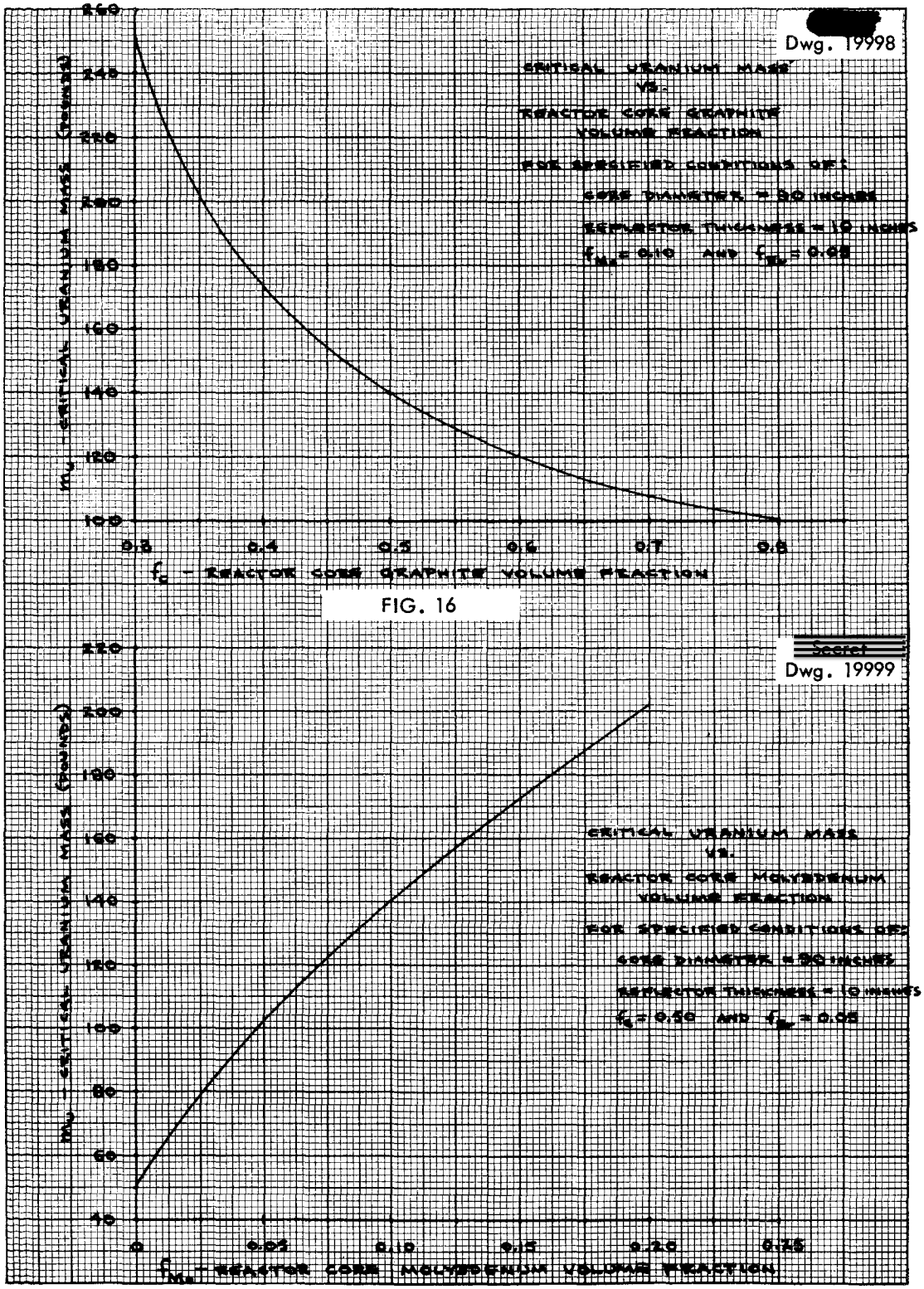
Dwg. 19998
CRITICAL URANIUM MASS VS. REACTOR CORE GRAPHITE VOLUME FRACTION
FOR SPECIFIED CONDITIONS OF:
CORE DIAMETER = 30 INCHES
REFLECTOR THICKNESS = 10 INCHES
f_{Mo} = 0.10 AND f_{Be} = 0.02
CRITICAL URANIUM MASS (POUNDS)
260
240
220
200
180
160
140
120
100
0.3
0.4
0.5
0.6
0.7
0.8
f_g - REACTOR CORE GRAPHITE VOLUME FRACTION

FIG. 16

Secret
Dwg. 19999
CRITICAL URANIUM MASS VS. REACTOR CORE MOLYBDENUM VOLUME FRACTION
FOR SPECIFIED CONDITIONS OF:
CORE DIAMETER = 30 INCHES
REFLECTOR THICKNESS = 10 INCHES
f_g = 0.50 AND f_{Be} = 0.05
CRITICAL URANIUM MASS (POUNDS)
220
200
180
160
140
120
100
80
60
40
0
0.05
0.10
0.15
0.20
0.25
f_{Mo} - REACTOR CORE MOLYBDENUM VOLUME FRACTION

FIG. 17

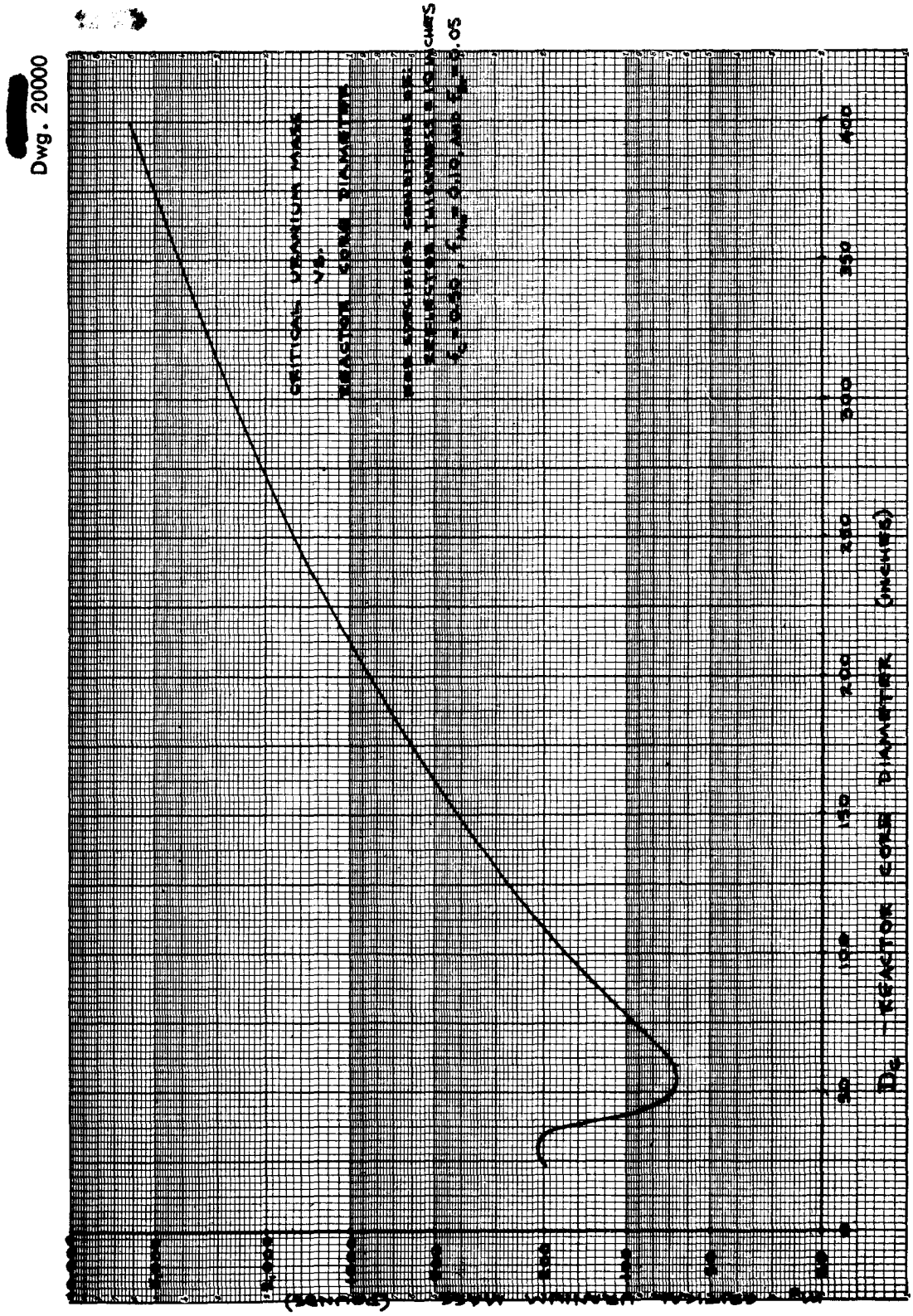
Dwg. 20000
CRITICAL URANIUM MASS
REACTOR CORE DIAMETER
Dc - REACTOR CORE DIAMETER (INCHES)

FIG. 18

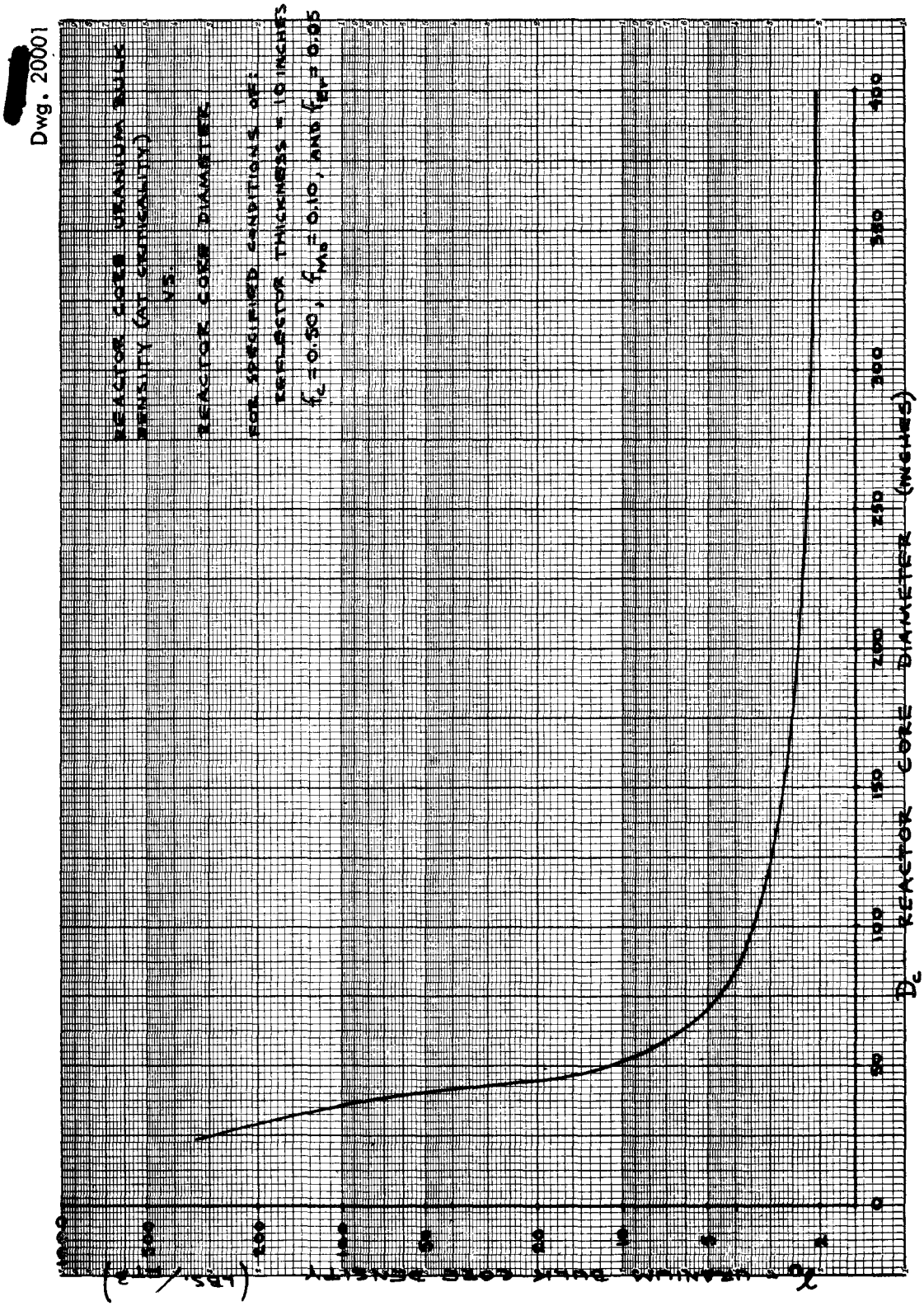
Dwg. 20001
REACTOR CORE URANIUM BULK DENSITY (AT CRITICALITY) VS. REACTOR CORE DIAMETER
FOR SPECIFIED CONDITIONS OF: REFLECTOR THICKNESS = 10 INCHES
$f_c = 0.50$, $f_{Mo} = 0.10$, AND $f_{Er} = 0.05$
χ_0 = URANIUM BULK CORE DENSITY (GRAMS/LITER)
D_c REACTOR CORE DIAMETER (INCHES)
0
50
100
150
200
250
300
350
400
4
6
8
10
12
14
16

FIG. 19

becomes smaller than 45 inches. For purposes of this study, the minimum core diameter was arbitrarily chosen as 25 inches. This specified minimum core size fixes the minimum rocket motor outside diameter; hence the minimum vehicle diameter.

ROCKET MOTOR STRUCTURE

In order to determine the effective specific power of the nuclear rocket motor, as previously defined, it is necessary to know the over-all weight density of the rocket motor and the bulk power density of the reactor core. The over-all weight density of the rocket motor, and hence the specific power, will depend upon the size of the reactor because the carbon reflector thickness is constant and independent of the reactor diameter and length. In order to determine the variation of the specific power with rocket motor size, the following conditions were assumed:

1. The material volume fractions within the core are: graphite, 0.50; Zr, 0.05; and Mo, 0.10; the remainder would be void volume for gas flow. The core length-to-diameter ratio was assumed to be 1.0.

2. The core would be reflected on the sides and top with a constant carbon reflector thickness of 10 inches.

3. The reactor pressure shell would be cylindrical, with a 2:1 ellipsoidal top end cap, and with a cylindrical length-to-diameter ratio of 1.0. This configuration would provide sufficient thickness above the core-top reflector for an adequate surge tank volume of liquid propellant which would also serve as a fast neutron shield and gamma radiation energy absorber. The pressure shell material could be 75ST-6 aluminum with a tensile yield strength of 67,000 psi.

4. The nozzle could be constructed with porous nickel walls, an outer shell of 75ST-6 aluminum, and an inner throat and gas entrance section liner of porous graphite. In order to simplify the equations, the nozzle was assumed to have 40% porosity and to be constructed entirely of nickel.

For a rocket motor external diameter D_r, in inches, the total volume of the pressure shell is given approximately by

$$(1)\quad V_s \cong [D_r^2 - (D_r - 2t_s)^2]\ (D_r)\ .$$

The shell thickness, t_s, is determined by allowable stress considerations to be

$$(2)\quad t_s = \frac{p_0 D_r\ f_s}{2s_s}\ .$$

Now, for a maximum system pressure of 1700 psi, a tensile yield strength of 67,000 psi, and a design safety factor of 2.5, Eq. 2 reduces to

$$(3)\quad t_s = 0.0317\ D_r\ .$$

Equations 1 and 3 may be combined to give pressure shell volume as

$$(4)\quad V_s = 0.1228\ D_r^3\ .$$

For a nozzle with exit-area to throat-area ratio of 35:1, the minimum nozzle bulk volume was determined to be approximately 30% of the pressure shell volume. Thus

$$(5)\quad V_{n(bulk)} = 0.30\ V_s$$

and the solid volume of the nozzle will be

$$(6)\quad V_n = (0.30)(1 - \text{porosity})V_s = 0.18\ V_s = 0.0221\ D_r^3\ .$$

The volume of the 10 in. thick carbon reflector is given by

$$(7)\quad V_{refl} = 34.45\ (D_r^2 - 25.62\ D_r + 182.3)$$

and the core volume is given by

$$(8)\quad V_c = 0.6453\ (D_r - 21.35)^3\ .$$

Now the nuclear rocket motor specific power, in megawatts per pound of total rocket motor weight, is given by

$$(9)\quad \overline{p} = \frac{\eta_c V_c}{1728\ m_r}$$

where m_r, the total rocket motor weight, is determined from the sum of the component weights to be

$$(10)\quad m_r = \gamma_s' V_s + \gamma_n' V_n + \gamma_{refl}' V_{refl} + V_c\ (\gamma_C' f_C + \gamma_{Zr}' f_{Zr} + \gamma_{Mo}' f_{Mo})\ .$$

The material densities and the core volume fractions for the rocket motor configuration discussed previously are given below.

	MATERIAL	γ' (lb/in.^{3})	f_{core}
γ'_C and γ'_{refl}	C	0.0615	0.50
γ'_{Zr}	Zr	0.2315	0.05
γ'_{Mo}	Mo	0.3686	0.10
γ'_s	Al	0.1009	
γ'_n	Ni	0.3219	

By using the above values, and combining Eqs. 4, 6, 7, and 8 with 9 and 10, the specific power is shown to be related to the bulk core power density and the rocket motor outside diameter by

$$(11) \qquad \frac{\eta_c}{\overline{p}} = \frac{52.23 + 5674\left(\frac{1}{D_r} - \frac{25.62}{D_r^2} + \frac{182.3}{D_r^3}\right)}{\left(1 - \frac{21.35}{D_r}\right)^3} + 136.8 \ .$$

Figure 20 shows the parameter $\eta_c/\overline{p}$ as a function of D_r.

From Fig. 20, it may be seen that the rocket motor specific power will be low for small size reactors; hence the rocket motor weight will be a large fraction of the total loaded vehicle weight for small vehicles. The motor weight per unit vehicle weight drops as the vehicle size increases; therefore it may be concluded that large nuclear-powered rocket vehicles are more practical than small vehicles from the standpoint of motor dead weight.

The variation of motor specific power with size is too great to permit the choice of a "typical" value for use in the vehicle study (Part I). For the vehicle study, it is necessary to know the rocket motor weight as a function of the reactor power output and thus as a function of the total loaded vehicle weight. This relation can be obtained by use of Eq. 11 or Fig. 20 and the equation

$$(12) \qquad P_r = m_r \overline{p} \ .$$

See Part I for the complete determination of the rocket motor weight equation.

In practice, Eq. 11 is cumbersome to work with, and it is therefore desirable to obtain a simple expression for $\eta_c/\overline{p}$ as a function of D_r. It was found possible to fit an equation of the form

$$\frac{\eta_c}{\overline{p}} = A + \frac{B}{D_r^n}$$

to Eq. 11 with fair accuracy. This equation and its deviation from Eq. 11 are given below.

$$(13) \qquad \frac{\eta_c}{\overline{p}} = 200 + \frac{3.46 \times 10^5}{D_r^{1.69}}$$

RANGE OF D_r (in.)	MAXIMUM DEVIATION (%)
$1000 < D_r < \infty$	5
$60 < D_r < 1000$	2½
$50 < D_r < 60$	11½

RADIATION HEATING OF PROPELLANT

In any nuclear fission process, some of the fission energy is given off as high-energy gamma rays (5 to 7 Mev per photon). This gamma ray energy, whether absorbed in a conventional shield of dense material or in the propellant itself, must be dissipated eventually by absorption in the propellant because there is no other coolant available in the rocket system.

[redacted] Dwg. 20002

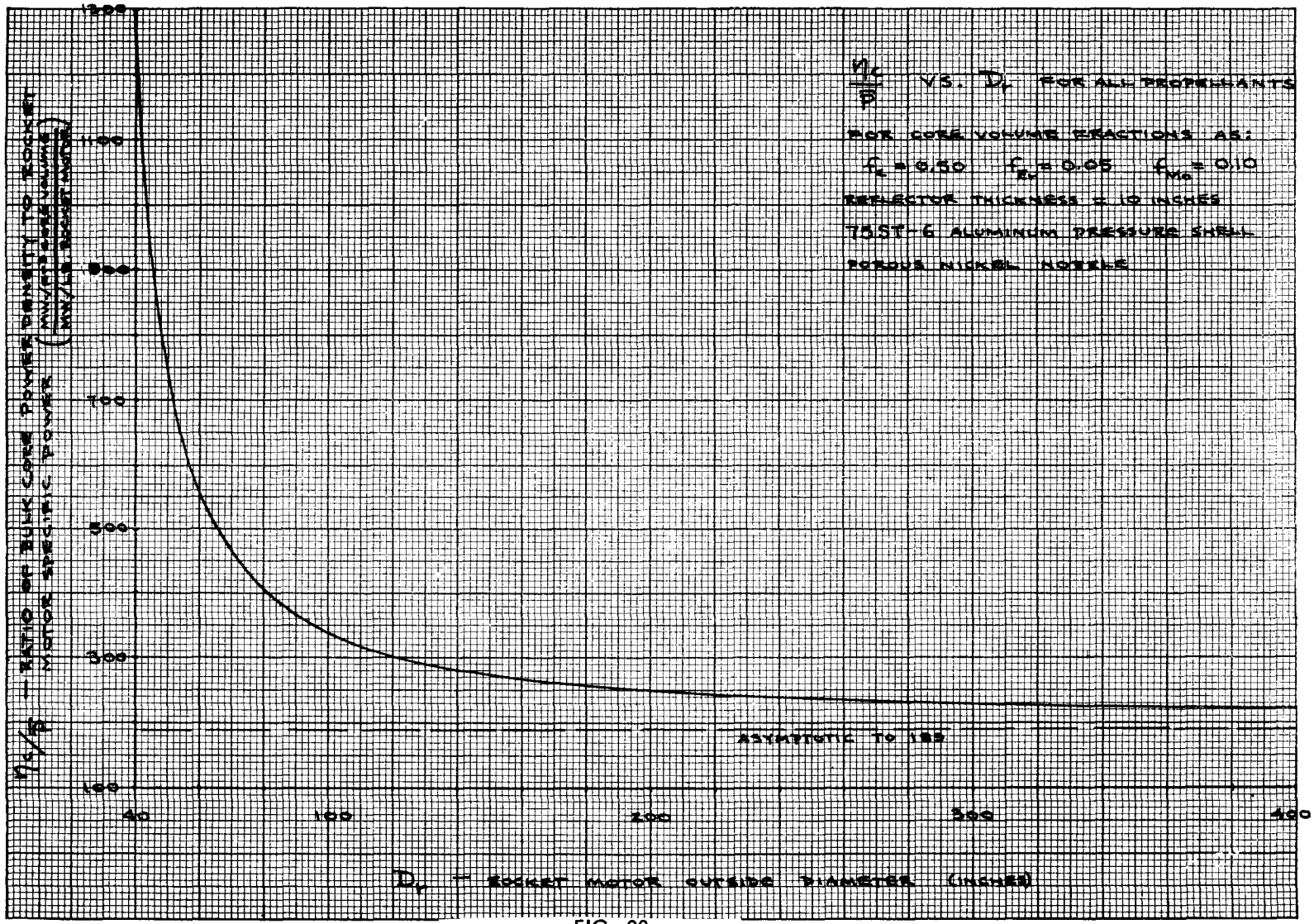

FIG. 20

A second source of volume heating external to the reactor core is that caused by thermalization of the high-energy neutrons that leak out of the core. It is desirable that these fast neutrons be thermalized and absorbed close to the reflector, before they reach a region of material with high absorption cross section (pumps, turbines, lines, valves, etc.), in order to minimize the production of secondary gamma rays by (n,γ) reactions. Neutron thermalization is best accomplished in media of low molecular weight and low neutron absorption cross section; thus the vehicle propellant (predominantly hydrogen, with hydrogen densities comparable to the hydrogen density of water) can serve as an excellent fast neutron shield. The thermal neutrons leaving this propellant shield region can be absorbed conveniently in a layer of boron carbide or other suitable material.

The rocket motor geometry, as previously specified, provides for several feet of liquid propellant above the core top reflector and inside the rocket motor pressure shell; thus the neutron thermalization will be essentially complete within the rocket motor, and secondary gamma emission from structure external to the rocket motor will be small compared to the primary gamma flux from the reactor core plus that from (n,γ) reactions within the propellant shield.

In order to avoid the use of conventional lead or iron gamma shielding, hence additional dead weight in the vehicle, it seems desirable to use the propellant directly as the gamma-energy absorber. By assuming that the density of hydrogen in the liquid propellant is about that of the hydrogen density of water and that the gamma absorption characteristics are the same, the attenuation of the gamma flux can be approximately expressed by

$$I = I_0 \, e^{-\mu_p x} \tag{1}$$

where μ_p is the gamma absorption coefficient of the propellant (in cm^{-1}), x is the absorber thickness (in centemeters), and I_0 and I are the radiation intensities before and after attenuation.

The approximate propellant thickness required for an attenuation of 100 in the gamma flux is given from Eq. 1 as

$$x_{100} = \left(\frac{1}{\mu_p}\right) \ln \left(\frac{I_0}{I}\right) = \frac{4.6}{\mu_p}. \tag{2}$$

The absorption coefficient for water is roughly 0.04 cm^{-1} for 3-Mev photons; thus the propellant thickness for an attenuation of 100 is determined from Eq. 2 is 115 cm, or 3.8 feet. Since the volumetric heating in the propellant is approximately proportional to the gamma flux at any point (if neutron thermalization is neglected), we find that 99% of the total power generated within the propellant will occur in the first 3.8 ft of propellant nearest the reactor. This internal heating is sufficient to cause vaporization of some of the propellant; in order to avoid propellant loss, this vaporization should be made to occur within the pressure shell of the rocket motor. For the rocket motor geometry previously described, which has a 2:1 ellipsoidal end cap on the motor pressure shell, the propellant-filled space between the reflector top and the end cap is about $[(D + 4)/4]$ ft in thickness; thus adequate gamma shield thickness for rocket motor diameters greater than 8 ft is provided. Rocket motors of smaller diameter will require longer, hence heavier, pressure shell structures per unit reactor core volume in order to attain the desired 3.8 ft of propellant above the top reflector and within the pressure shell. This propellant layer acts as both a fast-neutron shield and a gamma radiation shield for the main propellant tanks.

The power generated within the propellant is obviously equal to the total power leaking from the reactor core as neutron and gamma radiation, multiplied by the ratio of the effective

area radiating to the propellant to the total radiating area, plus the power that results from secondary radiation induced by the primary fast-neutron flux in the structure that is external to the rocket motor. This power can be expressed in Btu/sec by

$$Q_p = 946\,\bar{A}P_r f_e \quad , \tag{3}$$

where $\bar{A}$ is the area ratio defined above, P_r is total reactor power in megawatts, and f_e is the fraction of fission energy escaping the reactor core in the form of photon and fast neutron radiation. The loss-energy fraction, f_e, was taken as 0.08; thus 16 Mev/fission are considered to be to be dissipated external to the reactor core. This value must approximately account for power generation by secondary radiation as well as that caused by the primary neutron and gamma flux. Considerations of previous shielding studies made at ORNL indicate that 16 Mev/fission is a realistic figure for the purposes of this study. The effective area ratio, $\bar{A}$, is determined by geometrical considerations, as below.

In Fig. 21, assume that the propellant area normal to the radiating flux is the circle of diameter D at plane A-A, and that the total spherical area normal to the radiating flux is the sphere of diameter $\sqrt{2}\,D$. the effective area ratio is then given by

$$\bar{A} = \frac{\left(\frac{\pi}{4}\right)(D^2)}{(\pi)(\sqrt{2}\,D)^2} = 0.125 \ .$$

Now, the rate of vaporization of propellant will be given by

$$w_{vap} = \frac{946\,\bar{A}P_r f_e}{H_v} \tag{4}$$

where w_{vap} is in lb/sec and H_v is the latent heat of vaporization of the propellant, in Btu/lb.

The total weight flow rate of propellant required for the rocket vehicle propulsive system is obtained from Eqs. 18 and 19, Part I, this report, as

$$w_p = 47.5\frac{P_r}{\left(\frac{v_m}{10^3}\right)^2} \tag{5}$$

where v_m is the maximum theoretical exhaust velocity of the propellants used in this study and appears in Table 4, Part I.

When Eqs. 4 and 5 are combined, the fraction of propellant vaporized external to the reactor core is

$$\frac{w_{vap}}{w_p} = 19.9\frac{\bar{A}f_e\left(\frac{v_m}{10^3}\right)^2}{H_v} \ . \tag{6}$$

Using values for $\bar{A}$ and f_e as determined previously, Eq. 6 is reduced to

$$\frac{w_{vap}}{w_p} = 0.199\frac{\left(\frac{v_m}{10^3}\right)^2}{H_v} \ . \tag{7}$$

Values of H_v at atmospheric pressure, $(v_m/10^3)^2$, and w_{vap}/w_p are given in Table 7 for each propellant considered.

It can be seen from Table 7 that nearly all of the propellant in a pure hydrogen system will be vaporized within the rocket motor pressure shell before the propellant reaches the reactor core, while in the ammonia, hydrazine, and water systems, there will be relatively little vaporization external to the core.

Propellant vaporization outside the core, but within the pressure shell,

TABLE 7. HEAT OF VAPORIZATION AND FRACTION OF PROPELLANT VAPORIZED BY RADIATION HEATING

PROPELLANT	H_v*	$(v_m/10^3)^2$	w_{vap}/w_p
Hydrogen	197	962	0.972
Methane	248	268	0.215
Ammonia	587	227	0.077
Hydrazine	602	181	0.060
Water	969	152	0.031
Hydrogen and ammonia	513	367	0.142

*H_v data obtained from refs. 20, 21, and 22.

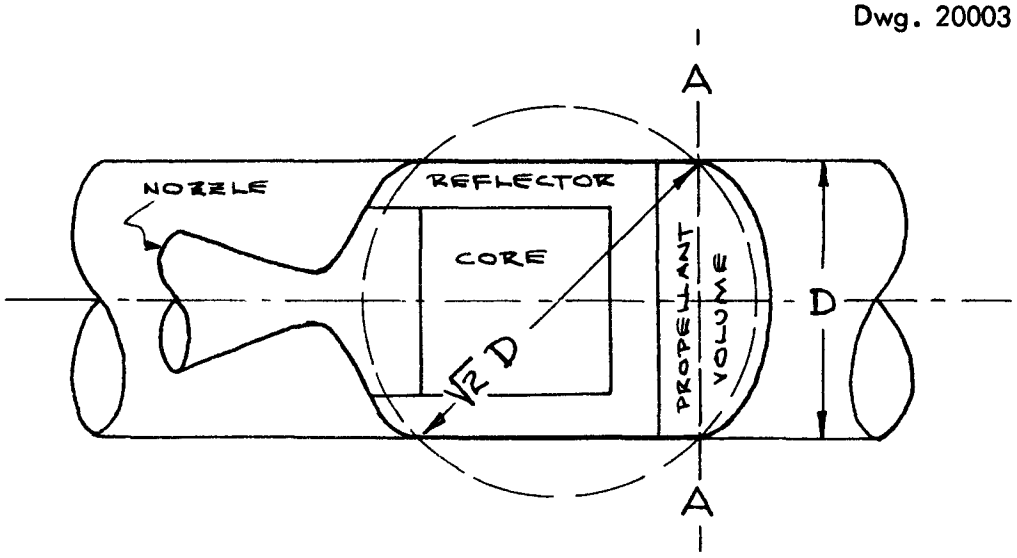

ROCKET MOTOR GEOMETRY ASSUMED FOR PROPELLANT SHIELD CALCULATIONS

FIG. 21

is certainly not detrimental to the reactor design or theoretical vehicle performance. The external vaporization serves to reduce the energy expenditure, hence heat transfer and gas pressure drop requirements within the reactor core itself; thus lighter weight reactors for the same total power output can be used.

REACTOR CORE DESIGN

Porous Tube Reactor. It is shown by the work of Green[8] that, for gas flow through a porous-wall heat source of high thermal conductivity, the temperature distribution across the porous wall of thickness t is given by

$$(1) \qquad (T - T_0) = \frac{qt}{Gc_{pg}} \left[\frac{x}{t} + \frac{1 - e^{-(Gc_{pg}t/k_s)(1-x/t)}}{\left(\frac{Gc_{pg}t}{k_s}\right)} \right],$$

from which the expression for the wall temperature drop, ΔT_H, is obtained:

$$(2) \qquad \Delta T_H = T_{x=t} - T_{x=0} = \frac{qt}{Gc_{pg}} \left[1 - \frac{1 - e^{-(Gc_{pg}t/k_s)}}{\left(\frac{Gc_{pg}t}{k_s}\right)} \right].$$

From ref. 8, for calculation of the gas pressure drop across the wall, it will be found convenient to use an average gas temperature defined as

$$(3) \qquad T_{avg} = \frac{1}{t}\int_0^t T dx$$

which becomes

$$T_{avg} = \frac{qt}{2Gc_{pg}} + \frac{k_s \Delta T_H}{Gc_{pg}t}$$

by use of Eqs. 1 and 2. Now from refs. 7 and 8, the gas flow through the wall is shown to be approximately

described by

$$(4)\quad \frac{p_0^2 - p_i^2}{t} = 2b\,\alpha\,\mu' T_{avg} G + \frac{6\beta}{6g_c} T_{avg} G^2 ,$$

but

$$(5)\quad p_0 = p_{avg} + \frac{\Delta p}{2}$$

and

$$p_i = p_{avg} - \frac{\Delta p}{2} ;$$

thus Eq. 4 can be written as

$$(6)\quad \frac{2p_{avg}\Delta p}{t} = (GT_{avg}) \left(2b\,\alpha\,\mu' + \frac{6\beta}{6g_c}\right) .$$

The stresses induced in the wall by external pressure loading are given by

$$(7)\quad s_L = \frac{\Delta p D_H}{2t}$$

for thin tube walls, while the thermal stresses can be closely approximated by

$$(8)\quad s_{th} = \frac{\Delta T_H EB}{2(1-\sigma)} .$$

For pressure loading, the stresses on the inner and outer tube surfaces are both compressive; however, for thermal loading under the conditions assumed for reactor operation, the inner surface stress will be a compressive stress, while the outer tube surface stress will be a tensile stress. The maximum hoop stress will thus be the sum of the thermal and pressure compressive stresses; hence

$$(9)\quad s_{tot} = s_L + s_{th} .$$

Only hoop stress is considered because the pressure loading axial stress will, in general, be approximately one-half as great as the pressure hoop stress; hence the sum of the axial pressure and thermal compressive stresses will be less than the sum of the compressive hoop stresses.

The total stress, of course, must not be greater than the desired allowable working stress, hence Eqs. 7, 8, and 9 become

$$(10)\quad \frac{s_c}{f_s} = \frac{D_H \Delta p}{2t} + \frac{\Delta T_H EB}{2(1-\sigma)} .$$

Certain subsidiary relations are necessary in order to arrive at the desired parameters that describe the reactor core system design. These relations are:

Power generation

$$(11)\quad P_r = \eta_H V_H = \frac{\eta_H m\pi D_H tL}{1728}$$

for thin walled tubes.

Tube volume

$$(12)\quad \frac{m\pi}{4}(D_H + t)^2 L = \frac{\epsilon_T \pi}{4}(D_c^2) L .$$

Power density

$$(13)\quad q = 0.5486\,\eta_H .$$

Weight flow rate of gas

$$(14)\quad G = \frac{w}{A_H} \frac{w}{\pi D_H Lm} ,$$

but the reactor power output must be equal to the power absorbed and dissipated by the propellant gas; hence

$$(15)\quad P_r = 0.678 \frac{w}{g_c} \left(\frac{v_m}{10^3}\right)^2 .$$

A combination of Eqs. 14 and 15 yields a relation between weight flow rate per unit area of tube surface and total reactor power:

$$(16)\quad G = \frac{1.474\, g_c P_r}{\pi \left(\frac{v_m}{10^3}\right)^2 D_H Lm} .$$

For optimum design of a cylindrical homogeneous reactor, the ratio of reactor length to diameter should be approximately 0.93. For convenience,

this ratio shall be taken as 1.0; hence

$$\frac{L}{D_c} = 1.0 \quad (17)$$

Thus, from Eqs. 20, 18, and 2, ΔT_H can be expressed as

$$\Delta T_H = \frac{c_2}{c_1 c_{pg}} \left\{ 1 - \frac{1 - \exp\left[- c_1 \frac{(D_H + t)^2}{D_H} \frac{P_r}{\epsilon_T D_c^3} \frac{c_{pg} t}{k_s} \right]}{\left[c_1 \frac{(D_H + t)^2}{D_H} \frac{P_r}{\epsilon_T D_c^3} \frac{c_{pg} t}{k_s} \right]} \right\}, \quad (21)$$

Now, combining Eqs. 12, 16, and 17 yields an expression for the gas weight flow rate

$$G = c_1 \frac{(D_H + t)^2}{D_H} \frac{P_r}{\epsilon_T D_c^3} \quad (18)$$

where

$$c_1 = \frac{1.474\ g_c}{\pi \left(\frac{v_m}{10^3} \right)^2} .$$

Equations 11, 12, 13 and 17, when combined, yield an expression for the core structure power density

$$q = c_2 \frac{(D_H + t)^2}{D_H t} \frac{P_r}{\epsilon_T D_c^3} \quad (19)$$

where

$$c_2 = \frac{(0.5486)(1728)}{\pi} .$$

Equations 18 and 19, when combined, yield

$$\frac{qt}{G} = \frac{c_2}{c_1} . \quad (20)$$

and from Eq. 3, T_{avg} can be written as

$$T_{avg} = \frac{c_2}{2 c_1 c_{pg}} + \frac{k_s}{c_1 c_{pg} t} \frac{D_H}{(D_H + t)^2} \frac{\epsilon_T D_c^3}{P_r} \Delta T_H . \quad (22)$$

The solution of Eq. 10 for $\Delta p/t$ yields

$$\frac{\Delta p}{t} = \left[\frac{2sc}{f_s} - \frac{\Delta T_H EB}{(1 - \sigma)} \right] \left(\frac{1}{D_H} \right) . \quad (23)$$

Now, by introducing the parameters

$$\lambda = \frac{(D_H + t)^2}{D_H}$$

and

$$\theta = \frac{P_r}{\epsilon_T D_c^3} ,$$

and by combining Eqs. 6, 18, 21, 22, and 23, the final relation involving gas flow, power generation, heat transfer, and thermal and pressure stresses in the reactor core is

$$2 p_{avg} \left[c_7 - 2 c_8 c_5 \left(1 - \frac{1 - e^{- c_6 \lambda \theta t}}{c_6 \lambda \theta t} \right) \right] = \left[c_3 \lambda \theta + c_4 (\lambda \theta)^2 \right] \left[c_5 D_H + \frac{2 c_5 D_H}{c_6 \lambda \theta t} \left(1 - \frac{1 - e^{- c_6 \lambda \theta t}}{c_6 \lambda \theta t} \right) \right] , \quad (24)$$

where

$$c_1 = \frac{1.474\ g_c}{\pi\left(\frac{v_m}{10^3}\right)^2} \text{ as before}$$

$$c_2 = \frac{(0.5486)(1728)}{\pi} \text{ as before}$$

$$c_3 = 2b\ \alpha\ \mu' c_1$$

$$c_4 = \frac{6\beta c_1^2}{6g_c}$$

$$c_5 = \frac{c_2}{2c_1 c_{pg}}$$

$$c_6 = \frac{c_1 c_{pg}}{k_s}$$

$$c_7 = \frac{2sc}{f_s}$$

$$c_8 = \frac{EB}{(1-\sigma)}$$

The material properties necessary to evaluate the foregoing constants are E, B, σ, s_c, k_s, α, and β. The necessary gas properties are b, μ', v_m and c_{pg}. Other information required for a useful solution of Eq. 24 is the average system pressure, P_{avg}, and the desired maximum gas temperature, T_c.

From the National Carbon Co. handbook, the following information was obtained for National Carbon Co. grade No. 30 porous graphite:

s_c = 520 psi
E = 0.2×10^6 psi
B = 5.9×10^{-6} in./in.·°F at 4500°F
σ = 0.2
k_s = 0.93×10^{-3} Btu/sec in.°F.

Reference 8 gives $\alpha = 8.4 \times 10^6/\text{in.}^2$ and $\beta = 4.9 \times 10^3/\text{in.}$ for grade No. 30 porous carbon.

The maximum theoretical propellant gas velocity is

$$v_m = \sqrt{\frac{2g_c k}{k-1}\frac{R_u}{mw}T_c}$$

(see Eq. 35, Part 1) and the gas constant is

$$b = \frac{1.856 \times 10^4}{mw}.$$

Now, since

$$(mw)(c_{pg}) = \frac{kR_u}{(k-1)J},$$

then

$$v_m^2 = 2g_c J c_{pg} T_c\ ;$$

thus

$$c_1 = \frac{6.06 \times 10^{-2}}{c_{pg}}$$

for any gas at T_c = 4960°R.

The other required conditions are P_{avg} = 1500 psi and T_c = 4960°R.

By using the data given above, Eq. 24 can be reduced to

$$(26)\quad \left[\frac{2sc}{f_s} - 7350\left(1 - \frac{1 - e^{-65.5\lambda\theta t}}{65.5\lambda\theta t}\right)\right] = \left[1.89 \times 10^{10}\ \frac{\mu'\lambda\theta}{(mw)c_{pg}} + \frac{1727(\lambda\theta)^2}{(mw)c_{pg}}\right]\left[0.83 D_H + \frac{0.02535}{\lambda\theta t}\left(1 - \frac{1 - e^{-65.5\lambda\theta t}}{65.5\lambda\theta t}\right)\right].$$

The following values were used in preliminary calculations for hydrogen gas:

b = 0.93×10^4 in./°R
μ' = 4.01×10^{-9} lb·sec/in.^{2} at 2500 to 3000°F
v_m = 31,000 ft/sec (see Part I)
c_{pg} = 4.0 Btu/lb·°R.

By solving Eq. 26 graphically, it was found that the value of the right side of the equation, for the range of interest of D_H and t, was always less than 30 for all values of $\lambda\theta t$ less than 0.1 and was always close to zero for all $\lambda\theta t$ less than 0.01. Thus, when the right hand side of the

equation is denoted by Φ_R and the equation is rearranged,

$$(27)\quad \frac{1 - e^{-65.5\lambda\theta t}}{65.5\,\lambda\theta t} = 1 - \frac{\frac{2sc}{f_s} - \Phi_R}{7350},$$

or for $\Phi_R \approx 0$,

$$(28)\quad \frac{1 - e^{-65.5\lambda\theta t}}{65.5\lambda\theta t} = 1 - \frac{2sc}{7350 f_s}.$$

From Eqs. 24, 26, 27, and 28, it can be seen that for temperatures, pressures, and porosities of the order of magnitude considered, the relation between λ, θ, and t within the reactor core is virtually independent of the gas properties and the viscous and inertial flow coefficients of the porous material. This relation depends only upon the desired design safety factor and the physical properties of the porous material.

Using the materials properties data given previously and a design safety factor of 1.0, Eq. 28 was solved to determine that

$$(29)\quad \lambda\theta t = 4.75 \times 10^{-3}.$$

Now, the reactor bulk core power density, defined as the ratio of the total reactor power output to the total core volume, is given by

$$(30)\quad \eta_c = 2200\frac{P_r}{D_c^3} = 2200\,\theta\epsilon_T.$$

Combining Eqs. 29 and 30 and reintroducing the defined expression for λ, an equation relating porous tube diameter and wall thickness to reactor core power density is obtained as

$$(31)\quad \frac{\eta_c}{\epsilon_T} = \frac{10.45\,D_H}{t(D_H + t)^2}.$$

The maximum possible value for the tube core volume fraction, ϵ_T, occurs for equilateral triangular packing of the porous tubes, and is $\epsilon_T = 0.907$.

Figure 12*a* shows porous graphite tube diameters and wall thicknesses required for any given bulk core power density, as given by Eq. 31. Figure 12*b* shows the effect of the design safety factor on the power density for any given conditions of porous tube diameter and wall thickness.

Packed Sphere Reactor. For flow of gases through packed spherical beds, ref. 9 gives the gas pressure drop as the following dimensionless equation:

$$(1)\quad \frac{dF}{dx} = \frac{f' f''}{72 g_c D_s}\frac{V_0^2}{},$$

which can be written as

$$(2)\quad \frac{dF}{dx} = .288\,\frac{f' f'' G^2}{g_c \rho^2 D_s}$$

by means of the relation

$$V_0 = \frac{144\,G}{\rho}.$$

However,

$$\frac{dp}{dx} = \rho\frac{dF}{dx};$$

thus

$$(3)\quad \frac{dp}{dx} = 288\,\frac{f' f'' G^2}{g_c \rho D_s}.$$

Now, the gas density ρ at any point x through the reactor core, is given by

$$(4)\quad \rho_x = \frac{P_x(mw)}{R_u' T_{gx}}.$$

Thus, Eq. 2 becomes

$$(5)\quad p\frac{dp}{dx} = 288\,\frac{f' f'' G^2 R_u' T_{gx}}{g_c D_s (mw)} = \frac{1}{2}\frac{d(p^2)}{dx}.$$

Now, assuming that the gas temperature through the reactor length can be approximated by

$$T_{gx} = A - Be^{-x/L_c},$$

the gas temperature is then expressed by

$$(6)\quad T_{gx} = T_0 + \frac{(T_c - T_0)\, e}{(e-1)}\left(1 - e^{-x/L_c}\right)$$

for boundary conditions of

$$x = 0\,, \qquad T_g = T_0\,,$$

and

$$x = L_c\,, \qquad T_g = T_c\,.$$

Substituting Eq. 6 into Eq. 5, utilizing the relations $p_0 = p_{avg} + \Delta p/2$, and $p_L = p_{avg} - \Delta p/2$, and integrating from $x = 0$ to $x = L_c$,

$$(7)\quad \Delta p = \frac{288\, f' f'' L_c G^2 R'_u T_c}{(e-1)\, g_c D_s (mw)\, p_{avg}}$$

within 5% for $T_0 = 460°\mathrm{R}$.

Now, if the gas exit temperature, T_c, is specified to be 4960°R, the average reactor gas pressure, p_{avg}, is specified to be 1600 psi, and appropriate values for R'_u and g_c are substituted, Eq. 6 reduces to

$$(8)\quad \Delta p = 171\, f' f'' \frac{G^2 L_c}{(mw) D_s}\,.$$

As for the porous tube reactor, the weight flow rate per unit area (based upon total core cross section) may now be expressed by

$$(9)\quad G = \frac{w}{\left(\frac{\pi}{4}\right) D_c^2}\,,$$

and again, as for the porous tube reactor, the power generation is given as

$$(10)\quad P_r = 0.678\, \frac{w}{g_c} \left(\frac{v_m}{10^3}\right)^2\,.$$

If Eqs. 9 and 10 are combined with Eq. 25 in the porous tube reactor study and reduced numerically, it is found that

$$(11)\quad G = 0.242\, \frac{P_r}{c_{pg} D_c^2}\,.$$

For values of $D_s/D_c \leq 0.05$, the factor f'' in Eq. 8 is given by $0.9 < f'' < 1.0$. The factor f', for all values of D_s/D_c, is given by the relation

$$(12)\quad f' = \frac{800}{N_{Re_f}} + \frac{39}{(N_{Re_f})^{0.16}}\,,$$

where N_{Re_f} is the Reynolds number for flow purposes and is defined as

$$(13)\quad N_{Re_f} = \frac{D_s G}{\mu}\,.$$

Combining Eqs. 11, 12, and 13, f' is determined to be

$$(14)\quad f' = 2610 \left(\frac{k_g D_c^2}{P_r D_s}\right) + 47.1 \left(\frac{k_g D_c^2}{P_r D_s}\right)^{0.16}\,.$$

A combination of Eqs. 8, 11, and 14 produces the following equation for Δp:

$$(15)\quad (\Delta p)(D_s^2) = 2.352 \times 10^4\ (k_g) \left(\frac{mw}{\bar{c}_p^2}\right)\left(\frac{P_r}{D_c}\right) + 424.5\ (k_g)^{0.16} \left(\frac{mw}{\bar{c}_p^2}\right)\left(\frac{P_r}{D_c}\right)^{1.84}\left(\frac{D_s}{D_c}\right)^{0.84}\,.$$

In order to evaluate this and other equations, it is necessary to specify values of the gas properties (mw, $\bar{c}_p$, k_g, and μ) to be used in the equations. Since the properties change with temperature, they will certainly vary widely in the flow through the reactor core, where the gas is heated from essentially 0 to 4500°F. This wide temperature variation indicates that all equations involving functions of the gas properties should be solved by numerical integration in which proper values for the gas properties are substituted at each point through the core. How-

ever, solutions sufficiently accurate for the purposes of this study may be obtained by use of gas properties evaluated at an average gas temperature defined as

$$T_{avg} = \frac{1}{L_c} \int_0^{L_c} T_{gx} dx \quad . \tag{16}$$

The solution of Eq. 16, by using T_{gx} from Eq. 6, is

$$T_{avg} = T_0 + \frac{(T_c - T_0)}{(e - 1)} \quad . \tag{17}$$

Now, by taking T_0 as 460°R and T_c as 4960°R, T_{avg} becomes 3080°R. The viscosity, conductivity, molecular weight, and molar specific heat for each of the propellant gases considered is given in Table 8 for this temperature. The data was obtained primarily from refs. 10, 11, 12, 13, and 14, and by use of the assumption that the Prandtl number of the gases considered is 0.79 and is invariant with temperature.

The average values of certain functions of these properties will be found useful later, and are given for reference.

$$\left.\begin{aligned} (k_g)^{0.21}_{avg} &= 0.073 \\ (k_g)^{0.20}_{avg} &= 0.083 \\ (k_g)^{0.18}_{avg} &= 0.107 \\ (k_g)^{0.16}_{avg} &= 0.137 \end{aligned}\right\} \quad \begin{aligned} &\text{mean error} < 6\% \\ &\text{maximum error} < 15\% \end{aligned}$$

$$(k_g)^{1.48} \left(\frac{mw}{\bar{c}_p^2}\right)\Bigg|_{avg} = 9.11 \times 10^{-10}$$

mean error < 7%
maximum error < 11%

$$(k_g)^{1.01} \left(\frac{mw}{\bar{c}_p^2}\right)^{0.5}\Bigg|_{avg} = 9.98 \times 10^{-5}$$

mean error < 9%
maximum error < 17%

$$(k_g)^{1.22} \left(\frac{mw}{\bar{c}_p^2}\right)\Bigg|_{avg} = 2.32 \times 10^{-8}$$

mean error < 14%
maximum error < 21%

TABLE 8. APPROXIMATE PROPELLANT GAS PROPERTIES AT T_{avg} = 3080°R (2620°F)

LIQUID PROPELLANT	APPROXIMATE GAS COMPOSITION	AVERAGE ACTUAL mw	$\bar{c}_p$ (Btu/mole·°F)	μ (lb/sec·in.)	k_g (Btu/sec·in.·°F)	$\left(\frac{mw}{\bar{c}_p^2}\right)$
Hydrogen	1.0 H_2	1.99	8.0	1.55×10^{-6}	7.89×10^{-6}	0.031
Ammonia	0.75 H_2 0.25 N_2	8.48	8.1	2.73×10^{-6}	3.30×10^{-6}	0.129
Hydrazine	0.67 H_2 0.33 N_2	10.64	8.2	2.88×10^{-6}	2.81×10^{-6}	0.159
Methane	0.25 C_2H_2 0.75 H_2	7.81	~10	2.3×10^{-6}	3.7×10^{-6}	0.078
Water	1.0 H_2O	17.92	12.0	3.75×10^{-6}	3.18×10^{-6}	0.124
Hydrogen and ammonia	0.875 H_2 0.125 N_2	5.23	8.05	2.34×10^{-6}	4.51×10^{-6}	0.081

$$(k_g)\left(\frac{mw}{\overline{c}_p^2}\right)\Bigg|_{avg} = 3.62 \times 10^{-7}$$

mean error < 18%
maximum error < 33%

By using data from Table 8, Eq. 15 is reduced to

$$(18)\quad (\Delta p)(D_s^2) = 8.51 \times 10^{-3}\left(\frac{P_r}{D_c}\right) + 58.16\left(\frac{mw}{\overline{c}_p^2}\right)\left(\frac{P_r}{D_c}\right)^{1.84}\left(\frac{D_s}{D_c}\right)^{0.84} .$$

If the parameters $\theta = P_r/D_c$ and $\lambda = D_c/D_s$ are introduced, Eq. 18 can be written

$$(19)\quad (\Delta p)(D_s^2) = 8.51 \times 10^{-3}\,\theta + 58.16\left(\frac{mw}{\overline{c}_p^2}\right)\frac{\theta^{1.84}}{\lambda^{0.84}} .$$

The load stresses on the graphite spheres are due primarily to the pressure loading as given by Eq. 19. At any sphere midplane cross section (across the reactor core) the compressive stress will be given as

$$(20)\qquad s_{x-x} = \Delta p + W_{sph_x} ,$$

where W_{sph_x} is the weight of all the spheres above the cross-section station. Obviously, s_{x-x} will be a maximum in the bottom row of spheres; thus

$$(21)\qquad s_{x-x_{max}} = \Delta p + \frac{a_m D_c \gamma_c \epsilon_V}{1728\ \epsilon_A g_c} ,$$

where a_m is the maximum acceleration of the rocket vehicle, ϵ_V is the volume fraction of the core occupied by the spheres and is given by

$$(22)\qquad \epsilon_V = \frac{\text{total sphere volume}}{\text{total core volume}} = 0.740$$

for tetrahedral packing. The fraction of the core cross sectional area occupied by the spheres at any section through the sphere midplanes is ϵ_A, and is given by

$$(23)\qquad \epsilon_A = \frac{\text{maximum sphere cross section}}{\text{core cross section}} = 0.907$$

for tetrahedral packing. When a specific gravity of 1.70 for graphite and a maximum vehicle acceleration of $9\,g_c$ are used, Eq. 21 reduces to

$$(24)\qquad s_{x-x_{max}} = \Delta p + 0.492\,D_c .$$

Stresses at the contact points of the stacked sphere structure are, in general, higher and more highly concentrated than the simple midplane compressive stress given by Eq. 24. The contact point compressive stress due to pressure and weight loading is given in ref. 15 as

$$(25)\qquad s_{L_{theo}} = 0.918\left[\frac{F_T E^2}{D_s^2(1-\sigma^2)^2}\right]^{1/3} .$$

It is pointed out in ref. 16 that this theoretical equation has been found by experiment to predict values of stresses 4 to 5 times higher than the normal allowable stresses for the materials which were tested. In these sphere loading tests, it was found that the spheres could withstand stresses 4 to 5 times the normal allowable stresses of the material when the applied stresses were computed by Eq. 25. Hence, in order to deal only with numbers which are comparable to the normal allowable stresses of the sphere material, s_L shall be taken as equal to $s_{L_{theo}}/4$. Thus

$$(26)\qquad s_L = 0.23\left[\frac{F_T E^2}{D_s^2(1-\sigma^2)^2}\right]^{1/3} .$$

F_T is the total normal load at any one contact point between any two spheres and is a maximum on the bottom row of spheres. For tetrahedral packing, F_T is found to be

$$(27)\qquad F_T = 0.392\,(\Delta p)(D_s^2) + 5.0 \times 10^{-4}\,a_m\,(D_c)(D_s^2) .$$

Thus, combining Eqs. 26 and 27, s_L is obtained as

$$(28)\quad s_L = 0.23\left[\frac{E^2}{(1-\sigma^2)^2}\,(0.392\,\Delta p + 5.0\times 10^{-4}\,a_m\,D_c)\right]^{1/3}.$$

For solid graphite at a temperature of 4500°F, $E = 1\times 10^6$ psi and $\sigma \approx 0.2$. When these values are used, and the maximum vehicle acceleration is specified as $9\,g_c$ (see Part I), Eq. 28 becomes

$$(29)\quad s_L = 1242\,(2.705\,\Delta p + D_c)^{1/3}.$$

From ref. 17, the maximum thermal stresses that result from internal power generation in the spheres are

$$(30)\quad R_{rm} = \frac{2EB}{(1-\sigma)}\,\frac{\Delta T_s}{5},$$

which is the radial compressive stress at the sphere center, and

$$(31)\quad \Phi_{\phi m} = \frac{EB}{(1-\sigma)}\,\Delta T_s\left(\frac{17}{15} + \frac{4k_s}{3D_s h_c}\right),$$

which is the tangential tensile stress at the sphere surface. The temperature drop from the sphere center to the sphere surface, ΔT_s, is given by

$$(32)\quad \Delta T_s = \frac{qD_s^2}{24k_s}.$$

The power generation within the solid graphite spheres is given by

$$(33)\quad q = 0.5486\,\eta_c\,\frac{\epsilon_p}{\epsilon_V},$$

where ϵ_p is the fraction of the total reactor power generated within the graphite spheres by neutron and gamma heating.

The bulk core power density is, as for the porous tube reactor,

$$(34)\quad \eta_c = \frac{1728\,P_r}{\left(\frac{\pi}{4}\right)D_c^3} = 2200\frac{P_r}{D_c^3}.$$

A combination of Eqs. 33 and 34 yields

$$(35)\quad q = 1207\frac{\epsilon_p}{\epsilon_V}\frac{P_r}{D_c^3}.$$

Now, for turbulent gas flow, the sphere surface heat transfer coefficient, h_c, is given from ref. 18 as

$$(36)\quad h_c = 0.023\frac{k_g}{d_h}\left(N_{\mathrm{Re}_H}\right)^{0.8}(N_{\mathrm{Pr}})^{0.4},$$

where N_{Re_H} is the heat transfer Reynolds number and is given by

$$(37)\quad N_{\mathrm{Re}_H} = \frac{2GL_cD_s}{3\epsilon_V D_c\mu}.$$

As for the porous tube reactor, the optimum core length to diameter ratio is taken as 1.0, thus

$$(38)\quad \frac{L_c}{D_c} = 1.0$$

and Eq. 37, when combined with Eqs. 11, 22, and 38, becomes

$$(39)\quad N_{\mathrm{Re}_H} = 0.218\frac{P_r D_s}{\mu c_{pg} D_c^2},$$

and for $N_{\mathrm{Pr}} = 0.79$, as before (Table 8),

$$(40)\quad N_{\mathrm{Re}_H} = \frac{0.276\,P_rD_s}{k_gD_c^2}$$

or

$$N_{\mathrm{Re}_H} = \frac{0.276}{k_g}\,\frac{\theta}{\lambda}.$$

The "hydraulic" diameter, d_h, is defined as four times the total flow volume divided by the total "wetted" sphere surface area, and is given by

$$(41)\quad d_h = \frac{2}{3}D_s\left(\frac{1-\epsilon_V}{\epsilon_V}\right),$$

which can be reduced by Eq. 22 to obtain

$$d_h = 0.234\,D_s.$$

Now, combining Eqs. 36, 40, and 41, an equation for h_c is obtained as follows:

$$(42)\quad h_e = 0.032\,k_g^{0.2}\left(\frac{P_rD_s}{D_c^2}\right)^{0.8}\left(\frac{1}{D_s}\right).$$

From Table 8, $k_g^{0.2}|_{avg}$ is seen to be approximately 0.083; thus Eq. 42 is reduced to

$$(43)\quad h_c = 2.66 \times 10^{-3}\left(\frac{P_r D_s}{D_c^2}\right)^{0.8}\left(\frac{1}{D_s}\right).$$

When Eqs. 32 and 35 are combined and it is specified that 10% of the total reactor power is generated within the graphite spheres (thus $\epsilon_p = 0.10$), the expression for ΔT_s becomes

$$(44)\quad \Delta T_s = \frac{6.80}{k_s}\,\frac{P_r D_s^2}{D_c^3}.$$

By combining Eqs. 30 and 31 with 43 and 44, the final thermal stress equations are obtained as

$$(45)\quad R_{rm} = \frac{2.72\,EB}{(1-\sigma)}\,\frac{P_r D_s^2}{k_s D_c^3},$$

and

$$(46)\quad \Phi_{\phi m} = \frac{EB}{(1-\sigma)}\left[\frac{7.7\,P_r D_s^2}{k_s D_c^3} + 3410\left(\frac{P_r}{D_c}\right)^{0.2}\left(\frac{D_s}{D_c}\right)^{1.2}\right].$$

If the graphite properties, as specified previously, are taken to be

$E = 1 \times 10^6$ psi ,
$\sigma = 0.2$,
$B = 3.1 \times 10^{-6}$ in./in.·°F ,
$k_s = 4.17 \times 10^{-4}$ Btu/sec·in.·°F ,

and the λ and θ notation introduced for Eq. 19 is used, Eqs. 45 and 46 become

$$(47)\quad R_{rm} = 2.53 \times 10^4 \frac{\theta}{\lambda^2},$$

and

$$(48)\quad \Phi_{\phi m} = 7.18 \times 10^4 \frac{\theta}{\lambda^2} + 1.32 \times 10^4 \frac{\theta^{0.2}}{\lambda^{1.2}}.$$

The rate of heat transmission from the spheres to the gas must be equal to the power generation within the spheres plus the power generation within the uranium carbide layer; thus a heat transfer balance may be set up as

$$(49)\quad h_c A_{sph} \Delta T_m = 948 P_r .$$

Since A_{sph} is the "wetted" surface area of all the spheres, we have

$$(50)\quad \Delta T_m = \frac{272\,P_r D_s}{h_c D_c^3},$$

and, from Eq. 43, Eq. 50 is reduced to

$$(51)\quad \Delta T_m = 1.02 \times 10^5 \left(\frac{P_r}{D_c}\right)^{0.2}\left(\frac{D_s}{D_c}\right)^{1.2},$$

or

$$(52)\quad \Delta T_m = 1.02 \times 10^5 \frac{\theta^{0.2}}{\lambda^{1.2}}.$$

Now, the bulk core power density, η_c, may be rewritten from Eq. 34 as

$$(53)\quad \eta_c = 2200\left(\frac{P_r}{D_c}\right)\left(\frac{D_s}{D_c}\right)^2\left(\frac{1}{D_s^2}\right),$$

or

$$(54)\quad \eta_c = 2200\,\frac{\theta}{(\lambda D_s)^2}.$$

Now by solving for D_s^2 from Eq. 19, and λ^2 from Eq. 52, and by introducing the parameters $(\Delta T_m/360)$ and $(\Delta p/200)$, η_c is approximately expressed by

$$(55)\quad \eta_c = \frac{32.3}{\left(\frac{mw}{\bar{c}_p^2}\right)}\,\frac{\left(\frac{\Delta p}{200}\right)\left(\frac{\Delta T_m}{360}\right)^{0.967}}{\theta^{1.033}}$$

for $\theta > \lambda/100$.

For hydrogen gas, $mw/\bar{c}_p^2$ is given in Table 8 as approximately 3.1×10^{-2}; thus

$$(56)\quad \eta_c|_{H_2} = 1042\,\frac{\left(\frac{\Delta p}{200}\right)\left(\frac{\Delta T_m}{360}\right)^{0.967}}{\theta^{1.033}}.$$

As determined from Eq. 52, λ is

$$(57)\quad \lambda = 111.0\,\frac{\theta^{0.167}}{\left(\frac{\Delta T_m}{360}\right)^{0.833}}.$$

This expression for λ, when combined with Eq. 40, yields the following relation between heat transfer Reynolds number, N_{Re_H}, and the reactor power factor θ:

$$(58)\quad N_{Re_H} = \frac{2.49 \times 10^{-3}}{k_g}\left(\frac{\Delta T_m}{360}\right)^{0.833}(\theta)^{0.833}.$$

Again from Table 8, k_g for hydrogen at the conditions stated is given as 7.89×10^{-6} Btu/sec·in.·°F; thus

$$(59)\quad N_{Re_H}\Big|_{H_2} = 316\left(\frac{\Delta T_m}{360}\right)^{0.833}(\theta)^{0.833}.$$

Since the primary parameter determining the feasibility of construction of the packed sphere reactor core is the required sphere diameter, it is of interest to determine the relation between sphere diameter and bulk core power density.

By combining Eqs. 19 and 57, the sphere diameter is given by

$$(60)\quad D_s = 7.471 \times 10^{-2}\,\frac{\left(\frac{mw}{\bar{c}_p^2}\right)^{0.5}(\theta)^{0.85}}{\left(\frac{\Delta p}{200}\right)^{0.5}\left(\frac{\Delta T_m}{360}\right)^{0.35}}.$$

When Eq. 60 is solved for θ and the value substituted into Eq. 55, the following relation between sphere diameter and reactor power density is obtained:

$$(61)\quad D_s = \frac{1.305\left(\frac{\Delta p}{200}\right)^{0.323}\left(\frac{\Delta T_m}{360}\right)^{0.446}}{(\eta_c)^{0.823}\left(\frac{mw}{\bar{c}_p^2}\right)^{0.323}}.$$

For hydrogen gas, this reduces to

$$(62)\quad D_s\Big|_{H_2} = \frac{4.01}{(\eta_c)^{0.823}}\left(\frac{\Delta p}{200}\right)^{0.323}\left(\frac{\Delta T_m}{360}\right)^{0.446}.$$

Figure 13 shows the required sphere diameter as a function of the desired bulk core power density for all the propellant gases considered, as given by Eq. 61. The heat transfer Reynolds number is given at various points along the curve.

Packed Rod Reactor. The pressure stresses in the packed rod core arise from axial compressive loads on the rods. The loads result from the gas pressure drop from the core top to bottom. The thermal stresses caused by volumetric power generation within the rods are compressive at the rod center and tensile on the rod surface under the assumed conditions of reactor operation.

From ref. 19, the gas pressure drop is found as the dimensionless equation

$$(1)\quad \frac{dF}{dx} = 288\,\frac{fG^2}{g_c\rho^2 d_h}.$$

In a manner identical to that used in Eqs. 1 through 8 in the section on the packed sphere reactor, the gas pressure drop is determined to be

$$(2)\quad \Delta p = 171\, f\,\frac{G^2}{mw}\,\frac{L_c}{d_h}$$

for an assumed axial gas temperature given by

$$T_{gx} = T_0 + \frac{(T_c - T_0)\,e}{(e-1)}\left(1 - e^{-x/L_c}\right).$$

For purposes of this study, G is based upon flow cross sectional area; thus

$$(3)\quad G = \frac{w}{\left(\frac{\pi}{4}\right)D_c^2\,\epsilon_f}$$

where ϵ_f is the gas volume fraction of the core and is given by

$$(4)\quad \epsilon_f = \frac{\text{total core cross section} - \text{rod cross section}}{\text{total core cross section}},$$

which, for rod packing in equilateral triangular array, is 0.093. Now, since the reactor power output must be balanced by the rate of energy gain of the propellant, the following equation

may be written:

$$(5) \qquad P_r = 0.678 \frac{w}{g_c}\left(\frac{v_m}{10^3}\right)^2 .$$

From Eq. 25 in the porous tube reactor study, it can be shown that the maximum theoretical exhaust velocity, v_m, is given by

$$(6) \qquad v_m^2 = 1556\, g_c \frac{\bar{c}_p T_c}{mw} .$$

Now, combining Eqs. 3, 5, and 6 yields an expression for the weight flow rate per unit flow area as:

$$(7). \qquad G = 0.242\left(\frac{P_r}{D_c^2}\right)\left(\frac{mw}{\epsilon_f \bar{c}_p}\right),$$

when T_c is specified as 4960°R.

The friction factor, f, in Eqs. 1 and 2 is given by

$$(8) \qquad f = \frac{128}{(N_{Re})^{1.48}} + \frac{0.0453}{(N_{Re})^{0.18}}$$

for all $10^2 < N_{Re} < 10^7$ where N_{Re} is the Reynolds number of the flow and is applicable throughout this section of the study to both flow and heat transfer expressions. Here N_{Re} is defined as:

$$(9) \qquad N_{Re} = \frac{d_h G}{\mu} .$$

The "hydraulic" diameter, d_h, is given by

$$(10) \quad d_{h(theo)} = \frac{(4)\ (\text{gas flow area between rods})}{\text{flow channel perimeter}} = 0.103\, D_s$$

for rod packing in an equilateral triangular array. Actually, because of laminar flow effects near the points of tangency of adjacent rods, it was felt more conservative to use a slightly higher value for d_h than that given by Eq. 10. For convenience, d_h was increased by a factor of $\pi/2$; thus giving

$$(11) \qquad d_h = 0.162\, D_s .$$

By combining Eqs. 7, 8, 9, and 11 with Eq. 2, and by specifying that the gas Prandtl number be 0.79, the following equation for Δp was obtained:

$$(12) \quad (\Delta p)(D_s^2) = 1.735 \times 10^6 \left(k_g^{1.48} \frac{mw}{\bar{c}_p^2}\right)\left(\frac{D_c}{D_s}\right)^{0.48}\left(\frac{P_r}{D_c}\right)^{0.52} + 615\left(k_g^{0.18} \frac{mw}{\bar{c}_p^2}\right)\left(\frac{P_r}{D_c}\right)^{1.82}\left(\frac{D_s}{D_c}\right)^{0.82} .$$

From the propellant gas data in Table 8, it was found that $k_g^{0.18}\big|_{avg}$ is 0.107, and that the average value of the $k_g^{1.48}\ (mw/\bar{c}_p^2)$ term is 9.11×10^{-10} with an average deviation of 7% for the propellants considered. By using these values and introducing the notation $\lambda = D_c/D_s$ and $\theta = P_r/D_c$, Eq. 12 becomes

$$(13) \quad (\Delta p)(D_s^2) = 1.58 \times 10^{-3}\, \theta^{0.52}\, \lambda^{0.48} + 65.8\left(\frac{mw}{\bar{c}_p^2}\right)\frac{\theta^{1.82}}{\lambda^{0.82}} .$$

The load stresses on the graphite rods are entirely compressive in nature (when side loads imposed by vehicle maneuvers are neglected) and the maximum load compressive stress is given by:

$$(14) \qquad s_L = \Delta p + w_{rods} ,$$

or

$$(15) \qquad s_L = \Delta p + \frac{a_m L_c \gamma_c}{1728\, g_c} .$$

In this reactor, as for the others, the core is assumed to be a square

cylinder; thus

$$\frac{L_c}{D_c} = 1.0 \quad (16)$$

Furthermore, the maximum vehicle acceleration is given in Part I as $9 g_c$. If a specific gravity of 1.70 is used for graphite, Eq. 15 can be reduced to

$$s_L = \Delta p + 0.553 D_c \quad (17)$$

The maximum thermal stress resulting from internal power generation in the rods is given by

$$s_{th} = \frac{\Delta T_s}{2} \frac{EB}{(1-\sigma)} \quad (18)$$

which is axial compressive stress at the rod center and axial and tangential tensile stress at the rod surface. The temperature drop from the rod center to the rod surface is given by

$$\Delta T_s = \frac{D_s^2}{16 k_s} \quad (19)$$

The power generation within the graphite rods is given by

$$q = 0.5486 \frac{\epsilon_p}{1-\epsilon_f} \eta_c \quad (20)$$

where ϵ_p is the fraction of the total reactor power generated within the graphite rods by neutron and gamma ray heating, and is taken as $\epsilon_p = 0.10$.

The bulk core power density is given, as previously, by

$$\eta_c = 2000 \frac{P_r}{D_c^3} \quad (21)$$

which, when combined with Eq. 20, yields

$$q = 1207 \frac{\epsilon_p}{1-\epsilon_f} \frac{P_r}{D_c^3} \quad (22)$$

When Eqs. 18, 19, and 22 are combined, the thermal stress is given by

$$s_{th} = 37.72 \frac{\epsilon_p}{(1-\epsilon_f)} \frac{EB}{(1-\sigma)} \frac{P_r D_s^2}{D_c^3} \quad (23)$$

For $\epsilon_p = 0.10$, $\epsilon_f = 0.093$, and graphite properties of $k_s = 4.17 \times 10^{-4}$ Btu/sec·in.·°F, $\sigma = 0.2$, $E = 1 \times 10^6$ psi, and $B = 3.1 \times 10^{-6}$ in./in.·°F, Eq. 23 reduces to

$$s_{th} = 3.87 \times 10^4 \left(\frac{P_r D_s^2}{D_c^3}\right) \quad (24)$$

or in the λ and θ notation,

$$s_{th} = 3.87 \times 10^4 \frac{\theta}{\lambda^2} \quad (25)$$

Now, for turbulent gas flow, the rod surface heat transfer coefficient is given by ref. 18 as

$$h_c = 0.023 \frac{k_g}{d_h} (N_{Re})^{0.8} (N_{Pr})^{0.4} \quad (26)$$

By combining Eqs. 7, 9, and 11 with Eq. 23 and by using N_{Pr} as 0.79 (Table 8), h_c becomes

$$h_c = 0.0781 k_g^{0.2} \left(\frac{P_r D_s}{D_c^2}\right)^{0.8} \left(\frac{1}{D_s}\right) \quad (27)$$

From Table 8, $k_g^{0.2}|_{avg}$ is seen to be approximately 0.083; thus

$$h_c = 6.482 \times 10^{-3} \left(\frac{P_r D_s}{D_c^2}\right)^{0.8} \left(\frac{1}{D_s}\right) \quad (28)$$

For conservation of energy, the rate of heat removal from the rods to the gas must exactly balance the power generation of the reactor; thus

$$h_c A_{rods} \Delta T_m = 948 P_r \quad (29)$$

When Eqs. 28 and 29 are combined and the relation

$$A_{rods} = \frac{\pi \epsilon_f D_c^3}{D_s}$$

is used, the solution of the equation for ΔT_m yields

$$\Delta T_m = \frac{333 P_r D_s}{h_c D_c^3} \quad (30)$$

and from Eq. 28, Eq. 30 becomes

$$\Delta T_m = 5.14 \times 10^4 \left(\frac{P_r}{D_c}\right)^{0.2} \left(\frac{D_s}{D_c}\right)^{1.2} \quad (31)$$

or by using λ and θ,

$$(32) \qquad \Delta T_m = 5.14 \times 10^4 \frac{\theta^{0.2}}{\lambda^{1.2}} .$$

As in the previous reactor studies, bulk power density, η_c, may be determined from

$$(33) \qquad \eta_c = 2200 \frac{\theta}{(\lambda D_s)^2} ,$$

where D_s^2 may be determined from Eq. 13 and λ^2 may be found from Eq. 32. By performing the required operations and by introducing the parameters $\Delta p/200$ and $\Delta T_m/360$, bulk power density can be approximately expressed as

$$(34) \qquad \eta_c = \frac{50.7}{\left(\frac{mw}{\bar{c}_p^2}\right)} \frac{\left(\frac{\Delta p}{200}\right)\left(\frac{\Delta T_m}{360}\right)^{0.984}}{\theta^{1.017}}$$

for $\theta > n$ with $\lambda < 100\ n$.

For hydrogen gas, Eq. 34 reduces to

$$(35) \qquad \eta_c\big|_{H_2} = 1640 \frac{\left(\frac{\Delta p}{200}\right)\left(\frac{\Delta T_m}{360}\right)^{0.984}}{\theta^{1.017}} .$$

Now, from Eq. 32, λ is determined to be

$$(36) \qquad \lambda = \frac{62.3\ \theta^{0.1667}}{\left(\frac{\Delta T_m}{360}\right)^{0.833}} .$$

Equation 9, combined with Eqs. 7 and 11, becomes

$$(37) \qquad N_{Re} = \frac{0.534}{k_g} \frac{\theta}{\lambda} .$$

A combination of Eqs. 36 and 37 yields a relation between the Reynolds number and the reactor power factor, θ, as:

$$(38) \qquad N_{Re} = \frac{8.57 \times 10^{-3}}{k_g} \left(\frac{\Delta T_m}{360}\right)^{0.833} \theta^{0.833} .$$

For hydrogen at the reactor conditions, this reduces to

$$(39) \qquad N_{Re}\big|_{H_2} = 1086 \left(\frac{\Delta T_m}{360}\right)^{0.833} \theta^{0.833} .$$

It is obvious that the maximum stress in the rods will be the sum of the pressure load and thermal axial compressive stresses at the rod center; hence Eqs. 17 and 25 can be combined to yield

$$(40) \qquad s_{tot} = \Delta p + 0.553\ D_c + 3.87 \times 10^4 \frac{\theta}{\lambda^2} .$$

The total stress must not be greater than the maximum strength of the graphite divided by the design safety factor. Also, the term $0.553\ D_c$ in Eq. 40 will be small (or can be made small by physically slicing the core into several short sections) compared to $(\Delta p + 3.87 \times 10^4\ \theta/\lambda^2)$ for all reactors of interest; hence Eq. 40 can be rewritten as

$$(41) \qquad \frac{s_c}{f_s} = \Delta p + 3.87 \times 10^4 \frac{\theta}{\lambda^2} ,$$

which, when combined with Eq. 36, yields

$$(42) \qquad \theta^{0.667} = 20.1 \frac{\left(\frac{s_c}{200\ f_s}\right) - \left(\frac{\Delta p}{200}\right)}{\left(\frac{\Delta T_m}{360}\right)} .$$

When Eq. 42 is combined with Eq. 34 to eliminate θ, an expression for reactor core power density is obtained as a function of allowable stresses, gas pressure drops, and wall-to-gas temperature drops as

$$(43) \qquad \eta_c = \frac{0.523}{\left(\frac{mw}{\bar{c}_p^2}\right)} \frac{\left(\frac{\Delta p}{200}\right)\left(\frac{\Delta T_m}{360}\right)^{3.524}}{\left[\left(\frac{s_c}{200\ f_s}\right) - \left(\frac{\Delta p}{200}\right)\right]^{1.525}} .$$

For hydrogen gas, this reduces to

$$(44)\quad \eta_c\big|_{H_2} = \frac{16.87\left(\frac{\Delta p}{200}\right)\left(\frac{\Delta T_m}{360}\right)^{3.524}}{\left[\left(\frac{s_c}{200\ f_s}\right)-\left(\frac{\Delta p}{200}\right)\right]^{1.525}}.$$

Since the feasibility of the packed rod reactor design will depend in large part upon the required sizes of rods to be used in the graphite core structure, the rod diameter, D_s, is derived below. By combination of Eqs. 13 and 32 (with Eq. 13 modified to

$$(\Delta p)(D_s^2) = 65.8\ \frac{mw}{\bar{c}_p^2}\ \frac{\theta^{1.82}}{\lambda^{1.82}};$$

valid for $\theta > \lambda/100$), the rod diameter was determined as

$$(45)\quad D_s = 0.1054\ \frac{\left(\frac{mw}{\bar{c}_p^2}\right)^{0.50}}{\left(\frac{\Delta p}{200}\right)^{0.50}}\left(\frac{\Delta T_m}{360}\right)^{0.341}\theta^{0.841}.$$

By introducing the limiting stress condition, Eq. 45 may be combined with Eqs. 42 and 43 to yield a relation between rod diameter and the stress, pressure drop, and wall-to-gas temperature drop parameters, and the bulk core power density as:

$$(46)\quad D_s = 2.717\frac{\left(\frac{\Delta p}{200}\right)^{0.328}\left(\frac{\Delta T_m}{360}\right)^{1.154}}{\left(\frac{mw}{\bar{c}_p^2}\right)^{0.328}(\eta_c)^{0.828}}.$$

For hydrogen, this reduces to

$$(47)\quad D_s\big|_{H_2} = 8.491\frac{\left(\frac{\Delta p}{200}\right)^{0.328}\left(\frac{\Delta T_m}{360}\right)^{1.154}}{(\eta_c)^{0.828}}.$$

The use of thicker rods means simpler and sturdier construction; however, Eq. 46 shows that rod diameter is an inverse function of the core power density. Since the nuclear rocket vehicle is feasible only for high power-density reactors, the parameter η_c must be held to its highest possible value. Reference to Eq. 34 shows that the bulk core power density is maximized for minimum values of θ; however, the minimum allowable value of θ is specified from Eq. 38 by the requirement that the flow Reynolds number be greater than 5000. Thus, from Eq. 38, we may write:

$$(48)\quad \theta_{min}^{0.833} = 5.834\times 10^5\ \frac{k_g}{\left(\frac{\Delta T_m}{360}\right)^{0.833}}.$$

Solving for θ and combining with Eq. 34 yields

$$(49)\quad \eta_{c_{max}} = \frac{4.690\times 10^{-6}\left(\frac{\Delta p}{200}\right)\left(\frac{\Delta T_m}{360}\right)^2}{\left(\frac{mw}{\bar{c}_p^2}\right)k_g^{1.22}}.$$

From the data in Table 8, the average value of the term $k_g^{1.22}\ (mw/\bar{c}_p^2)$ is found to be 2.32×10^{-8} for all propellants considered; thus Eq. 49 reduces to

$$(50)\quad \eta_{c_{max}} = 202.2\left(\frac{\Delta p}{200}\right)\left(\frac{\Delta T_m}{360}\right)^2.$$

Now, by combining Eqs. 46 and 49, the rod diameter for maximum core power density is given by

$$(51)\quad D_s = 6.90\times 10^4\ \frac{\left(\frac{mw}{\bar{c}_p^2}\right)^{0.500}k_g^{1.01}}{\left(\frac{\Delta p}{200}\right)^{0.500}\left(\frac{\Delta T_m}{360}\right)^{0.502}}.$$

For hydrogen, this reduces to

$$(52)\quad D_s\big|_{H_2} = \frac{0.0852}{\left(\frac{\Delta p}{200}\right)^{0.500}\left(\frac{\Delta T_m}{360}\right)^{0.502}}$$

for maximum core power density.

Figure 14 shows the rod diameter as a function of the desired bulk core power density, for all the propellants considered, as given by Eq. 46. Values of the flow Reynolds number are shown at various points along the curve.

Stacked Plate Reactor. To aid in the analysis of the stacked plate reactor, the reactor core was thought of as consisting of N parallel flat plates of thickness t, separation u, length L, and width c. This model was then replaced by *two* parallel plates of separation u, length L, width C (where $C = Nc$), and thickness t. The gas flow is taken as being in the L direction (that is, perpendicular to the C dimension) between the plates.

The loads that result from pressure drops within the core appear as compressive stresses on the graphite plates, while the thermal stresses will be compressive at the plate center planes and tensile at the plate surfaces.

As derived previously (Eq. 2 - packed rod reactor study), the gas pressure drop is given by

$$(1) \qquad \Delta p = 171 f \frac{G^2}{mw} \frac{L}{d_h}$$

for an assumed axial gas temperature given by

$$T_{gx} = T_0 + \frac{(T_c - T_0)\, e}{(e - 1)} \left(1 - e^{-x/L}\right).$$

For semi-infinite parallel flat plates, the "hydraulic" diameter is simply

$$(2) \qquad d_h = 2u .$$

In this study, G, the weight flow rate per unit area, is based upon free flow area only; thus

$$(3) \qquad G = \frac{w}{Cu} .$$

The reactor power is related to G through Eq. 3 and the expression

$$(4) \qquad P_r = 0.678 \frac{w}{g_c} \left(\frac{v_m}{10^3}\right)^2 .$$

By combining Eqs. 3 and 4 with Eq. 8 of the packed rod reactor study, and by specifying operation at a gas core outlet temperature of 4500°F, an equation for G is obtained as

$$(5) \qquad G = 0.190 \left(\frac{mw}{\bar{c}_p}\right)\left(\frac{P_r}{Cu}\right) .$$

The flow friction factor, f, in Eq. 1 is found from data in ref. 19 to be

$$(6) \qquad f = \frac{128}{(N_{Re})^{1.48}} + \frac{0.0453}{(N_{Re})^{0.18}} ,$$

where Reynolds number is given by

$$(7) \qquad N_{Re} = \frac{d_h G}{\mu} .$$

Now, when Eqs. 2, 5, and 7 are combined and the Prandtl number of the propellant gas is specified to be 0.79 (see Table 8), N_{Re} becomes

$$(8) \qquad N_{Re} = 0.481 \frac{P_r}{C k_g} .$$

Hence, Eq. 6 can be reduced to

$$(9) \qquad f = 379 \left(\frac{Ck_g}{P_r}\right)^{1.48} + 0.0517 \left(\frac{Ck_g}{P_r}\right)^{0.18} .$$

When Eqs. 1, 2, 5, and 9 are combined and the parameters $\lambda = L/u$ and $\theta = P_r/C$ are introduced, the following relation involving Δp is obtained:

$$(10) \qquad (\Delta p)(u^2) = 1170\, k_g^{1.48} \left(\frac{mw}{\bar{c}_p^2}\right) \lambda \theta^{0.52} + 0.1597\, k_g^{0.18} \left(\frac{mw}{\bar{c}_p^2}\right) \lambda \theta^{1.82} .$$

From the propellant gas data in Table 8, $k_g^{0.18}\big|_{avg}$ is found to be 0.107, while the average value of the $k_g^{1.48}\,(mw/\bar{c}_p^2)$ term is equal to 9.11×10^{-10} (see Eq. 12 - packed rod reactor study). By using these values, Eq. 10 is reduced to

$$(11)\quad (\Delta p)(u^2) = 1.066 \times 10^{-6}\ \lambda\theta^{0.52} + 0.0171\left(\frac{mw}{\overline{c}_p^2}\right)\lambda\theta^{1.82}\ .$$

The pressure load stresses on the graphite plates are entirely compressive (if side loads due to vehicle maneuvers are neglected) with the maximum compressive stress being given by

$$(12)\quad s_L = \Delta p + \frac{L\gamma_c a_m}{1728\ g_c}\ .$$

For graphite of specific gravity equal to 1.70, and for a maximum vehicle acceleration of $9\,g_c$, Eq. 12 reduces to

$$(13)\quad s_L = \Delta p + 0.553\ L\ .$$

The maximum thermal stress in the rods due to internal neutron and gamma ray heating is given by

$$(14)\quad s_{th} = \frac{2\Delta T_s}{3}\ \frac{EB}{(1-\sigma)}\ ,$$

which is axial compressive stress at the plate center and axial tensile stress at the plate surface. The temperature drop from the plate center to the plate surface is given by

$$(15)\quad \Delta T_s = \frac{qt^2}{8k_s}\ .$$

The power generation within the graphite plates is given by

$$(16)\quad q = 0.5486\ \epsilon_p \eta_c \left(\frac{t+u}{t}\right)\ ,$$

where ϵ_p is the fraction of total reactor power generated within the plates by neutron and gamma heating and is here taken to be 0.10, as previously. The bulk core power density is given by

$$(17)\quad \eta_c = 1728\ \frac{P_r}{LC(t+u)}\ ,$$

which, when combined with Eq. 16, yields

$$(18)\quad q = 948\ \frac{\epsilon_p P_r}{LCt}\ .$$

When Eqs. 14, 15, and 18 are combined, the thermal stress is given by

$$(19)\quad s_{th} = \frac{79\ \epsilon_p P_r t\ EB}{k_s LC\ (1-\sigma)}\ .$$

Now, for $\epsilon_p = 0.10$, $k_s = 4.17 \times 10^{-4}$ Btu/sec·in.·°F, $E = 1.0 \times 10^6$ psi, $B = 3.1 \times 10^{-6}$ in./in.·°F, and $\sigma = 0.2$, Eq. 19 is reduced to

$$(20)\quad s_{th} = 7.34 \times 10^4\ \frac{P_r t}{LC}\ ,$$

or, when the parameter $\delta = t/u$ is introduced,

$$(21)\quad s_{th} = 7.34 \times 10^4\ \frac{\theta\delta}{\lambda}\ .$$

For turbulent gas flow, the plate surface heat transfer coefficient is given by

$$(22)\quad h_c = 0.023\ \frac{k_g}{d_h}\ (N_{Re})^{0.8}\ (N_{Pr})^{0.4}\ ,$$

as previously.

When $N_{Pr} = 0.79$ (see Table 8) and Eqs. 2, 8, and 22 are combined, h_c becomes

$$(23)\quad h_c = 5.83 \times 10^{-3}\ k_g^{0.2}\left(\frac{P_r}{C}\right)^{0.8}\left(\frac{1}{u}\right).$$

Table 8 gives $k_g^{0.2}\big|_{avg}$ as 0.083; thus Eq. 23 is reduced to

$$(24)\quad h_c = 4.84 \times 10^{-4}\left(\frac{P_r}{C}\right)^{0.8}\left(\frac{1}{u}\right).$$

As previously, a heat balance may be set up between energy transferred to the gas and power generated within the plates as

$$(25)\quad h_c\ A_{plate}\ \Delta T_m = 948\ P_r\ ,$$

where A_{plate} is equal to $2CL$.

Now, when Eqs. 24 and 25 are combined and solved for ΔT_m,

$$(26)\quad \Delta T_m = 0.979 \times 10^6\left(\frac{P_r}{C}\right)^{0.2}\left(\frac{u}{L}\right)\ ,$$

or, in the λ and θ notation previously introduced,

$$(27)\quad \Delta T_m = 0.979 \times 10^6\ \frac{\theta^{0.2}}{\lambda}\ .$$

The bulk core power density may now be determined from Eq. 17 to be

$$(28)\quad \eta_c = 1728\left(\frac{P_r}{C}\right)\left(\frac{u}{L}\right)\left(\frac{1}{u^2}\right)\left(\frac{1}{1+\frac{t}{u}}\right),$$

or, if rewritten with the λ, θ, and δ parameters,

$$(29)\quad \eta_c = \frac{1728\,\theta}{\lambda u^2(\delta+1)}.$$

In order to solve for δ from Eq. 21 it is necessary to know the relation between Δp, s_{th}, and total stress. The maximum allowable stress in the graphite plates can not be greater than the maximum compressive strength divided by the design safety factor; thus

$$(30)\quad \frac{sc}{f_s} = s_L + s_{th}$$

or, from Eqs. 13 and 21,

$$(31)\quad \frac{sc}{f_s} = \Delta p + 0.553L + 7.34\times 10^4\,\frac{\theta\delta}{\lambda}.$$

For practical purposes, the term $0.553\,L$ can be neglected in comparison with $(\Delta p + 7.34\times 10^4\,\theta\delta/\lambda)$; thus Eq. 31 can be solved for δ as

$$(32)\quad \delta = 2.72\times 10^{-3}\left(\frac{sc}{200\,f_s}-\frac{\Delta p}{200}\right)\left(\frac{\lambda}{\theta}\right).$$

Equation 8 may be rewritten as

$$(33)\quad N_{Re} = \frac{0.481}{k_g}\,\theta,$$

which reduces to

$$(34)\quad N_{Re}\big|_{H_2} = 6.10\times 10^4\,\theta$$

for hydrogen at the reactor conditions (see Table 8 for values of k_g).

It can be seen from Eq. 33 and Table 8 that θ must be greater than 3×10^{-2} for all propellants considered in order for flow conditions to be in the turbulent regime. Now, for values of θ greater than 3×10^{-2}, the first term of Eq. 11 can be shown to be negligible compared to the second term; thus Eq. 11 can be reduced to

$$(35)\quad (\Delta p)(u^2) = 0.0171\left(\frac{mw}{\bar{c}_p^2}\right)\lambda\theta^{1.82}$$

for $\theta > 3\times 10^{-2}$.

From Eq. 35, u^2 may be determined as

$$(36)\quad u^2 = 8.55\times 10^{-5}\,\frac{\left(\frac{mw}{\bar{c}_p^2}\right)}{\left(\frac{\Delta p}{200}\right)}\,\lambda\theta^{1.82}.$$

Now, from Eq. 27, the following solution for λ may be obtained:

$$(37)\quad \lambda = 2720\,\frac{\theta^{0.2}}{\left(\frac{\Delta T_m}{360}\right)}.$$

When Eqs. 36 and 37 are combined with Eq. 29, the bulk core power density is given as

$$(38)\quad \eta_c = \frac{2.731}{\left(\frac{mw}{\bar{c}_p^2}\right)}\,\frac{\left(\frac{\Delta p}{200}\right)\left(\frac{\Delta T_m}{360}\right)^2}{(\delta+1)\,\theta^{1.22}}.$$

For hydrogen gas, the coefficient, $2.731/(mw/\bar{c}_p^2)$, in Eq. 38 becomes 88.1.

The feasibility of construction of any of the reactor systems discussed depends to a large extent upon the required quantity and sizes of individual core structure elements. In the present case, the parameter of importance from the fabrication standpoint is the plate thickness, t. Since $\delta = t/u$ (see Eq. 21), the plate thickness may be related to the core power density by a combination of Eqs. 29, 36, and 37 as

$$(39)\quad t = 1.317\,\frac{\left(\frac{\Delta p}{200}\right)^{0.500}\left(\frac{\Delta T_m}{360}\right)^{1.500}}{\left(\frac{mw}{\bar{c}_p^2}\right)^{0.500}\eta_c\,\theta^{0.21}} - 0.4823\,\frac{\left(\frac{mw}{\bar{c}_p^2}\right)^{0.500}\theta^{1.01}}{\left(\frac{\Delta p}{200}\right)^{0.500}\left(\frac{\Delta T_m}{360}\right)^{0.500}}.$$

For hydrogen, this becomes

$$(40)\quad t\big|_{H_2} = 7.48\,\frac{\left(\frac{\Delta p}{200}\right)^{0.500}\left(\frac{\Delta T_m}{360}\right)^{1.500}}{\eta_c\,\theta^{0.21}} - \frac{0.085\,\theta^{1.01}}{\left(\frac{\Delta p}{200}\right)^{0.500}\left(\frac{\Delta T_m}{360}\right)^{0.500}}.$$

The use of thicker plates (within limits) makes for simpler and less fragile construction; thus it would be desirable to utilize a low value of θ in Eq. 39. The minimum value of θ, however, may be specified from Eq. 33 as being that value which gives flow conditions at a Reynolds number of 5000 or greater. Thus, from Eq. 33, we may write

$$(41)\qquad \theta_{min} = 1.04 \times 10^4\, k_g\,.$$

Now, combining Eqs. 39 and 41 yields the following equation for maximum plate thickness:

$$(42)\quad t_{max} = 0.189\,\frac{\left(\frac{\Delta p}{200}\right)^{0.500}\left(\frac{\Delta T_m}{360}\right)^{1.500}}{\left(\frac{mw}{\bar{c}_p^2}\right)^{0.500} k_g^{0.21}\,\eta_c} - 5500\,\frac{k_g^{1.01}\left(\frac{mw}{\bar{c}_p^2}\right)^{0.500}}{\left(\frac{\Delta p}{200}\right)^{0.500}\left(\frac{\Delta T_m}{360}\right)^{0.500}}.$$

The average value of $k_g^{1.01}\,(mw/\bar{c}_p^2)^{0.500}$ is found from Table 8 to be 9.98×10^{-5}; thus Eq. 42 can be reduced to

$$(43)\quad t_{max} = \frac{0.189\left(\frac{\Delta p}{200}\right)^{0.500}\left(\frac{\Delta T_m}{360}\right)^{1.500}}{k_g^{0.21}\left(\frac{mw}{\bar{c}_p^2}\right)^{0.500}\eta_c} - \frac{5.49 \times 10^{-3}}{\left(\frac{\Delta p}{200}\right)^{0.500}\left(\frac{\Delta T_m}{360}\right)^{0.500}}.$$

It can be seen from Eqs. 42 and 43 that thick plates will be given by low values of $mw/\bar{c}_p^2$, all other parameters being fixed; thus the plate thickness is definitely a function of the characteristics of the propellant gas.

For hydrogen, Eq. 42 reduces to

$$(44)\quad t_{max}\big|_{H_2} = 12.63\,\frac{\left(\frac{\Delta p}{200}\right)^{0.500}\left(\frac{\Delta T_m}{360}\right)^{0.500}}{\eta_c} - \frac{6.43 \times 10^{-3}}{\left(\frac{\Delta p}{200}\right)^{0.500}\left(\frac{\Delta T_m}{360}\right)^{0.500}}.$$

Furthermore, by combination of Eqs. 29, 36, and 37 with Eq. 41, the maximum bulk core power density is given as

$$(45)\quad \eta_{c_{max}} = 3.430 \times 10^{-5}\,\frac{\left(\frac{\Delta p}{200}\right)\left(\frac{\Delta T_m}{360}\right)^2}{(\delta + 1)\left(\frac{mw}{\bar{c}_p^2}\right)k_g^{1.22}}.$$

Now, for maximum power densities it is obvious that the value of δ should be as small as possible; however, δ is related to the core void volume fraction by

$$(46)\qquad \delta = \frac{1 - f_v}{f_v}.$$

Critical mass studies indicate that reactors with greater than 50% void volume within the core require excessive amounts of uranium for criticality; hence the minimum value for δ is herein defined as 1.0. By the average value of $k_g^{1.22}\ (mw/\bar{c}_p^2)$ as 2.32×10^{-8} for all propellants (see Table 8), the maximum bulk core power density possible in the stacked plate core, for a flow Reynolds number of 5000, becomes

$$(47)\quad \eta_{c_{max}} = \frac{1478}{(\delta + 1)} \left(\frac{\Delta p}{200}\right)\left(\frac{\Delta T_m}{360}\right)^2 = 739 \left(\frac{\Delta p}{200}\right)\left(\frac{\Delta T_m}{360}\right)^2$$

for the minimum value of δ of 1.0.

As a matter of interest, Eq. 45 may be combined with Eq. 49 in the packed rod reactor study to show that

$$(48)\quad \frac{\eta_{c_{max}}\ (\text{stacked plates})}{\eta_{c_{max}}\ (\text{packed rods})} = \frac{7.31}{(\delta + 1)}$$

for a flow Reynolds number of 5000 in both systems.

To show the relation between flow Reynolds number, bulk core power density, and plate thickness, Eqs. 33 and 39 may be combined to eliminate θ and yield

$$(49)\quad t = \frac{1.130 \left(\frac{\Delta p}{200}\right)^{1/2} \left(\frac{\Delta T_m}{360}\right)^{3/2}}{\eta_c\ (N_{Re})^{0.21}\ (k_g)^{0.21} \left(\frac{mw}{\bar{c}_p^2}\right)^{1/2}} - \frac{1.009 \left(\frac{mw}{\bar{c}_p^2}\right)^{1/2}\ (k_g)^{1.01}\ (N_{Re})^{1.01}}{\left(\frac{\Delta p}{200}\right)^{1/2} \left(\frac{\Delta T_m}{360}\right)^{1/2}}.$$

Figure 15 shows the plate thickness as a function of the bulk core power density for various Reynolds numbers for all the propellants considered, as given by Eq. 49.

REFERENCES

1. C. B. Mills, *A Simple Criticality Relation for Be Moderated Intermediate Reactors,* Y-F10-93 (March 10, 1952).
2. A. E. Ruark *et al.*, *Nuclear Powered Flight,* NP-378 (APL/JHU TG-20) chap. IV and app. 2 and 4 (Jan 14, 1947).
3. H. S. Tsien, *Rockets and Other Thermal Jets Using Nuclear Energy;* C. Goodman (ed.), *The Science and Engineering of Nuclear Power,* vol. 2, chap. 11, Addison-Wesley Press (1949).
4. W. K. Ergen, *Preliminary Remarks on Hsue-Shen Tsien's Seminars "Rockets and Other Thermal Jets Using Nuclear Energy,"* NEPA 544-STR-2 (June 1, 1948).
5. C. Malmstrom, R. Keen, and L. Green, Jr., *Some Mechanical Properties of Graphite at Elevated Temperatures,* NAA-SR-79, Fig. 18 (Sept. 28, 1950).
6. *Feasibility of Nuclear Powered Rockets and Ramjets,* NA-47-15, app. 3-F (Feb. 11, 1947).
7. L. Green, Jr. and P. Duwez, "Fluid Flow Through Porous Metals," *J. Appl. Mechanics* **18**, 39 (1951).
8. L. Green, Jr., "Gas Cooling of a Porous Heat Source," *J. Appl. Mechanics* **19**, 173 (1952).
9. W. H. McAdams, *Heat Transmission,* pp. 124-125, McGraw-Hill, New York, 1942.
10. F. G. Keyes, "A Summary of Viscosity and Heat Conductivity Data for He, A, H_2, O_2, N_2, CO, CO_2, H_2O, and Air," *Trans. Am. Soc. Mech. Engrs.* **73**, 589.
11. J. O. Hirschfelder, B. B. Bird, and E. L. Spotz, "The Transport Properties for Non-Polar Gases," *J. Chem. Phys.* **16**, 968 (1948).
12. L. A. Bromley, *Calculation of Gas Viscosity as a Function of Temperature,* UCRL-525 (Nov. 1949).
13. L. A. Bromley, *Thermal Conductivity of Gases at Moderate Pressures,* UCRL-1852 (June 12, 1952).

F. J. Krieger, *Calculation of the Viscosity of Gas Mixtures*, RM-649 (July 13, 1951).

R. J. Roark, *Formulas for Stress and Strain*, pp. 274-281, McGraw-Hill, New York, 1943.

S. Timoshenko, *Theory of Elasticity*, pp. 339-344, McGraw-Hill, New York, 1934.

L. M. K. Boelter, V. H. Cherry, H. A. Johnson, and R. C. Martinelli, *Heat Transfer Notes*, chap. XVII, University of California Press, Berkeley and Los Angeles, 1948.

Ref. 9, p. 168.

Ref. 9, pp. 118-119.

20. G. P. Sutton, *Rocket Propulsion Elements*, Table 5-2, John Wiley and Sons, New York, 1949.

21. D. W. Scott, G. D. Oliver, M. E. Gross, W. N. Hubbard, and H. M. Huffman, "Thermodynamic Properties of Hydrazine," *J. Am. Chem. Soc.* **71**, 2293 (1949).

22. E. W. Washburn (ed.), *International Critical Tables of Numerical Data, Physics, Chemistry, and Technology*, vol. 5, p. 136, McGraw-Hill, New York, 1926-33.

23. L. Green, *High Temperature Compression Tests on Graphite*, NAA-SR-165, Fig. 6 (Jan 7, 1952).

ACKNOWLEDGEMENT

In any investigation of the type covered in this report, the end result is necessarily an integration of the thoughts and efforts of a number of people. Accordingly, the author wishes to express his indebtedness to J. R. Johnson and F. Kertesz for their helpful discussions of possible methods of solving the provlem of a protective coating for the reactor heat transfer structure. The contribution of C. B. Mills, who performed the criticality calculations, was also of great importance. F. H. Abernathy was very helpful with his discussions of the shielding problems associated with nuclear-powered rockets. A. P. Fraas aided in correcting the manuscript.

ERRATA

ORNL
Central Files Number
53-6-6

This document consists of 6 pages.
Copy 7 of 29 copies. Series A.

NUCLEAR ENERGY

FOR ROCKET PROPULSION

TABLE OF CONTENTS

LIST OF TABLES

LIST OF FIGURES